

Doctoral Thesis

Retrofitting Methods for Existing Historical Clay Buildings against Earthquake Events

submitted in satisfaction of the requirements for the degree of
Doctor of Science in Civil Engineering
of the Vienna University of Technology, Faculty of Civil Engineering

Dissertation

Methoden zum Ertüchtigung des Bestehende Historisches Lehmgebäude gegen Erdbeben Events

ausgeführt zum Zwecke der Erlangung des akademischen Grades eines
Doktors der technischen Wissenschaft
eingereicht an der Technischen Universität Wien Fakultät für Bauingenieurwesen
von

Dipl.-Ing. Israa Jabur
Matrikelnummer 9825053
Brigittenauerlände 156-158/2/35, 1200 Wien

Gutachter: o. Univ. Prof. Dipl.-Ing. Dr.-techn. Andreas KOLBITSCH

Institut für Hochbau und Technologie Zentrum für Hochbaukonstruktionen und
Gebäudeerhaltung E206

Gutachter: Ao. Univ. Prof. Dipl.-Ing. DDr.-techn. Elemer BÖLCSKEY

Institut für Hochbau und Technologie Zentrum für Hochbaukonstruktionen und
Gebäudeerhaltung E206

Wien, im Oktober 2013

ACKNOWLEDGMENTS

I want to express my sincere gratitude to everyone who has helped and supported me during this work. I want to send special thanks to:

- o. Univ. Prof. Dipl.-Ing. Dr.-techn. Andreas KOLBITSCH, my advisor, for trusting and supporting me during all the work with enthusiasm and precious supervision.
- ao. Univ. Prof. Dipl.-Ing. DDr.-techn. Elemer BÖLCSKEY, for sharing his knowledge in the earthquake retrofitting field with me and giving me the opportunity to research such an exciting subject.

TABLE OF CONTENTS

1.	STATEMENT OF THE PROBLEM	1
1.1	OBJECTIVES AND SCOPE	2
1.2	THESIS ORGANIZATION	3
2.	THE CURRENT STATE OF TECHNOLOGY AND LITERATURE REVIEW	5
2.1	HISTORY OF MUD BUILDING IN THE ARAB WORLD AND WORLDWIDE	5
2.1.1	Characteristics of Mud as a Building Material	7
2.1.2	Techniques for the Use of Mud as a Building Material	10
2.2	CURRENTLY AVAILABLE CALCULATION METHODS FOR THE ASSESSMENT OF EARTHQUAKE LOADS	13
2.2.1	Earthquake Effects and Structure Behaviour	13
2.2.2	Calculation Methods of the Seismic Effect According to EC 8:	21
2.3	THE STATE OF CURRENT RESEARCH	28
3.	MATERIAL PROPERTIES	32
3.1	SELECTIONS OF MUD BUILDING MATERIALS	33
3.2	SELECTION OF THE EXPERIMENTAL ARRANGEMENTS	36
3.2.1	Strength of clay	36
3.3	EVALUATION OF THE ENVISAGED TESTS	46
4.	STRUCTURAL ANALYSIS	48
4.1	SETTING MUD PROPERTIES USED FOR THE EXPERIMENTS	48
4.1.1	Clay produced in Austria	48
4.1.2	Clay produced in the Dubai region	49
4.2	CARRYING OUT THE EXPERIMENTS	49
4.2.1	Compressive strength	50
4.2.2	Tensile strength	59
4.2.3	Elastic modulus	62
4.2.4	Shear strength	65
4.3	EVALUATION OF TEST RESULTS	76
5.	DEVELOPMENT OF THE ANALYTICAL AND NUMERICAL MODEL FOR SEISMIC LOADS	77
5.1	MODIFICATION OF EQUIVALENT LATERAL FORCE METHOD FOR CLAY BUILDING	83
5.1.1	Material Characteristics	83
5.1.2	Geometry	84
5.1.3	Loads	88
5.1.4	Mass Calculation	90
5.1.5	Geometric characteristic data	90
5.1.6	Building Geometric characteristic data	92
5.1.7	Criteria for structural regularity	101

5.1.8	Simplified response spectrum method.....	103
5.1.9	Earthquake forces due to the torsional effect	104
5.2	MODIFICATION OF RESPONSE SPECTRUM METHOD FOR CLAY BUILDING.....	111
5.3	INELASTIC STATIC INVESTIGATION OF PUSHOVER METHODS	118
5.3.1	Determination of the elastic response spectrum.....	119
5.3.2	Determination of the building load-deformation curve.....	120
5.3.3	Creating the building load-deformation curve.....	123
5.3.4	Creation of the building pushover-curve for an equivalent mass.....	124
5.3.5	Determination of the period for an equivalent mass system	125
5.3.6	Determination of the maximum deformation for an equivalent mass system	125
5.3.7	Determination of the target deformation for mass system	126
5.3.8	Checking the allowable target deformation	126
5.3.9	Determining the Ductility μ	127
5.3.10	Determining the verified graph of the S_e - S_d Diagram.....	127
5.3.11	Pushover simulation Analysis.....	128
5.4	TIME HISTORY METHOD	137
5.4.1	Horizontal strength calculation according to the time history method	139
5.4.2	Deformation capacity calculation according to the time history method	143
6.	RETROFITTING METHODS AND NUMERICAL MODELING.....	145
6.1	RETROFITTING METHODS FOR UNREINFORCED WALLS.....	145
6.1.1	Surface Treatment.....	146
6.1.2	Post-Tensioning.....	148
6.1.3	Injection	149
6.1.4	Add new structural members to scale up the seismic performance.....	150
6.1.5	Reduce the seismic force inputted to the building	151
6.2	NUMERICAL MODELLING AND RESPONSE SPECTRUM ANALYSIS FOR SEISMIC EXCITATION	152
6.2.1	Model simulation without retrofitting	153
6.2.2	Model simulation with wood cross-bracing retrofitting.....	154
6.2.3	Model simulation with wood X-Bracing and fixed wooden plate retrofitting	156
6.2.4	Numerical analysis for the top displacement	158
6.3	COMPARISON OF THE NUMERICAL ANALYSIS RESULTS	159
7.	SUMMARY AND CONCLUSION.....	161
8.	REFERENCES.....	163

LIST OF TABLES

Table 2-1 Abbreviated European Intensity Scale EMS 1992	19
Table 2-2 Comparison of the essential characteristics of the calculation methods	28
Table 3-1 Different types of clay according to [24]	33
Table 3-2 Summary of the grain sizes of the various fillers	36
Table 3-3 Classification of construction clays according to the binding strength [24].....	42
Table 3-4 Compilation of the general parameters of clay from [30], [31], [32], [33]	47
Table 4-1 Compression test results	53
Table 4-2 Determination of flexural strength	56
Table 4-3 Compressive strength results (S1-S16).....	58
Table 4-4 Elasticity modulus results – Prism 1	64
Table 4-5 Elasticity modulus results for Prism 2	65
Table 4-6 Shear test specimen	66
Table 4-7 Test and simulation results comparison for Wood Frame	69
Table 4-8 Test and simulation results comparison for wall sections B1 and B2	71
Table 4-9 Test and simulation results comparison for wall sections C1 and C2	73
Table 4-10 Test and simulation results comparison for wall section D1	74
Table 4-11 Test and simulation results comparison for wall section E1	76
Table 4-12 Summary of the obtained results	76
Table 5-1 Mass calculation.....	90
Table 5-2 Determination of geometric data for earthquake loads in the x-direction.....	93
Table 5-3 Determination of geometric data for earthquake loads in the y-direction.....	95
Table 5-4 Determination of the shear areas and moments of inertia.....	97
Table 5-5 Determine of the Torsion radii according to the stiffness center.....	99
Table 5-6 Calculating the ceiling moments of inertia	100
Table 5-7 Calculating the Column moments of inertia.....	100
Table 5-8 Stress in X direction	106
Table 5-9 Stress in the Y direction	107
Table 5-10 Stress in the Y direction	108
Table 5-11 Stress in the X direction	109
Table 5-12 Seismic forces with torsional effect	110
Table 5-13 Shear forces due to the earthquake of an individual wall.....	110
Table 5-14 Model material specification	111
Table 5-15 Model mass participation factor	112
Table 5-16 Frequency mode and its vibration time	114
Table 5-17 Wall shear stress according to response spectrum analysis	117
Table 5-18 Approximate shear strength and maximum final deformations of shear walls in x- direction.....	123
Table 5-19 Approximate shear forces on shear walls in x-direction	143
Table 6-1 Comparison of the numerical analysis results.....	160

LIST OF FIGURES

Figure 1-1 Typical modes of failure in adobe structures [1]	2
Figure 2-1 Examples of mud architecture in Arabic cities (Egypt, Saudi Arabia, Yemen, and Algeria) ..	7
Figure 2-2 building with air-dried mud bricks	11
Figure 2-3 Collision mechanism of plate tectonics	14
Figure 2-4 various types of earthquake waves	16
Figure 2-5 Dependency of the expected magnitude on the recurrence period for various regions ...	17
Figure 2-6 Scale of magnitude according to Richter	18
Figure 2-7 Equivalent lateral force method: Structure (left) and lateral bar with equivalent lateral forces (right).....	23
Figure 2-8 Response spectra method: structure (left) and the deformation parts out of the three horizontal natural vibration forms (right).....	25
Figure 2-9 Non-linear static calculation: structure with horizontal equivalent lateral forces F_i (left) and horizontal force – displacement curve (pushover curve) (right).....	26
Figure 2-10 Capacity spectrum method: acceleration-displacement diagram of the structure (capacity curve) and the assessment spectrum (demand spectrum)	26
Figure 2-11 Compression strength test by Jeanette Gasparini	29
Figure 2-12 specimen of Adobe-masonry strengthen with sisal rope at the mortar joint [Janet]	30
Figure 2-13 External wire mesh reinforcement introduced by Marcial and Rafael	31
Figure 2-14 External geogrid mesh reinforcement	31
Figure 3-1 Example of a modern earthen structure in Riyadh, Saudi Arabia [23]	32
Figure 3-2 Dimensions (in mm) for testing arrangement of the flexural tension strength	38
Figure 3-3 Test specimen preparation (in mm) and the test arrangement	41
Figure 3-4 Diagrammatic representation of the stress-strain relation for concrete.....	44
Figure 3-5 clay wall sections specimens	45
Figure 3-6 Experimental arrangement sketch for determining shear strength capacity	46
Figure 4-1 Clay obtained from Austria.....	48
Figure 4-2 Clay obtained from the Al-Aali Company	49
Figure 4-3 formwork preparation for the compression test.....	50
Figure 4-4 Slump test for prepared clay	51
Figure 4-5 Prepared clay in the formwork for the compression test	51
Figure 4-6 Prepared clay specimens for the compression test.....	52
Figure 4-7 Compression test carried out on the prepared clay specimens	52
Figure 4-8 Compressive strength result.....	54
Figure 4-9 Clay specimen preparation.....	55
Figure 4-10 Flexural bending test on clay prisms.....	55
Figure 4-11 Carrying out the compression test.....	57
Figure 4-12 the relation between the drying time and compressive strength for series (S1-S16)	58
Figure 4-13 (right) A mechanical tensile test machine. (left) A universal tensile testing machine (Hegewald & Peschke).....	59
Figure 4-14 Tensile test specimens	60
Figure 4-15 Tensile test results. (a&b) Using the electrical machine. (c) The test performed using a mechanical machine.....	61

Figure 4-16 Preparation of clay prisms for the elasticity modulus test.....	62
Figure 4-17 Test setup for determining the elasticity modulus.....	63
Figure 4-18 Elasticity modulus results for Prism 1	64
Figure 4-19 Elasticity modulus results for Prism 2	65
Figure 4-20 Shear test setup	66
Figure 4-21 Shear strength test for wood frame A1 and A2.....	67
Figure 4-22 Shear strength test simulation for wood frame A1 and A2.....	68
Figure 4-23 (a) and (b) Force –Top displacement test results for wood frame A1 and A2	68
Figure 4-24 Shear strength test for wall section B1	69
Figure 4-25 Shear strength test for wall section B2	69
Figure 4-26 Shear strength test simulation for wall section B.....	70
Figure 4-27 (a) and (b) Force –Top displacement test results for wall sections B1 and B2.....	70
Figure 4-28 Shear strength test for wall section C1	71
Figure 4-29 Shear strength test for wall section C2	72
Figure 4-30 Shear strength test simulation wall section C	72
Figure 4-31 Force –Top displacement test results for wall section C2.....	72
Figure 4-32 Shear strength test for wall section D1	73
Figure 4-33 Shear strength test simulation wall section D.....	74
Figure 4-34 Force –Top displacement test results for wall section D1	74
Figure 4-35 Shear strength test for wall section E1	75
Figure 4-36 Shear strength test simulation wall section E	75
Figure 4-37 Force –Top displacement test results for wall section E1.....	75
Figure 5-1 Dubai seismic zones [35]	78
Figure 5-2 the elastic response spectrum’s shape of 5%.....	80
Figure 5-3 Layout of the ground floor with associated coordinate system.....	84
Figure 5-4 North View	85
Figure 5-5 South View.....	85
Figure 5-6 West View.....	86
Figure 5-7 Door View Section.....	86
Figure 5-8 (a, b and c) Prayer Hall	87
Figure 5-9 Ceiling and roof overloaded distribution	89
Figure 5-10 General design spectrum according to EC-8	103
Figure 5-11 6 th Model mode shape	113
Figure 5-12 7 th Model mode shape	113
Figure 5-13 Shear stress in XY-direction	115
Figure 5-14 Shear stress in XZ-direction	115
Figure 5-15 Shear stress in YZ-direction	116
Figure 5-16 Resultant wall deformation.....	116
Figure 5-17 Capacity spectrum method [43]	118
Figure 5-18 Normative response spectrum of soil type 1, class A according to the EC8	120
Figure 5-19 Load-deformation curve of the prayer hall for the mosque for walls in the x-direction	123
Figure 5-20 the idealization of the Pushover-curve	124
Figure 5-21 Determination of the performance point using the load deformation curve.....	127
Figure 5-22 Determination of the performance point using the idealization of the pushover-curve	128

Figure 5-23 Capacity curve in W-E direction.....	129
Figure 5-24 Deformed building in W-E direction (for the capacity curve steps - first perspective)...	130
Figure 5-25 Deformed building in W-E direction (for the capacity curve steps - second perspective)	131
Figure 5-26 Tensile principal strain for all analysis steps of W-E direction	132
Figure 5-27 Capacity curve in N-S direction.....	133
Figure 5-28 Deformed building in N-S direction (for the capacity curve steps - first perspective)....	134
Figure 5-29 Deformed building in N-S direction (for the capacity curve steps - second perspective)135	
Figure 5-30 Tensile principal strain for all analysis steps of N-S direction	136
Figure 5-31 Response spectrum based on DIN EN 1998-1 (Type 1 – Class A) soil condition.....	138
Figure 5-32 Time history of the peak ground horizontal acceleration	138
Figure 5-33 Horizontal shear stress due to the earthquake effect for Wall 1 in yz-plane.....	139
Figure 5-34 Horizontal shear stress due to the earthquake effect for Wall 4 in yz-plane.....	140
Figure 5-35 Horizontal shear stress due to the earthquake effect for Wall 1 in xy-plane	141
Figure 5-36 Horizontal shear stress due to the earthquake effect for Wall 4 in xy-plane	142
Figure 5-37 Accumulated absolute total deformation for the building through 10 sec.	143
Figure 6-1 Preparing and applying bamboo-band mesh	146
Figure 6-2 Applying Shotcrete.....	147
Figure 6-3 FRP retrofitting method	148
Figure 6-4 Applying post-tensioning method	148
Figure 6-5 Applying the injection method to an existing masonry brick wall.....	149
Figure 6-6 Examples of seismic retrofitting methods.....	150
Figure 6-7 Examples of reducing seismic force	151
Figure 6-8 Clay mosque	152
Figure 6-9 Shear stresses in x-y, y-z and x-z directions for the Mosque without retrofitting	153
Figure 6-10 Model with wood X-bracing retrofitting	154
Figure 6-11 Shear stresses in x-y, y-z and x-z directions for the mosque after wood X-Bracing retrofitting	155
Figure 6-12 Model with wood x-Bracing and fixed wooden plate retrofitting	156
Figure 6-13 Shear stresses in x-y, y-z and x-z directions for the mosque wood X-bracing and fix plate retrofitting	157
Figure 6-14 Maximum top displacement for the model before and after the two methods of retrofitting	159
Figure 6-15 Walls numbering as used for the compression	160

ABBREVIATIONS

ADRS	Acceleration-Displacement Response Spectrum
ASCE	American Society of Civil Engineers
CQC	Complete Quadratic Combination
EMS	European Macroseismic Scale
Eurocode 6	European Standards - Bemessung und Konstruktion von Mauerwerksbauten
Eurocode 8	European Standards - Design of structures for earthquake resistance
FPA	Fiber -Reinforced Polymer
MM	Modified Mercalli scale
MSK	Medvedev-Sponheuer-Karnik scale
ÖNORM	Österreichisches Normungsinstitut
SDOF	Single-Degree Of-Freedom

ZUSAMMENFASSUNG

Die vorliegende Arbeit ist eine Untersuchung des Verhaltens eines vorhandenen Lehmbaus unter seismischen Effekten mit dem Ziel, eine Nachrüstungsmethode für eine historische Lehm-Moschee in der arabischen Golfregion zu entwickeln, die einfach umzusetzen ist und Erdbeben widerstehen kann.

Zunächst wird ein Überblick über die historische Nutzung von Schlamm und Lehm im Bauwesen sowie eine Übersicht über die chemischen Eigenschaften verschiedener Lehmarten gegeben.

Mittels Materialtests im Labor wurden die mechanischen Lehmeigenschaften gemessen und als Eingabeparameter für analytische und numerische Modellierungstechniken definiert.

Anschließend werden konkurrierende Standards seismischer Bauplanung verglichen. Entsprechend Euro-Code 8 erfolgte die Implementierung linearer und nicht-linearer Analysemethoden, um die Schubspannung und die Wandverformungen während eines Erdbebens zu bewerten.

Um den Erdbebeneinfluss auf die Lehm-Moschee zu spezifizieren, wurde zur Durchführung einer dynamischen Analyse eine Finite-Elemente-Methode in Verbindung mit dem Computerprogramm Solid Works (Version 2013) genutzt.

Abschließend werden Beispiele für Nachrüstungsverfahren präsentiert. Für die richtige Wahl zur Nachrüstung der Moschee wurden die Ergebnisse der statischen und dynamischen Analyse hinzugezogen. Ein Kreuzverband aus Holz in Verbindung mit einem festen hölzernen Rahmen stellt sich als das am besten geeignete Verfahren heraus, um den erhöhten Beanspruchungen standzuhalten und gleichzeitig den bestehenden architektonischen Stil zu ergänzen.

SUMMARY

This thesis is an investigation into the behaviour of existing clay buildings under seismic effects. The goal is to develop a retrofitting method for a historical clay mosque in the Arabic Gulf region which is simple to construct and will allow it to withstand an earthquake.

An overview is provided of the historical uses of mud and clay in construction, as well as an outline of the chemical properties of various kinds of clay.

Through material tests in the laboratory, the mechanical properties of clay are measured and defined as input parameters for analytical and numerical modelling techniques.

The competing standards for seismic building design are then compared. Following Euro code 8, linear and non-linear analysis methods are implemented to evaluate shear stress and wall deformation during an earthquake.

A finite element method is used in conjunction with the Solid Works computer program (Version 2013) to perform a dynamic analysis to specify the earthquake influence on the clay mosque.

Examples of retrofitting construction methods are presented, and the results of the static and dynamic analyses are used to determine the appropriate choice for retrofitting the mosque. A wooden cross-bracing technique in combination with a fixed wooden frame is found to best meet the stress requirements while complementing the existing architectural style.

1. STATEMENT OF THE PROBLEM

Mud is a low-cost, readily available construction material, usually manufactured by local communities. Mud structures are generally self-made, because the construction practice is simple and does not require additional energy resources. Worldwide, the use of adobe is mainly in rural areas, where houses are typically one storey, 3 m high, with wall thicknesses ranging from 0.25 m to 0.80 m. In parts of the Middle East, one finds that the roof of one house is used as the floor of the house above. Urban adobe houses are found in most developing countries.

Mud as a building material is soft and of low bearing capacity. In the event of an earthquake, these material properties turn out to be very unfavourable. Ground accelerations, such as those resulting from earthquakes, induce the mass of the massive adobe walls, high loads that are ablate by design. Due to the lower elastic modulus of clay, these constructions are more excited than those of stone. The low tensile strength and the absence of mud structural constructive elements, such as roof stiffeners, often lead directly to load loss and the collapse of the building.

Architectural characteristics are similar in most countries: rectangular plan, single door, and small lateral windows are predominant. Quality of construction in urban areas is generally superior to that in rural areas. Foundations, if present, are made of medium to large stones joined with mud or coarse mortar. Walls are made with adobe blocks joined with mud mortar. Sometimes straw or wheat husk is added to the soil used to make the blocks and mortar. The size of adobe blocks varies from region to region. In traditional constructions, wall thickness depends on regional weather conditions. Thus in coastal areas with a mild climate walls are thinner than in the cold highlands or in the hottest deserts. Roofs are made of wood joists (usually from locally available tree trunks) resting directly on the walls or supported inside indentations on top of the walls. Roof coverings may be corrugated zinc sheets or clay tiles, depending on the economic situation of the owner and the cultural inclinations of the region. However, most traditional adobe construction responds very poorly to earthquake ground shaking, suffering serious structural damage or collapse and causing a significant loss of life and property.

Adobe buildings are not safe in seismic areas because their walls are heavy and they have low strength and brittle behaviour. During strong earthquakes, due to their large mass, these structures develop high levels of seismic forces, which they are unable to resist, and therefore they fail abruptly. Typical modes of failure during earthquakes are severe cracking and disintegration of walls, separation of walls at the corners, and separation of roofs from the walls, which can lead to collapse. Seismic deficiencies characteristic of adobe construction are summarized in figure (1-1) below.

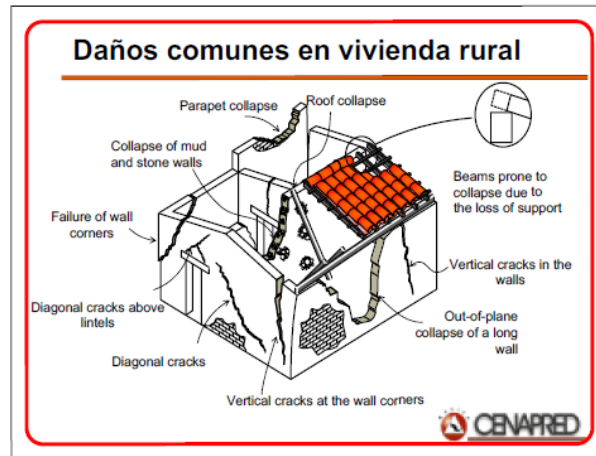


Figure 1-1 Typical modes of failure in adobe structures [1]

The carrying capacity of simple mud buildings is rarely documented in the literature. The application of standard design method to clay construction is not documented. A method for determining the compressive strength is provided. Further, the determination of mechanical properties such as modulus of elasticity, Poisson ratio, tensile strength and bending strength are not performed consistently. The haphazard approach taken by previous investigations into adobe masonry structures means few reliable conclusions about material properties can be drawn.

1.1 OBJECTIVES AND SCOPE

The aim of this dissertation is to estimate the seismic effect on existing historical mud buildings in the Arab world, especially in Gulf countries. Earthquake effects can be analysed through different mathematical methods according to international standards such as Eurocode 8 [2] and many others guidelines which take into consideration building behaviour during earthquake events.

A historical mud mosque has been chosen as the model to investigate seismic dangers and to develop a strengthening method to upgrade structural capacity during earthquake events. The mosque lies in a historical and tourist village called Hatta near Dubai.

Since very complex approaches are unsuitable for use in a historical mud building, opportunities are identified in this work to determine linear and non-linear structural behaviour with sufficient accuracy by means of simplified approaches. This is achieved on the basis of results of the material mechanical characteristics from experiments on the mud specimen and mud section walls.

In addition, a dynamic analysis has been performed using a finite element method and the Solid Works program (version 2013) [3] to deduce the dynamic behaviour of the building and compare it with other statics methods. Based on established design rules, an example of a clay house shows the design and method of retrofitting construction is developed.

1.2 THESIS ORGANIZATION

This work includes two areas of investigations: first, the determination of the carrying capacity of a mud specimen and mud wall section by identifying the mechanical characteristics; and, second, the implementation of a static and dynamic structural analysis of seismic effects.

The thesis is divided into seven chapters:

In Chapter 2, typical construction methods used in the Arab world are identified and classified. This classification of construction is the basis for further development of construction methods and construction techniques, with the aim of increasing carrying capacity during earthquakes. In addition, assessment methods for calculating earthquake loads are briefly presented and common linear and non-linear detection methods are introduced.

Chapter 3 describes the mechanical properties and the experimental arrangements of typical mud specimens and the clay wall sections.

Chapter 4 presents the experimental results and compares these with finite element values which have been obtained through numerical analysis by using a finite element program to deduce the max shear strength and deformation for the clay wall sections.

In Chapter 5, the mud building module is analysed using the four computational methods given by EN 1998 to determine the influence of the seismic effects. The analytic approach and numerical analysis are discussed and compared for earthquake influences such as shear forces and mud building deformation.

Chapter 6 illustrates a strengthening method for the mud building after determining the mechanical properties and the capacities of the mud material; this method is presented and analysed using finite element analysis. It provides a good retrofitting method against earthquake events.

Chapter 7 provides a summary, evaluates the results of the work for practical application and provides an outlook on open issues.

2. THE CURRENT STATE OF TECHNOLOGY AND LITERATURE REVIEW

Background

Mud is one of the oldest, most widely used building materials known to man. Among other things, it was used to insulate half-timbered houses. Because mud could historically be found in close proximity to settlements, about a third of all people in the world still live in mud buildings. Mud differs in its composition and its clay content depending on the source and the climate where it is found, and can be processed using very little energy. Mud is also of interest with regards to the environment, due to the ease and repeatability of recycling. The excellent absorption qualities of mud also facilitate an agreeable indoor climate due to absorption and discharge of air humidity.

2.1 HISTORY OF MUD BUILDING IN THE ARAB WORLD AND WORLDWIDE

Mud is one of the best-known and oldest building materials known to man. It has many advantages, including its texture and performance as a building material, but also some disadvantages which need to be taken into account [4]. The use of mud in construction varies greatly depending on the environmental conditions, such as climate and soil quality, availability and experience. Mud building has experienced renewed interest in recent times as a solution to problems in both industrialised and developing nations: these include problems with energy supply and pollution in the industrialised world and lack of housing and employment in the Third World.

Mud has been used as a building material in most countries of the world, principally in urban settlements near valleys, rivers and their subsidiaries, as well as mountainsides, oases and all areas with suitable ground.

Mud was used to a great extent in antiquity, in the cultures of Mesopotamia, Egypt and later by the Romans and the peoples of the Near East, in India and by the great Emperors of China. During the middle Ages many European buildings were made of mud, and it was frequently used by the Indians in North America and Mexico. This mud architecture was often employed by the peoples of Africa, including the Berbers, the Hausa and many other high cultures. The archaeological remains of many settlements in various regions of the

world are testament to the importance of mud. Most of these settlements were built with sun- and air-dried mud and not fired mud bricks; one example is the city of Jericho in Palestine, considered the oldest city in history.

The second half of the 20th century saw an unprecedented improvement in the production and development of modern building materials and in methods of transport and communication. As a result, many countries experienced a reduction in the use of traditional methods and materials for building. However, mud building survived in many cities and urban areas, particularly in developing countries and on the African continent, because of its numerous advantages, including wide availability of mud and low or very low price. In non-urban regions mud constructions are still the most common type of building; particularly in Asia, Africa and Latin America, but less so in Europe, North America and Australia. Currently, more than a third of the world's population live in mud buildings.

Arab countries contain the earliest and greatest amount of surviving historic evidence of mud building, as well as the first cities constructed completely with natural mud floors. Since the dawn of civilization, it is particularly this region of the world which has developed the concept of city architecture and its building arts through the use of mud building methods. Over the centuries people have developed and refined these methods to enable the construction of more complex building types, be they civilian, military or various types of luxury buildings.

Some of the most well-known examples are the Arab cities with imposing mud architecture: Shibam and Sa'ada in Yemen, Marrakech in Morocco, Adrar in Algeria, Ghadames in Libya and Aleppo in Syria. Some cities in Saudi Arabia, such as Hael, Najran, Hofuf, Dir'ya and Riyadh are further proof of the spread of mud building and the renewed rise of mud architecture over the last two or three decades (see Figure 2-1).

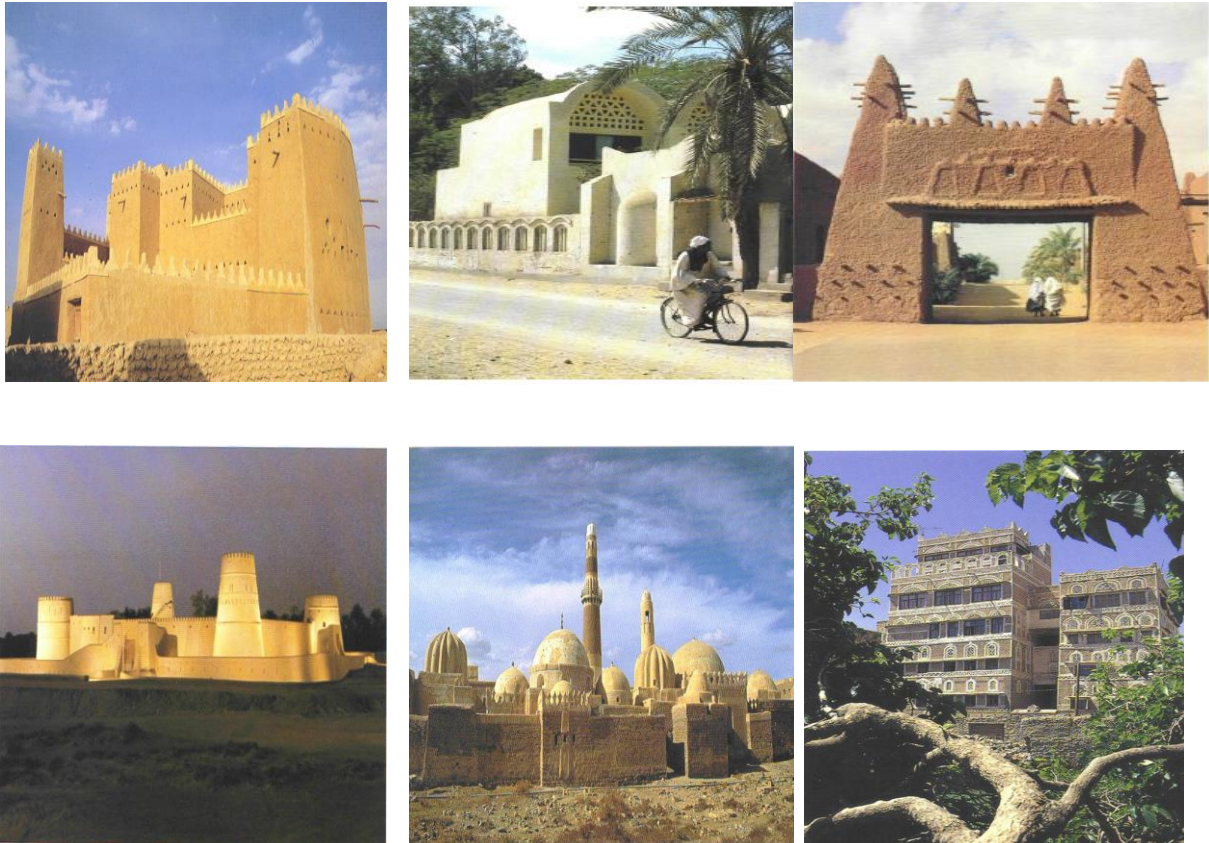


Figure 2-1 Examples of mud architecture in Arabic cities (Egypt, Saudi Arabia, Yemen, and Algeria)

2.1.1 Characteristics of Mud as a Building Material

There are numerous advantages to the use of mud, as shown by its deep connection to the history of human habitation on earth. A case for its continued use can be summarised in the following points:

Advantages of Mud as a Building Material:

- The existence of this material in the vicinity of most building sites makes it extremely cost-effective, mud being the only building material which is so widely available and free of cost. This makes large investments for the transport of modern building materials unnecessary, meaning less depletion of natural resources and reduced environmental pollution.
- Due to the simplicity of building with mud, which requires minimal use of machinery and simple tools, there is no need for special techniques. In addition, developing countries have high availability of unskilled labour and high unemployment rates.

Employing these workers in the building industry, will contribute to the development of the economy.

- The variety of mud building methods allows investors or employers to choose the method most suited to the region. Through the study of soil quality, employment of available inexpensive labour, and the use of existing building methods a unique local style can be developed, as shown through the mud brick architecture found around the world.
- Great savings can be made in the transport of materials, as transport is not necessary where mud is found on site. This is in contrast to more modern materials such as bricks, concrete, cement blocks, etc., which carry high costs of transport and loading at factories and also require storage on site. This presents particular difficulties in countries lacking in transport infrastructure, such as roads and waterways, as is the case in many developing countries.
- Savings can be made in energy consumption, whether during building, through the use of simple machinery with low energy needs, or through the use of solar energy in drying. The use of building designs which make use of the positive thermic properties of mud in reserving and conducting heat, and give the interior spaces effective protection against outer temperatures also increases energy efficiency. It is well-known and documented that mud buildings are cooler in summer and warmer in winter.
- Mud has technical properties related to sound insulation and fire safety which offer more privacy and resistance against the effects of fire, adding to the comfort and safety of the occupants.
- Mud is simple to recycle, re-use and dispose of. There is little waste or excess building materials resulting from the building and demolition process. Mud is recycled naturally, through environmental factors, such as wind, rain etc., and most

importantly without the use of toxic gases or chemicals or any other environmental pollution.

Disadvantages of Mud as a Building Material:

Despite the many positive qualities of mud as a building material, there is still substantial resistance to this material worldwide, due to a lack of information and a lack of optimal uses of this material and its by-products. Most of these negative qualities can be summed up as follows:

- Mud displays low resistance in the presence of water. Rain and flooding, or the capillary impact which allows water to penetrate into mud, represents one of the most important causes of damage and the subsequent rapid collapse of mud buildings. Furthermore, the absorption of water by the roof leads to an increase in the loads on the supporting structures. This can cause support failure in the mud and lead to building collapse. Another problem is the evaporation of ground water, which leads to salt deposits on the surface of the material and contributes to weaknesses and a decrease in the strength of the mud.
- The relative weakness of mud in terms of carrying weight has led to a reduction of its use in heavy roof constructions and the bracings supporting them. Mud also has relatively low resistance to tension and shear forces, making its use in earthquake-threatened areas limited or nearly impossible. The use of mud for constructions with bending moment demands, such as bridges and roofs, is also very limited to impossible. For this reason, mud has in the past been limited to walls and as filler material in ceilings where it will only be subject to compression force, such as cupolas and cellar arches.
- The volumetric changes in mud, particularly mud with a high silt content, leads to cracking when subjected to cycles of varying weather influences, such as humidity and dryness. This can make the plastering of surfaces impossible, and is clearly observable in the style of construction (Madmak).

- The surfaces of mud buildings erode at a significantly high rate under various environmental effects, such as wind, sandstorms and corrosion, resulting in weaknesses and low durability of this building material, and leads to frequent and recurring maintenance. This is particularly true in countries with heavy rainfall, where the owners re-surface and renovate the buildings every year after the rainy season.
- The joints between mud and other building materials are so weak that it is difficult to construct with windows, doors, and other details, requiring particularly good architectonic detail solutions.
- The properties of mud make it easy for rodents and insects to find shelter. The cracks resulting in mud and its good thermic qualities make it attractive for rodents and insects to inhabit and reproduce, leading to documented negative effects on the bearing capacity and damage to mud structures, as well as the health of the occupant.

2.1.2 Techniques for the Use of Mud as a Building Material

There are many mud building methods and techniques from past and present. The student of mud architecture can count more than 15 widespread building techniques using this material.

Many methods and techniques can be derived and adapted depending on whether they are used for the entire building or only isolated parts. Construction of mud walls is generally based on the choice of suitable soil, which is mixed with the correct amount of water, forming a solid mass suitable for the chosen building type and construction. In this way, the essential bonding is created in the mud mixture and dries either through the evaporation of the existing water from this mixture, or with the help of the sun and/or air. Another way of creating bonding using mud and water is mixing and pressing them together in a special mould using external pressure, as seen in the Rammed Earth method.

The most famous mud building techniques:

- plaster, as found in Hadramaut, Yemen
- Madamik, as found in Asir, Saudi Arabia
- tamped mud bricks, as found in Morocco
- modern bricks, as in the case of many modern companies and projects
- the use of hand-pressing equipment in the production of air-dried mud bricks (e.g. in Mali)
- the use of modern machinery in the production of mud bricks in commercial quantities in North America

The construction methods can be briefly described as follows:

1. Building with air-dried mud bricks (adobe);

This mud building method is very widespread in the Arab World, most of all in Egypt, Iraq, and Yemen, as well as the regions of Nedsched and Al Ahseer in Saudi Arabia. In the past, these mud bricks were prepared by mixing soil containing a great amount of silt with chopped straw. The mixing is achieved through heavy stamping by man or animals, such as oxen or cows. A brick shape is created through the use of an open wooden mould. The volume and size of the moulds varies by region. The mould is laid on the ground and pressed down to ensure a homogenous mud mixture without any air bubbles.

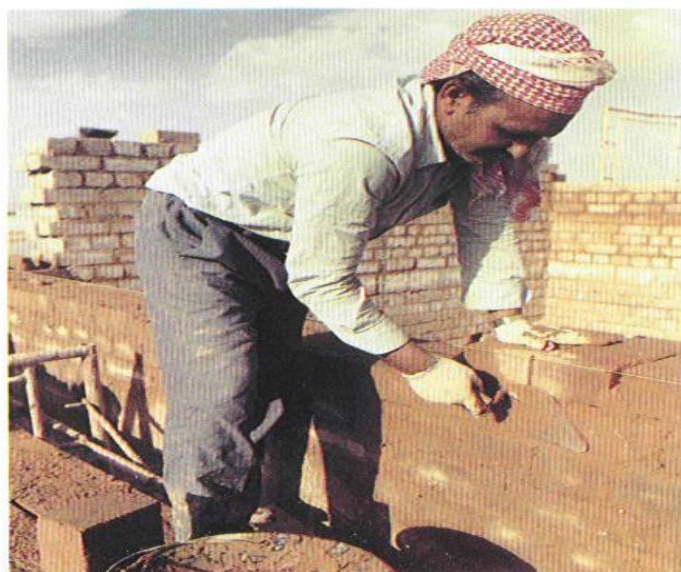


Figure 2-2 building with air-dried mud bricks

The wooden mould is then removed and the mud mass stays on the ground to dry for several days. The mud bricks are lined up with small gaps between them, to allow them to dry in the sunlight and to make it possible to turn them on their sides, encouraging air flow and completing the drying process (Figure 2-2). This method is still the most widely used.

2. Building with mud bricks (cob)

This method of mud building is used in the Arab world, in the Saada region in Yemen, and also Hael and Asir in Saudi Arabia. This building method is largely the same as that of the air-dried mud bricks: the mud preparation and mixing methods are the same, but additional amounts of hay are added in order to avoid the cracks which are created during the drying process. The hay binds the mixture together with a degree of plasticity in order to increase resistance against rainwater. The mass is then cut into spheres and shaped by hand into bricks. Through this process, the builder becomes very familiar with the handling of the mud. The mud bricks are lined up in a row with a height for the row of around 30 cm. Two days are left for drying before building begins on the next row. Despite the strength and stability which it lent buildings in the past, this method no longer plays a significant role.

3. Building with tamped mud bricks (rammed earth)

This building method has spread in the Arab world, focused mainly in Maghreb, which comprises Tunisia, Algeria and the Kingdom of Morocco. Unlike the methods previously described, about 10% volume of water is added to the mixture, providing a moisture base, plasticity and firmness. The mud is laid in forms similar to the mould used with reinforced concrete, which gives the walls shape. The mixture is shaken with compressors and wooden instruments, or simply using hand-held instruments, as is often the case in developing countries. After filling the mould with the tamped mud mass, it is moved horizontally until a complete layer is achieved. The wooden mould is then lifted upwards in order to begin the next rows and layers and so on, until roof level is reached.

4. Building with stabilized earth blocks (more stable earth blocks)

This expanded version of the tamped mud building method was first developed after the Second World War. This method combines the mud brick method with tamped mud method, but is considered a very modern method, and is used only in certain countries, and in specific projects, for example in Egypt, Morocco, Yemen and Saudi Arabia. Using this method, suitable mud is mixed thoroughly and improved with certain additives, such as cement, bitumen, or lime, in order to increase water resistance. After that, the mixture is tamped in the same way as the tamped mud bricks. It is pressed into moulds and then the tamped bricks are removed and used like conventional bricks. A number of simple machines and a compressor have been developed for the mixing and tamping.

2.2 CURRENTLY AVAILABLE CALCULATION METHODS FOR THE ASSESSMENT OF EARTHQUAKE LOADS

2.2.1 Earthquake Effects and Structure Behaviour

Causes of Earthquakes

Earthquakes are caused by ground movements, most commonly as tectonic quakes brought on by shifts in the fracture joints of the lithosphere.

The particular plate boundaries where these shifts take place can move away from each other (spreading zones), toward each other (collision zones) or past each other (transform faults). When the plates get locked or cant against each other, pressure and stresses builds up in the bedrock. If the shear strength of the bedrock is then exceeded, these tensions are released as sudden movements of the earth's crust, resulting in a tectonic earthquake. Since the built-up tension stresses are not limited to the immediate surroundings of the plate boundaries, the resulting release of tension can, in some rare cases, also occur in the inside of the plate, if the crustal rocks have a weakness zone. Figure (2-3)

Earthquakes usually consist of a series of quakes. These are referred to as pre-shock and aftershock, in relation to the stronger main quake [5].

Further Causes of earthquakes:

- volcanic activity
- artificial influences e.g. extraction of raw materials/mineral oil
- collapse of underground cavities in the mining industry
- submarine landslides

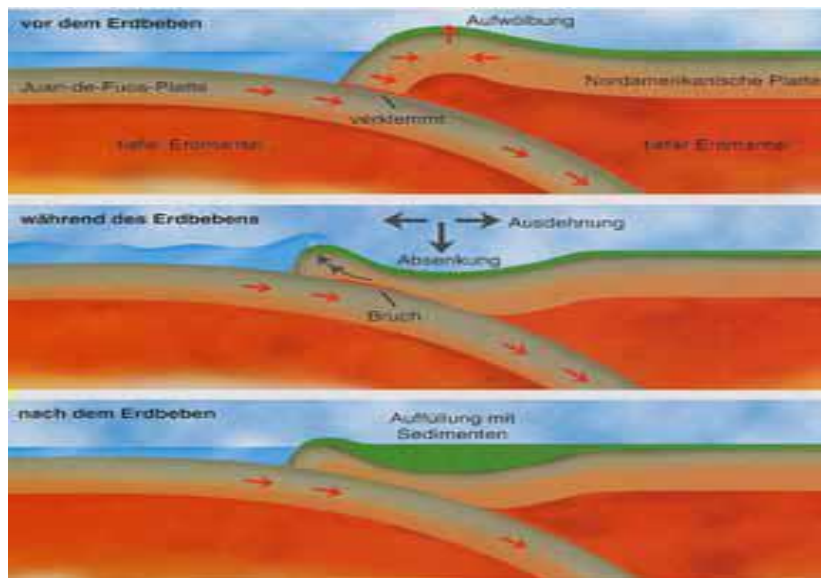


Figure 2-3 Collision mechanism of plate tectonics

Seismic Waves

Earthquake waves or seismic waves are caused by an epicenter process, and as a rule, spread out in a radial formation in the interior of the earth. These waves are absorbed, refracted and also reflected on their way into the earth. The speed at which they diffuse is dependent on the manner in which and the material through which these waves travel. For both earthquakes (seismology) or waves resulting from explosions or vibrations (artificial), the manner in which these waves course through the earth is particularly dependent on material properties.

There are several categories of waves, figure (2-4):

- Longitudinal waves: P waves or primary waves are so-called compaction waves, also called compression waves. Vibrating in the direction in which they diffuse, they pass through gases, liquids and solids. Acoustic waves or sound waves are a well-known

example of compression waves in the air. P waves can diffuse not only in solid rock, but also in liquids such as water and the quasi-liquid parts of the earth's interior. The particles in the earth are pushed and pulled in the same manner as acoustic waves; the movement occurs in the direction of travel of the wave.

- Transversal waves: the S wave or secondary wave moves transversely to the direction of travel. S waves can only travel through solids. They cannot travel in liquids or gases, as these have no (or only a nominal) shear resistance. Liquid areas of the interior of the earth can be recognised by the lack of S waves.
- Love waves: the highest speed surface waves. They travel with a speed of approximately 2000 - 4400 m/s but are slower than S waves.
- Rayleigh waves: these roll similarly to ocean waves in a retrograde elliptical movement, that is, the rolling movement occurs transversely to the direction of travel. An up-and-down as well as a back-and-forth movement of the ground is created. The speed of travel is approximately 2000-4000 m/s. It is usually the Rayleigh waves which can be felt in an earthquake. The amplitudes are much greater than those of the other waves and apply their destructive effect in the form of earthquakes.

A differentiation is made between body waves (P-and S waves) and surface waves (Love and Rayleigh waves). Primary waves diffuse faster than secondary waves (S waves). Due to this, in the event of an earthquake P waves are recorded first, with S waves being detected later. The time differential between the P and S waves can be used to calculate the distance to the epicentre.

If it is possible to measure the distance to the epicentre and the direction of the waves from at least three different locations, the epicentre can be measured with a relatively high degree of accuracy.

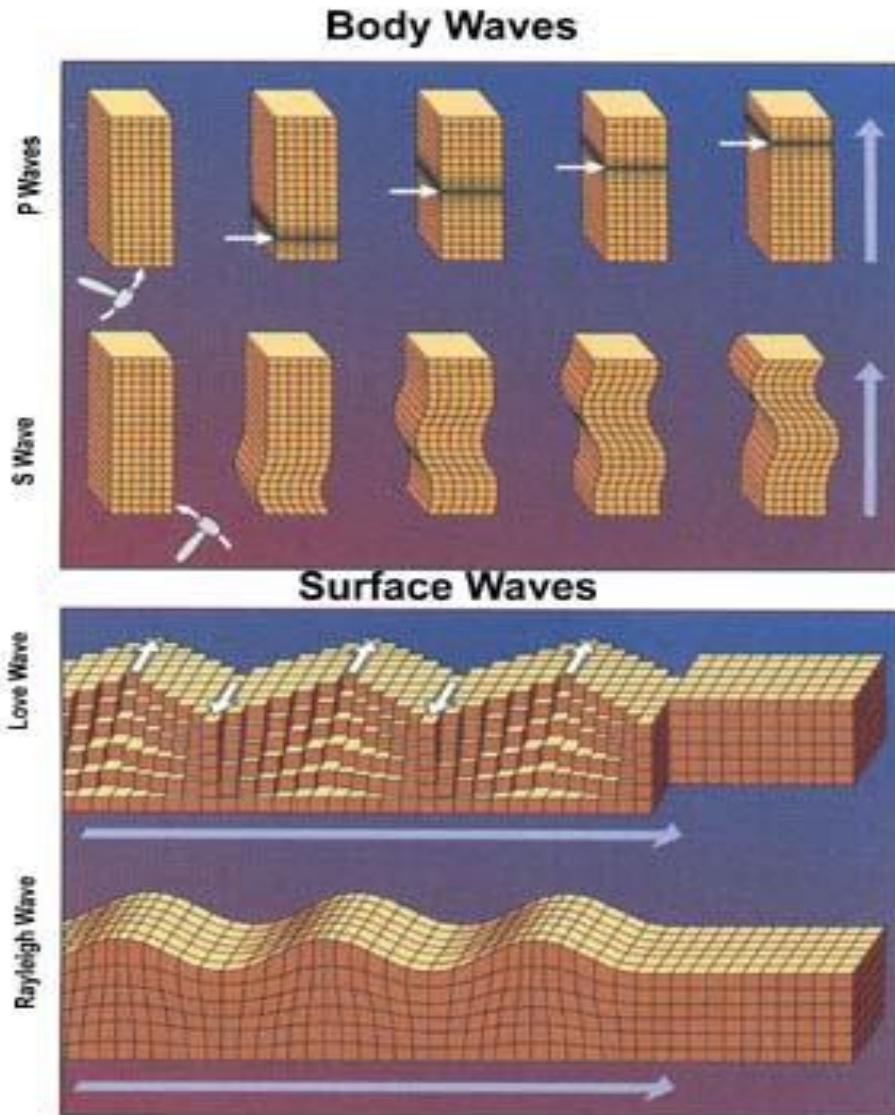


Figure 2-4 various types of earthquake waves

Earthquake Parameters

1. Magnitude

The measure of the strength of an earthquake is its magnitude (M). M is the description for the released wave energy (E), which is described for an earthquake event.

The definition is:

$$M = \frac{2}{3}(\lg E - 4.8) \quad 2-1$$

During an earthquake, the maximum measured speed of earthquake waves can be found by measuring the resultant magnitudes:

- The duration magnitude (M_d) describes aftershocks in the case of an epicentre at a distance of approximately 500 km.

- The surface wave magnitude (M_s) describes the maximum value of surface wave speed.
- The body wave magnitude (M_b) describes the maximum value of body wave speed.

When using the logarithmic magnitude scale, a difference of one level is equivalent to a factor $f = 10^{1.5} = 32$ times greater amount of released energy. The empirical correlations describe the difference between magnitude and size of the epicentres and dislocations.

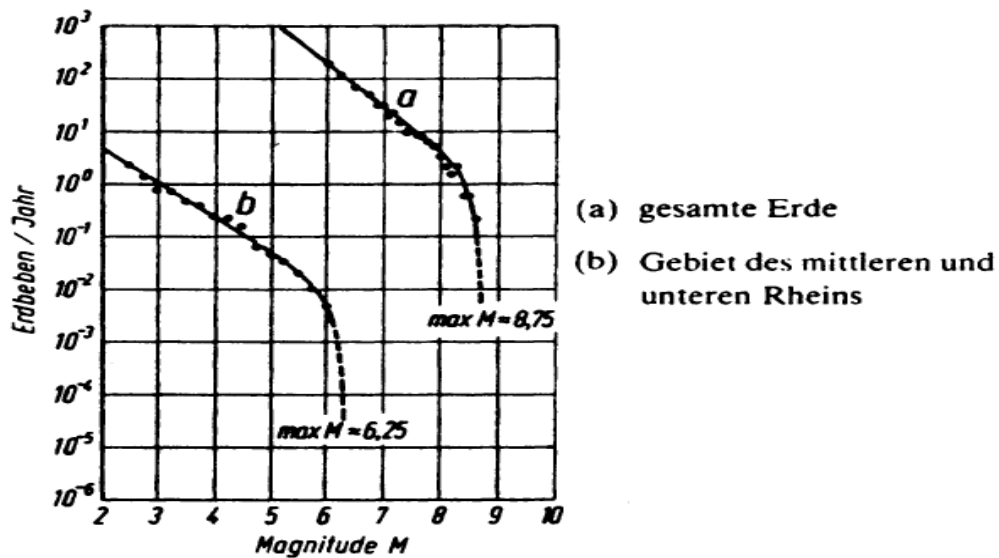


Figure 2-5 Dependency of the expected magnitude on the recurrence period for various regions

Maximum magnitudes are theoretically limited by the size of the fracture surface hardness of the rock and are about 9.0. The graphic visualisation below shows conditional probability occurrence and return periods of reference of the expected magnitudes in the central area and the Rhein respectively, as well as those for the entire earth , as explained in Figure (2-5) above.

The oldest and best known magnitude scale is the one developed by C. F. Richter. The relation between the maximum amplitude on the seismogram and the distance from the epicentre was recognised by Richter and derived from the decay behaviour of the amplitude of the earthquake. A ten-fold increase in amplitude is equivalent to one level of magnitude as illustrates in Figure (2-6).

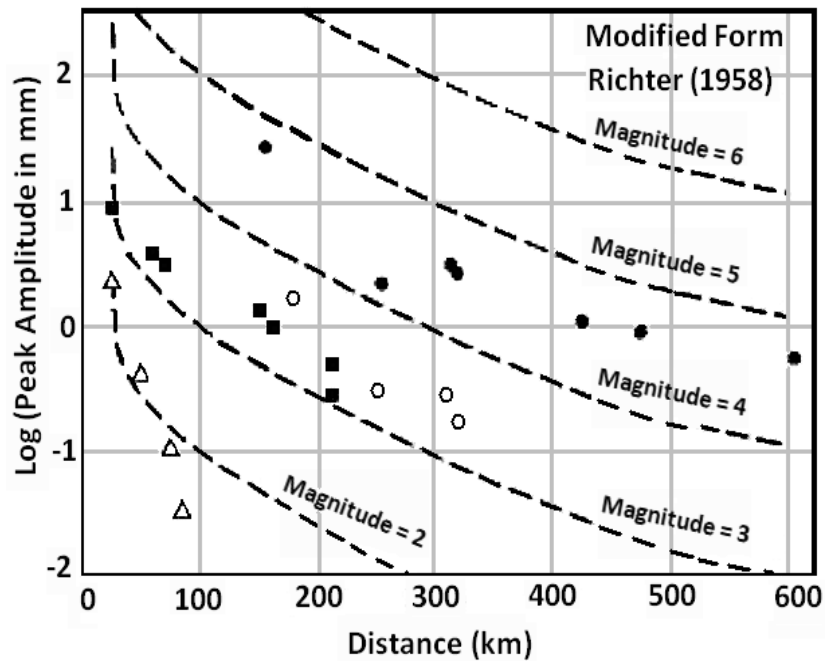


Figure 2-6 Scale of magnitude according to Richter

However, in order to assess and judge the degree of damage to buildings in certain locations, knowing the magnitude of the earthquake alone is not enough.

The transmission value of the waves caused by an earthquake, together with the distance to the epicentre gives information regarding the degree of damage. This is the reason the concept of earthquake intensity was introduced.

2. Intensity

Intensity is a measure of earthquake strength. In contrast to the magnitude, which is determined instrumentally, the intensity determines the effect of an earthquake on the landscape, streets and buildings. Earthquake intensity can be perceived with or without instruments (macroseismics). An earthquake, categorised by scale, can exhibit a different degree of intensity at different locations, depending on circumstances. Numerous scales exist, including the Modified Mercalli scale (MM), the Medvedev-Sponheuer-Karnik scale (MSK 64) and the current European Macroseismic Scale (EMS 1992). This last scale can be understood as follows:

Table 2-1 Abbreviated European Intensity Scale EMS 1992

EMS-Intensity	Definition	Description of Maximum Effect
I	Not felt	Not felt
II	Scarcely felt	Felt only by very few individual people at rest in houses.
III	Weak	Felt indoors by a few people. People at rest feel a swaying or light trembling
IV	Largely observed	Felt indoors by many people, outdoors by very few. A few people are awakened. Windows, doors and dishes rattle.
V	Strong	Felt indoors by most, outdoors by few. Many sleeping people awake. A few are frightened. Buildings tremble throughout. Hanging objects swing considerably. Small objects are shifted. Doors and windows swing open or shut.
VI	Slightly damaging	Many people are frightened and run outdoors. Some objects fall. Many houses suffer slight non-structural damage like hair-line cracks and fall of small pieces of plaster.
VII	Damaging	Most people are frightened and run outdoors. Furniture is shifted and objects fall from shelves in large numbers. Many well-built ordinary buildings suffer moderate damage: small cracks in walls, fall of plaster, parts of chimneys fall down; older buildings may show large cracks in walls and failure of fill-in walls.
VIII	Heavily damaging	Many people find it difficult to stand. Many houses have large cracks in walls. A few well-built ordinary buildings show serious failure of walls, while weak older structures may collapse.
IX	Destructive	General panic. Many weak structures collapse. Even well-built ordinary buildings show very heavy damage: serious failure of walls and partial structural failure.
X	Very destructive	Many ordinary well-built buildings collapse.
XI	Devastating	Most ordinary well-built buildings collapse; even some with good earthquake resistant design are destroyed.
XII	Completely devastating	Almost all buildings are destroyed.

The entries between I (earthquakes cannot be felt at this location) and XII (totally devastating) are derived and annotated in the classical sense, which is to be defined and understood subjectively.

There is more than one empirical relationship between epicentre intensity I_0 and the magnitude M and depth of epicentre. When epicentre depth, h , is less than 50 km the following correlation on the European scale can be made, according to Müller-Keintzel [6].

$$M = 0.5 \cdot I_0 + \lg h + 0.35$$

2-2

The range of variation in the correlations is generally too large to describe.

Ground Motion Characteristics:

Ground displacements can be caused by movement and activity at ground level during an earthquake. These are expressed in terms of acceleration and velocity. Usually only the acceleration of the ground is considered, as the displacements and velocity can be calculated through the simple integration of the acceleration time history. Over time a series of parameters are described. These are maximum value a_0 , frequency distribution of the excitation and time history. These serve to quantify the effect of the ground movement on buildings through the course of an earthquake. Normally the description of this effect is achieved with the help of the response spectrum. Following this method in the frequency range, the information regarding the size of the time history is lost, because the highest extreme value is indicated once.

The ground moves in all three spatial dimensions during an earthquake. When conducting a building assessment, it is necessary to take into account the resulting dynamic forces in all three dimensions. As the contingency reserves of structures based mainly on vertical loads are sufficiently great, the intensity of vertical movement for conventional constructions can be ignored. The shear stress of unreinforced masonry is the exception here; the shear stress must be reduced through the increase or reduction of the normal pressure forces and the resulting stresses.

Horizontal ground acceleration a_0 (greatest value) can be determined with the help of the empirical relationships with the intensity, I (example according to Müller-Keintzel).

$$I = b \cdot \lg(a_0) + c \qquad 2-3$$

Through the parameters $b = 2.0-3.0$ and $c = 1.5-2.7$.

Earthquake Duration:

Earthquake duration depends on the type and size of the fracture process and subsurface. In case of strong earthquake shaking, the duration can be from several seconds (at about magnitude 6) up to 3 min (at magnitude 9.5). The duration of the quakes and the movements have a great effect on the extent of damage.

In cases of equal distance to the epicentre, sites with soft, flat layers of sediment tend towards considerably longer quake duration than sites with rocky subsoil.

Starting with a magnitude of 7.5 (a so-called strong quake), the maximum values of ground movement barely increase. However, the duration of intense ground movement increases due to the longer epicentre time function.

The duration between exceeding the first and last acceleration threshold was defined by some researcher with a value of 0.05 *g*. Another definition of duration (Trifunac and Brady, 1975) [7] also takes into consideration the time between reaching 5% and 95% of the total energy at a site. In a preliminary definition from National Application Documents of the ENV 1998, the minimum duration of the stationary part of the acceleration time history was suggested as T_s .

In the case of enduring intense ground movement, the resulting correlation is dependent on the total intensity *I*, which is described as the area under the squared acceleration seismogram.

$$I = \int_0^{T_s} [a(t)]^2 \cdot dt \quad 2-4$$

A modification of the equation is equal to the *rms* acceleration,

$$a_{rms} = \sqrt{\frac{1}{T_s} \cdot \int_0^{T_s} [a(t)]^2 \cdot dt} \quad 2-5$$

Where:

- T_s is the duration of the shock and
- (a_{rms}) is mean square acceleration.

Numerous experiments are necessary in order to determine the real seismic design load.

2.2.2 Calculation Methods of the Seismic Effect According to EC 8:

There are a number of methods for calculating the stresses that structures are subjected to during earthquakes. In order to calculate the seismic effects of unreinforced masonry structures, four calculation methods are presented:

- the equivalent lateral force method
- the response spectrum method
- the non-linear static calculation method (the pushover method)
- the non-linear dynamic calculation method

The vibration of a building by rapid ground movements is dependent on its dynamic properties. The stresses and deformations generated in the structure are determined by simplified calculation methods.

Proof of an earthquake can be achieved independently of the chosen calculation method, under various safety requirements. Most European guidelines and standards are based on the safety requirements of the Ultimate Limit State. In order to exclude the possibility of a structural collapse, minimisation of the threat to life and limb underlies the ultimate limit state.

The Equivalent Lateral Force Method

This is currently the most useful method for earthquake norms. The dynamic earthquake effects are replaced by static equivalent lateral forces. These create stresses of a similar magnitude in the structure as the maximum created during the duration of an earthquake. Every structure is considered separately in both directions. Fundamental oscillation in the form of a multi mass oscillator is defined for each main direction for an equivalent bar; figure (2-7). The maximum value is read off a norm response spectrum at the corresponding fundamental frequency. The higher natural vibrations and the vertical excitation are neglected [8].

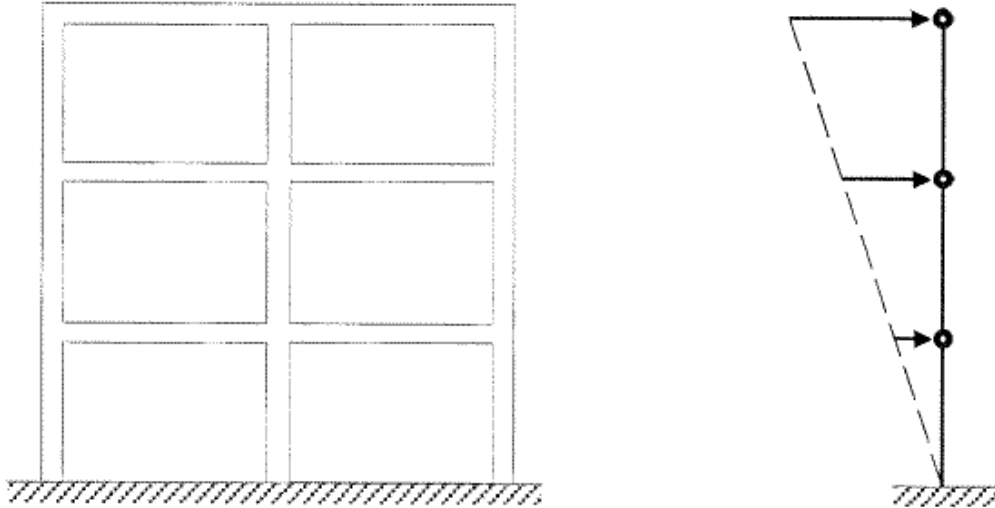


Figure 2-7 Equivalent lateral force method: Structure (left) and lateral bar with equivalent lateral forces (right)

In order to determine the equivalent lateral forces, usually the whole masses are used instead of the effective modal masses of the fundamental vibration mode. These simplifications serve to partially compensate for the neglected effects such as increasing the influence of higher natural vibrations. For the distribution of equivalent lateral forces over the height of a structure, the fundamental vibration mode is often approximated as a linear relation; Figure (2-7). The influence of non-linear plastic material behaviour is ascertained through a reduction factor. Non-linear behaviour (e.g. crack formation, plasticization), can also be taken into account by employing reduced average values in the determination of a fundamental frequency.

The equivalent lateral force method is described as the “Simplified Response Spectrum Method” and the reduction factor as “behaviour factor q ” [EC 8-1-2].

Response Spectrum Method

The Response Spectrum Method is a linear dynamic method for determining the maximum response during the excitation of the time history. It is based on this that the damping of a multi-mass oscillator can be transferred, as predicted, to be transmitted through

transformed variables on modal coordinates into a separate single-degree system. Every decoupled single-mass oscillator is equivalent to a natural vibration mode of a multi-mass oscillator in its original form.

The determination of an earthquake excitation via the response spectrum can be described through the maximum values of the individual natural vibration modes. The maximum values of the individual vibration modes, together with the upper limit for the response of a whole system, form the sum of the absolute values.

The squares root of sum squares is an approximate method for combining modal responses. In this method, the squares of a specific response are summed (e.g., displacement, drift, story/base shear, story/base overturning moments, elemental forces, etc.) The square root of this sum is taken to be the combined effect.

In the case of coupled vibrations of similar value, natural frequencies, it can be assumed that more complicated superposition rules are required. This is called Complete Quadratic Combination (CQC). If the linear dynamic behaviour of irregular structures through the response spectrum method allows, CQC should be calculated using a two-dimensional model (or three-dimensional if higher natural vibration forms must be considered) [9].

Thus earthquake excitation, in the form of response spectra, can occur in all three directions at the same time.

The equivalent force method is only an approximation if, for illustrative purposes, through a flat reduction factor, the non-linear behaviour is frequency-dependent, i.e. different from the individual mode shapes which can be detected.

The initial stiffness may provide another way of taking of non-linear behaviour into account, i.e. the tangent stiffness at zero deformation, the secant stiffness in the expected level of deformation can be used. This is also possible with the equivalent lateral force method as illustrates in Figure (2-8) [10].

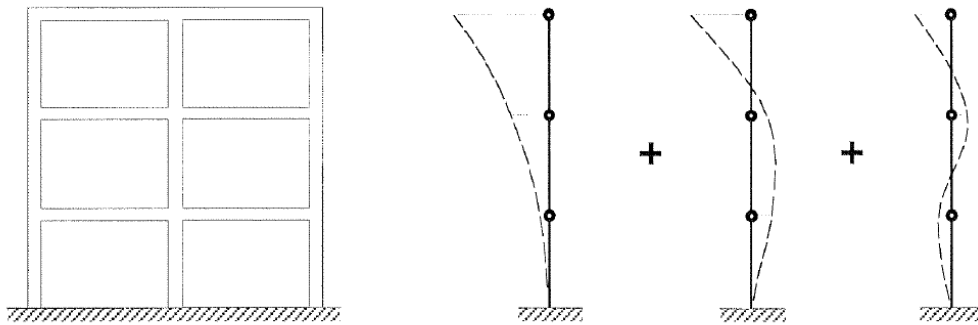


Figure 2-8 Response spectra method: structure (left) and the deformation parts out of the three horizontal natural vibration forms (right)

Non-linear Static Calculation Method

The force-deformation behaviour of a structure is defined through consideration of the plastic deformations in the non-linear static calculation.

The upper storey of a structure (the roof level) is typically the equivalent lateral displacement in the function of the total equivalent lateral forces, the so-called pushover curve, which is calculated step-by-step to the point of failure [11].

Linearly approximated in the equivalent lateral force method, this is the most common distribution of the individual equivalent lateral forces (F), which are distributed over the height of the structure based on its fundamental shape (Figure.2-9). With the influence of higher natural vibrations, it is possible to detect the pushover curve. A non-linear static calculation makes it possible to define the self-adjusting plasticity mechanism and to calculate the local displacement demand of the plastic zones for a given global displacement with a degree of accuracy.

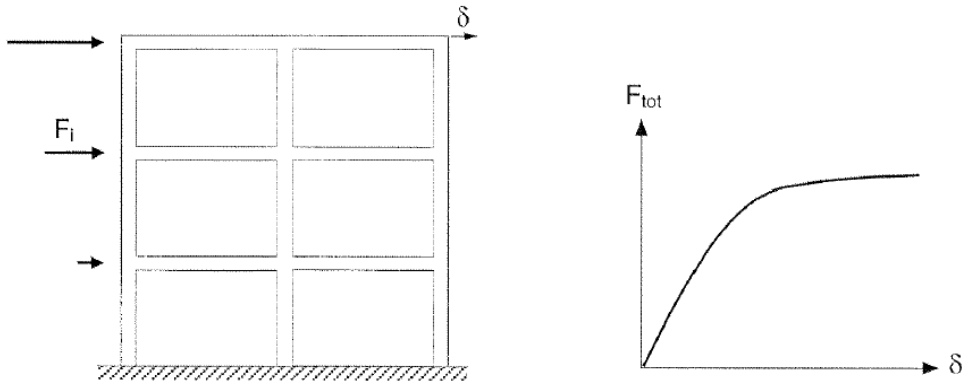


Figure 2-9 Non-linear static calculation: structure with horizontal equivalent lateral forces F_i (left) and horizontal force – displacement curve (pushover curve) (right)

The capacity spectrum method is a particularly descriptive method of non-linear statistical calculation; here the capacity of horizontal forces persists with the corresponding demand of a design spectrum, which can be compared graphically with each other [12][13]. Here the pushover curve is transformed from a force-deformation curve into an acceleration-displacement curve (A-D curve) by considering the dynamic properties of the structure.

With a certain viscous damping and the elastic design spectrum described as a demand curve, these can also be recorded into the acceleration-displacement graph, so that the corresponding spectral values can be plotted into the same A-D co-ordinate system (Figure 2-10). The design point is the intersection of the demand curve and the capacity curve.

The required value of the design spectrum (demand) is achieved by the presence of non-linear deformation capacity (capacity) under its mono-directional static load stresses.

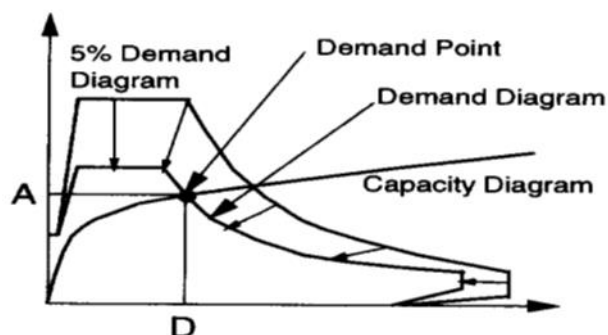


Figure 2-10 Capacity spectrum method: acceleration-displacement diagram of the structure (capacity curve) and the assessment spectrum (demand spectrum)

Applying the design spectrum for higher damping rates for elastic response spectra than the established standards common value of 5% of the equivalent viscous damping of the demand curve is very controversial.

Non-linear Dynamic Calculation Method

In the non-linear dynamic calculation method, a structure can be analysed through a single- or multi-mass oscillator. Numerical integration and the related systems of non-linear movement equations over the duration of the earthquake excitation are illustrated per time step [14].

The calculation is normally carried out using the method of finite elements [15]. Two different algorithms for time integration are applied: the implicit and explicit methods of central differences. The performance of modern computers allows a finer degree of detail in modelling with regards to geometry and material behaviour, but the boundaries of the highly complex work of the creation of numerical models and the interpretation of the extensive results are quickly reached.

Comparison of Calculation Methods

Following Bachmann 95 [8], the most important indicators of the four assessment methods discussed above are listed in the table (2-2).

The response spectrum method and the non-linear static calculation method are limited methods due to the number of assumptions. The fields of application of the equivalent lateral force method are also not widespread, as non-linear dynamic calculation method demonstrates a very powerful method.

Table 2-2 Comparison of the essential characteristics of the calculation methods

	Equivalent Lateral Force Method	Response Spectra Method	Non-linear Static Calculation	Non-linear Dynamic Calculation
Dynamic model	linear single-mass oscillator	linear multi-mass oscillator	non-linear single-mass oscillator	non-linear multi-mass oscillator
Geometric model	two-dimensional	two-or three-dimensional	two-dimensional	two- or three-dimensional
Material model	linear	linear	non-linear	non-linear
Damping model	viscous	viscous	viscous	viscous and hysterical
Taking into account natural vibration modes	only fundamental vibration mode	fundamental vibration and higher natural vibration modes	only natural vibration mode	N/A
Taking into account torsion	enlargement factor	linear	Increasing factor	non-linear
Taking into account material non-linearities	overall application of a reduction factor	overall application of a reduction factor	non-linear material model	non-linear material model
Earthquake excitation	response spectrum	response spectrum	response spectrum	time history
Magnitude of findings	shear forces and deformations	shear forces and deformations	local ductility demand: shear forces and deformations	local ductility demand: shear forces and deformations
Limitation in the field of use	regular structures	all structures	fundamental vibration mode dominates	proof of important structures; recalculation of results of experiments
Typical application	assessment	assessment	recalculation of existing structures	very large
Amount of effort required calculation	small	average	large	very large

2.3 THE STATE OF CURRENT RESEARCH

Many construction techniques using clay as the main material are employed throughout the world. The most common are adobe and rammed earth.

Extensive research has been carried out during the last decades in universities and building research stations in many parts of the world on the behaviour of earthen buildings under earthquake action and the way structures can be designed and strengthening to resist it.

As investigations through the current research regarding the clay properties, many experiments has been carried out with different type of clay specimens such as clay bricks, clay wall sections in order to determine the maximum compressive strength ,flexural bending strength and shear strength as well as the determination of the elasticity module. Jeanette Gasparini [16] investigated in her dissertation the behaviour of clay material in the location of Oaxaca, Mexico, figure (2-11). The experiments results on adobe wall section showed a mean compressive strength is 2.14 N / mm^2



Figure 2-11 Compression strength test by Jeanette Gasparini

While the shear strength has been evaluated with different mathematical approach such as ; according to MANN, MÜLLER [17] as 0.11 N/mm^2 and through the mathematical evaluation of BERNADINI, MODENA, TURNSÊK, VESCOVI [18] as 0.116 N/mm^2 as well as through GHANEM, ABU-EL-MAGD, HOSNY [19] evaluation as 0.074 N/mm^2 . Many other literature and the research results regarding the clay mechanical properties are presented in section 3.3.

Also through Jeanette's work; a recommendation for a retrofitting method has been analysed and developed by strengthen the Bed joint of the clay structure using sisal rope,

figure (2-12). The strengthening method has analyzed on a design model using finite element method to distinguish the ability of applying this method under the seismic effect.

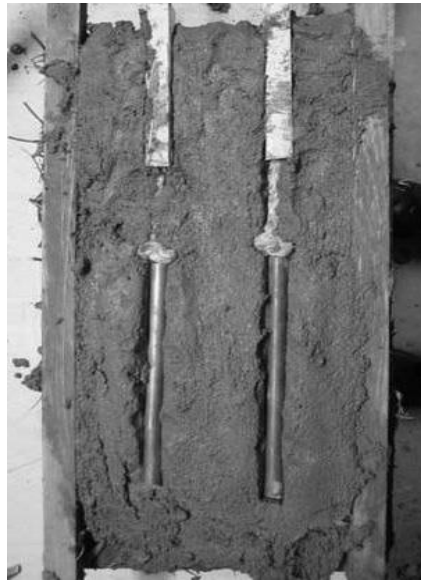


Figure 2-12 specimen of Adobe-masonry strengthen with sisal rope at the mortar joint [16]

Many retrofitting methods using different technics have been developed on the existing clay building in order to upgrade its capacity against earthquake violation.

The researchers at the Catholic University of Peru have attempted to find solutions for improving the seismic performance of clay buildings. One of the method that presented by Marcial Blondet and Rafael Aguilar [20] of the existing building is by using of External cane mesh reinforcement. This technique consists of nailing wire mesh bands against the adobe walls and then covering them with cement mortar. The mesh is placed in horizontal and vertical strips, following a layout similar to that of beams and columns as illustrates in Figure (2-13).



Figure 2-13 External wire mesh reinforcement introduced by Marcial and Rafael

Blondet [21] at university of Peru introduced many study to evaluate the possibility of using polymer mesh to reinforce clay buildings. Several similar full-scale adobe housing models with different amounts and types of polymer mesh were tested through shaking table test; figure (2-14). The reinforcement provided consisted of bands of polymer mesh tied to both sides of the walls with plastic string threaded through the walls. The results showed that; although the adobe walls suffered some damage, collapse was avoided. It has been proved that the amount and spread of damage on the adobe walls increased as the quantity of polymer mesh reinforcement decreased.



Figure 2-14 External geogrid mesh reinforcement

3. MATERIAL PROPERTIES

Introduction

Clay has been used since early history as a building material. The use of the material is varied; it is found in masonry walls and fortress construction, as well as an infill in wooden or grout of braids, or mortar, plaster, screed and furnace construction [22] (Figure 3-1).



Figure 3-1 Example of a modern earthen structure in Riyadh, Saudi Arabia [23]

In addition to its good structural properties, clay is available almost everywhere on earth and requires little transportation effort. However, clays differ in their individual composition, which can be problematic. Early knowledge of clay was passed down as traditional knowledge in each respective region; therefore, it was not necessary to check the composition or mechanical properties of clay from different regions.

In addition to the use of clay in old and historical buildings, today we also consider mud as a building material, especially for renovations and use in new buildings. Therefore it is necessary for engineers and architects to acquire practical knowledge of clay as a building material and in order to avoid damages. Furthermore it is important to pay attention to mud's behaviour in combination with other building materials.

3.1 SELECTIONS OF MUD BUILDING MATERIALS

General properties of clay

Clay is formed by the weathering of rock strata, which can be caused by different processes. Mechanical operations as well as exposure to water, wind and temperature differences can all be responsible for resulting the clay. Clays are divided into different categories, depending on locality. Table 3-1

Table 3-1 Different types of clay according to [24]

Mountain Clay	Stored on or underneath the rocks from which it was formed by weathering. The mineral skeleton consists mainly of angular rock debris of various grains.
Boulder Clay	Displaced by glacial clay. The mineral skeleton consists of rounded grains.
Marl Clay	Chalky boulder clay
Schwemm lehm	Has been slurried through water courses from earlier storage sites and dropped off in calm water. Schwemmlehm is occasionally interspersed with weak lenses of sand, gravel or rubble. Humus additions are possible
Loess Clay	Is developed from loess by leaching of the lime content. Loess is a wind shipper lime and fine clayey sand. Loess has a very fine-grained mineral skeleton and often a low clay content

Clay is essentially a mixture of clay minerals, silt and sand, which may also contain coarse rock units such as gravel and pebbles. These three main components are responsible for the covalence of the clay, which holds the remaining ingredients, known as fillers.

In the building industry, clays are distinguished according to their binding forces. A clay is lean when it is low in clay and a fat when it has increased clay content.

Clay minerals

Clay minerals are the most important chemical weathering product of the soil. They are formed by the alteration of existing minerals or by synthesis from elements when minerals weather to their elemental form. It is not possible to make clays by grinding up silt or sand particles. Clay has many uses today, including pottery, ceramics, linings for landfills, computer chips, cosmetics, and pharmaceuticals.

Clay minerals are important because of the negative charge they contribute for cat-ion exchange. They form part of the larger class of silicate minerals, which are called aluminosilicates. Aluminosilicates have a definite crystalline structure and very small size (diameter of less than 0.002 mm).

Clay minerals are composed of two basic building blocks

1. Silicon - Oxygen Tetrahedron ($\text{Si}_2\text{O}_5^{-2}$)

Tetrahedral sheets are composed of individual tetrahedrons which share every three out of four oxygens. They are arranged in a hexagonal pattern with the basal oxygens linked and the apical oxygens pointing up/down.

2. Aluminium Octahedron (Gibbsite Sheet) $\text{Al}(\text{OH})_6^{-3}$

Octahedral sheets are composed of individual octahedrons that share edges composed of oxygen and hydroxyl anion groups with Al, Mg, Fe^{3+} and Fe^{2+} typically serving as the coordinating cation. These octahedrons are also arranged in a hexagonal pattern called a gibbsite sheet.

Clay minerals are generally hexagonal crystalline platelets. These plates consist of a core of either silicon or aluminium. Silicon cores are surrounded by oxygen and aluminium cores by hydroxide groups, as follows:

A. 1:1 clay mineral: Kaolinite

Kaolinite occurs when the Si-tetrahedral and gibbsite sheets are brought together, with the apical oxygen ions of the tetrahedral layer also being in the octahedral layer. As a result, the charge on these oxygen ions is balanced by bonding to one silicon ion and two aluminum ions.

The kaolinite mineral is actually made up of many micelles (3-D structures) piled one atop the other. Since one surface of the micelle contains hydrogen ions and the other only oxygen ions there is a tendency for hydrogen bonds to form between micelles. While individual hydrogen bonds are very low energy, the bonding energy is additive and the sum of the many hydrogen bonds between micelles results in the

micelles being very strongly bonded together and nearly impossible to separate. This layer bonding makes kaolinite a nonexpanding clay mineral. Since each micelle is constructed of a layer of silicon tetrahedral units and a layer of octahedral units, kaolinite is called a 1:1 clay mineral.

B. 2:1 clay minerals

The basic structure of 2:1 clay minerals is two silicon tetrahedral layers and one aluminum octahedral layer. This layer is weakly held to another 2:1 layer. The interlayer or space between the sheets is an important difference between 2:1 and 1:1 clay minerals. Smectite and vermiculite are two kinds of 2:1 clay minerals.

i. Smectite

The term "smectite" is used to describe a family of expansible 2:1 phyllosilicate clay minerals having permanent layer charge due to the isomorphous substitution in either the octahedral sheet (typically from the substitution of low charge species such as Mg^{2+} , Fe^{2+} , or Mn^{2+} for Al^{3+}) or the tetrahedral sheet (where Al^{3+} or occasionally Fe^{3+} substitutes for Si^{4+}). It is common for smectites to have both tetrahedral and octahedral charges.

ii. Vermiculite

Vermiculite is a high-charge 2:1 phyllosilicate clay mineral. It is generally regarded as a weathering product of micas. The charge in vermiculites may be both tetrahedral and octahedral in nature, but most vermiculites have mainly tetrahedral charge due to the substitution of Al^{3+} for Si^{4+} . Typically, between 0.6 to 0.9 out of every 4 Si are replaced by Al. This negative charge must be balanced by the presence of positively-charged sites somewhere else in the mineral structure

Generally, cations have a decisive influence on the bonding strength of a clay due to their nature and number. The thinner the plate, the greater the specific surface area, which in turn causes an increase in cation exchange. This property is the decisive factor for the strength of the clay.

Silt, sand and gravel:

Silts, sands and gravels are the fillers of clay and are held together by the binding capacity of the clay (Table 3-2).

Table 3-2 Summary of the grain sizes of the various fillers

Filler	particle size [mm]
Silt	0.002 to 0.06
Sand	0.06 to 2
Gravel	2 to 60

3.2 SELECTION OF THE EXPERIMENTAL ARRANGEMENTS

3.2.1 Strength of clay

3.2.1.1 Compressive strength in accordance with DIN 18952 and DIN 18953 [25][26]

Both the DIN 18952 and DIN 18953 standards contained methods for determining compressive strength. However, in 1971 the two standards were deleted without replacement. Nevertheless, the process of determining compressive strength will be briefly described here.

Two methods described in DIN 18952 Part 2:

- Compressive strength for construction clay: A cube is made with an edge length of 70mm, then it is dried, firstly in air, and starting from the fifth drying day, drying is achieved using an oven at 80 °C. Once the cube is dry through to the core, the compressive strength can be determined. The test pressure should be exerted parallel to the cube surface.

- Compressive strength of dry and compacted clay material: Initially, five cubic specimens with an edge length of 300 mm are produced. For the test, the clay sample must be dried. For this purpose the test specimen is firstly dried in air, and after six days, the drying can be speeded up, with cubes stored in a climate cabinet

at a maximum of 60 ° C. The drying phase is to be completed when no more weight loss can be determined on the test specimen. As drying time increases, a rise in cracking on the cube specimen can be seen.

3.2.1.2 Compressive strength and flexural tension strength according to ÖNORM EN 1015-11 [27]

As mentioned in Section 3.2.1.1, currently there is a lack of a valid norm for determining the compressive and flexural tension strength of a mud construction. As a substitute, the ÖNORM EN 1015-11 standard was used for this purpose.

Test Specimens

The test specimens were made using two different types of clay, in order to compare the mechanical properties between regions. The first was produced in Austria and the second one was produced in Bahrain.

The test specimens used to determining flexural strength have dimensions of 40 x 40 x 160 mm, while the specimens for determining compressive strength are cubes with an edge length of 100 mm.

The production and testing of the test specimens was carried out using existing metal moulds and testing devices for concrete or mortar that call for the same experiments.

3.2.1.2.1 Determination of flexural tension strength

Since the clay construction parts will be subjected to no or minimal tension stresses, its flexural strength has little importance. But it may take on some relevance when using clay plaster or when the edge strength of the clay bricks needs to be considered. As tensile strength increases, the risk of damaging the edges of clay bricks during assembly or transportation will be reduced.

Tensile stress on the clay specimens leads to compression pressure. Because of the different stiffness of the aggregate and clay, an increase in the test load leads to force deflections, which act transversely and oblique to the direction of the acting tensile forces.

Test arrangement

The produced clay cubes are loaded on a three-point load up to the point of failure. The test setting must meet the requirements according to ÖNORM EN 1015-11. The distances of the three-point loading are shown in Figure 3-2.

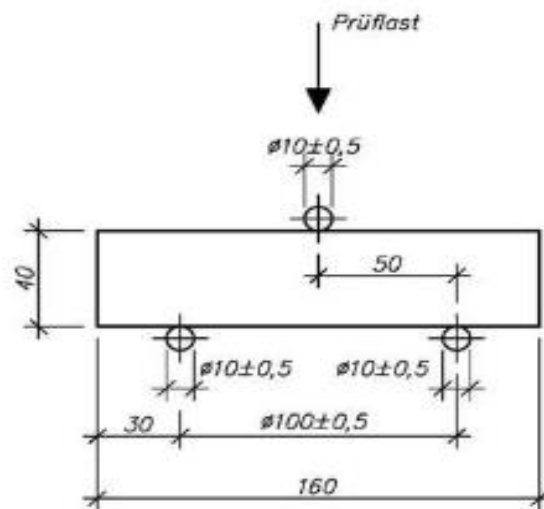


Figure 3-2 Dimensions (in mm) for testing arrangement of the flexural tension strength

The test machine essentially consists of three steel rollers with a diameter of 10 mm (+/- 0.5 mm) and a length of 45-50 mm. The two support rollers are arranged at a distance of 100mm (+/- 0.5 mm). The size of the test machine can vary according to its use. The test

machine which used for these experiments has a 130mm distance between the supports rollers.

Loading procedure

The test load is applied smoothly and at a uniform speed (between 10 N / s and 50 N / s), so that the fracturing of the specimens occurs within approximately 30 to 90 s.

Calculation of flexural tensile strength

According to the general formula for calculating single load stresses, the flexural tensile strength σ_{BZ} can be calculated from the obtained fracture load, F (which is central to the test).

$$\sigma_{BZ} = 1.5 \cdot \frac{F \cdot l}{b \cdot d^2} \quad [\text{N/mm}^2] \quad 3-1$$

Where:

b is the width of the specimen (in mm)

d is the height of the specimen (in mm)

l is the distance between the axes of support rollers (in mm)

3.2.1.2.2 Determination of compressive strength

The compressive strength of clay buildings depends on the following factors:

- The type and amount of clay minerals in the clay skeleton, which constitute the degree of strength of the construction material.
- The size and the amount of silt, sand and gravel has an important influence on compressive strength.
- The particle size and distribution of the construction material when the clay is prepared and compressed is essential.

- The compressive strength can be improved by the addition of various additives.

Carrying out the compression test

In order to determine the compressive strength of the clay, two types of clay specimens were used. The first ones were prepared from clay obtained from Wienerberger in Austria with dimensions of 100 x 100 x 100 mm. The second clay specimens were produced from clay obtained from the Al-Aali company in Bahrain, and comprised the two halves of the cube produced by carrying out the flexure tension experiment. The carrying load is continuously increased throughout the test until the specimens break.

Evaluating the results

The compressive strength σ_D can be calculated using formula (3-2) which considers F as the failure load, where A is the area at which the clay specimen is loaded.

$$\sigma_D = \frac{F}{A} \quad [\text{N/mm}^2] \quad 3-2$$

3.2.1.3 Binding strength

Binding strength is the resistance provided by a clay specimen against breaking up. It can be determined through the tensile test. This type of strength depends on the clay content, water content and the type of clay minerals present.

Producing standard stiff clay

Standard stiff clay is used throughout this work in order to determine mechanical properties. Its production is regulated through [25] and is described as follows:

- Step 1: In order to ensure a uniform moistening of clay, it should be stored at rest for a specific period of time. Fat clays need to be stored for 12 hours while lean clays need about 6 hours.
- Step 2: 200 g is taken from the stored clay, shaped into a ball and dropped from a height of 2 m onto a flat plate. Standard stiffness clay is obtained when the flattened portion has a diameter of 50mm. If the diameter is larger than 51 mm

this test should be repeated with lower water mixing. With a diameter smaller than 49 mm, the test should be repeated after adding more water.

Determination of the binding strength

The determination of the binding force is described in DIN 18952 sheet 2 and shown in Figure 3-3. The stiff clay is placed into the test mould in three layers and compacted using a rammer. The tamping should be carried out until no more compacting is possible. Then, the specimen is loosened on both sides using a knife and the test specimen taken from the test mould.

The obtained specimen and after 28 drying days is introduced into the test device shown, figure(3-3) and loaded by adding sand to the sand container until it tightens. Once the specimen breaks, the sand supply is stopped and the weight of the sand is measured. From the weight of the sand and the cross-sectional area of the specimen the tension stress and hence the binding strength can be determined. The final value is obtained from the mean of at least three samples. The deviations of the samples must not be greater than 10%, otherwise the complete testing procedure must be repeated.

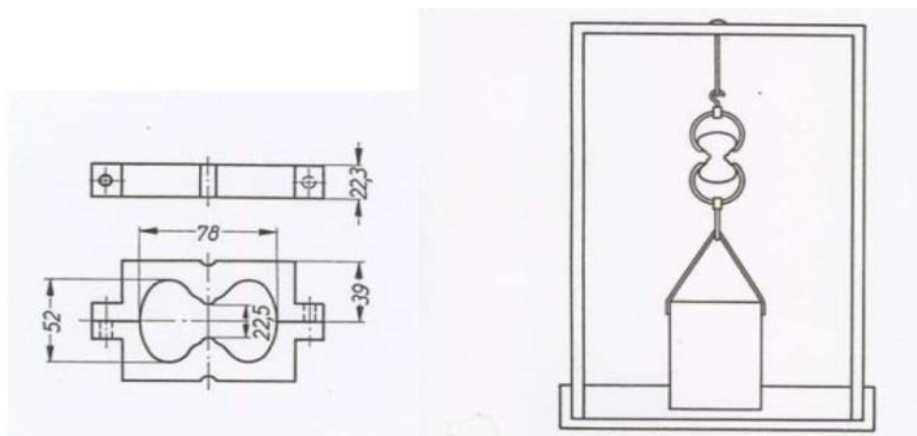


Figure 3-3 Test specimen preparation (in mm) and the test arrangement

Nowadays there are a lot of mechanical and electrical machines which can be used for the same purpose. The preparation of the test specimens is the same but the test machines are different. For example, in the University of Bahrain a mechanical machine for this test is operated by preparing the specimen inside the mould as shown in the figure 3-3. At the University of Vienna, the same mechanical procedure is employed with the help of an

electrical machine. Both mechanical and electrical producer has been implemented through this project.

The binding strength generally ranges from 0.005 to 0.036 N / mm ² (Table 3-3). Based on the binding force, the clay is divided into six different groups.

Table 3-3 Classification of construction clays according to the binding strength [24]

Binding Strength [N/mm ²]	0.005-0.008	>0.008-0.011	>0.011-0.02	>0.02-0.028	>0.02-0.036	>0.036
Designation	very lean clay	lean clay	almost fat clay	fat clay	very fat clay	clay

3.2.1.4 Moisture effects on clay

3.2.1.4.1 Water effects

Once clay comes into contact with water, it begins to swell and may also deform plastically. Clay building materials have a microporous structure. Water can be passed rapidly through capillary forces.

In principle, clay buildings should be protected absolutely from any direct effects of water, such as rainfall or rising ground moisture.

Furthermore, it must be ensured during production of clay construction materials that the shrinkage phase is complete, and that equilibrium moisture content has reached a stable level.

Throughout this work, the determination of the drying time was highly important.

3.2.1.4.2 Drying time

The drying time is the period that wet building material requires for its moisture content to reach a state of equilibrium.

Laboratory investigations at the University of Kassel into building experimental institute showed that the equilibrium moisture content of adobe bricks is reached after 20 to 30 days, while burnt bricks have not yet reached this state even after 100 days.

Drying time was calculated throughout this work for the specimens used for the flexure bending test. The specimens were observed and weighted each week until they reached the equilibrium moisture content. The drying time was approximately 28 days.

3.2.1.5 Elasticity of Model

Definition of Elastic Modulus

The modulus of elasticity, or “Young’s Modulus”, is defined as the slope of the stress-strain curve within the proportional limit of a material. There is no specific test for determining the elastic modulus of a clay material; therefore, the same test procedure as used for concrete specimens was employed.

Test arrangement

The specimen produced for this test has dimensions of 100mm x 100mm x 400mm. The test machine is programmed to load the specimen in a cyclic loading loop in order to obtain the stress-strain curve. The maximum value of the loading stress is recommended in the standard codes as approximately 25-30% of the maximum material compression stress.

Evaluating the results

After carrying out the experiments, a stress-strain curve is obtained. The secant modulus is defined as the slope of the straight line drawn from the origin to the stress-strain curve at some percentage of the ultimate strength. This is the value most commonly used in structural design. Since no portion of the stress-strain curve is a straight line, the usual method of determining the modulus of elasticity is to measure the tangent modulus, which is defined as the slope of the tangent to the stress-strain curve at some percentage of the ultimate strength of the material as determined by compression tests. Figure 3-4 [28] shows the stress-strain plot of a concrete as it is loaded and unloaded. From this figure, we can see that the secant modulus is almost identical to the tangent modulus obtained at some lower percentage of the ultimate strength.

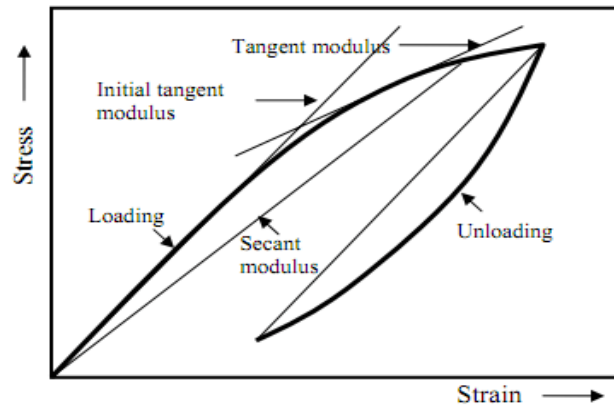


Figure 3-4 Diagrammatic representation of the stress-strain relation for concrete

From three or four loops of the stress-strain curve, the elasticity modulus can be calculated from the following formula:

$$E = \frac{\sigma}{\varepsilon} [N/mm^2] \quad 3-3$$

Where:

E is the elasticity modulus [N/mm²]

σ is the max stress in [N/mm²]

ε is the strain

Another important material property which can be calculated from the elasticity modulus is the shear module, G . According to EC6 [29], the shear modulus can be calculated as 40 % of the measured elastic modulus.

3.2.1.5.1 Shear strength

Shear strength is one of the important mechanical properties for studying the seismic capacity of clay material. Tamped clay walls (also called rammed earth walls), like any other form of clay construction, have relatively good strength in compression but generally poor strength in shear and tension, especially when moist.

Test specimens

The shear strength for clay materials depends on the construction method used for the mud building. For the purposes of this thesis, the properties of tamped clay wall sections will be investigated. The prepared wall section specimens consist of clay and clay with a wooden frame. The combination of clay and wood has been developed in order to increase the shear strength capacity of the wall section.



Figure 3-5 clay wall sections specimens

The specimens are poured into a formwork in layers 10 to 15 cm thick and compacted by ramming. The formwork consists of two parallel panels, separated and interconnected by spacers, see Figure3-5. The compaction of the layer inside the formwork is achieved by using manual tampers (ramming) with conical or flat heads. Conical tampers give a better bond between the different clay layers, but the process takes longer.

Test device

After fabrication and conservation, the wall sections were lifted and fixed under a reaction beam. Constant vertical pressure was applied to simulate the real stress produced by the ceiling load. A uniaxial lateral load was applied to the test walls from a force piston set to one side in order to determine the shear strength capacity against earthquake events.

The tester should record at which load the first cracks appear in the wall section and at which load the wall section specimen fails. The test setup is shown in Figure 3-6.

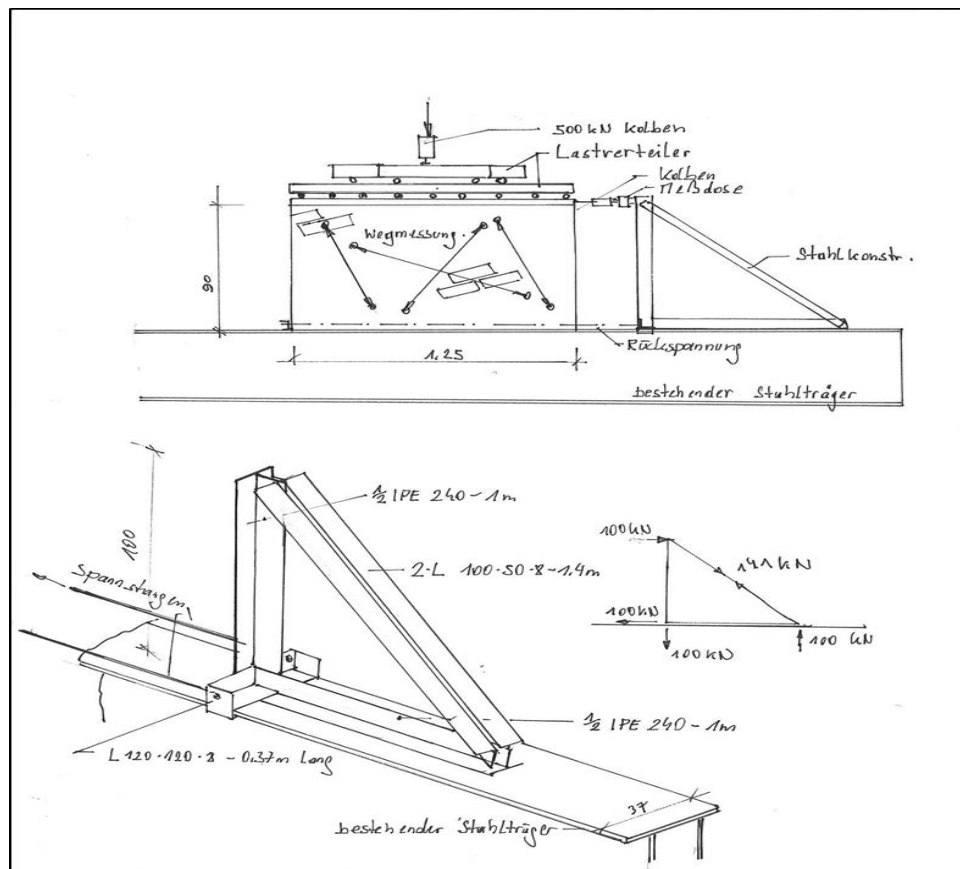


Figure 3-6 Experimental arrangement sketch for determining shear strength capacity

3.3 EVALUATION OF THE ENVISAGED TESTS

Before beginning earthquake analysis modelling, it is important to evaluate the tests to be carried out. The tests should be performed according to the standards and guidelines in order to reach real and logical material mechanical properties values from which analytical and numerical analysis can be applied to deduce the correct shear stresses and deformations due to seismic effects.

Furthermore, it is important to search the literature for recommended values for the main mechanical properties of clay in order to envisage the appropriate range for test results carried out during this work (see Table 3-4).

Table 3-4 Compilation of the general parameters of clay from [30], [31], [32], [33]

Flexural bending strength	1.1 -1.6 N/mm ²
Compression strength	2-6 N/mm ²
Bind strength	0.005 – 0.036 N/mm ²
Elasticity model	6000 – 8500 N/mm ²
Density	1700 – 2200 kg/m ³
Shear strength	0.01 – 0.1 N/mm ²

4. STRUCTURAL ANALYSIS

To determine the characteristic values of the mechanical properties of clay (mud), an extensive investigation was carried out in the materials laboratory of the Institute for Building Construction and Technology, Department of Building Materials, Materials Technology and Fire Safety at the University of Vienna. In order to obtain good knowledge of the clay in Dubai region, some mechanical properties were also determined through experiments in the civil Engineering laboratory of the University of Bahrain.

4.1 SETTING MUD PROPERTIES USED FOR THE EXPERIMENTS

4.1.1 Clay produced in Austria

In order to determine the mechanical properties of clay, an amount of clay was obtained from clay deposits in Vienna, Austria (see Figure 4-1).



Figure 4-1 Clay obtained from Austria

To prepare for the experiments, the clay specimens were mixed with a small amount of water and stored for 12 hours at rest. The amount of the water should not affect the plasticity of the clay.

4.1.2 Clay produced in the Dubai region

The clay used in the laboratory experiments at the University of Bahrain was obtained from the Al-Aali Company. This type of clay is crushed with a grain size of 0 to 0.5 mm, which is suitable for preparing clay specimens. Because of the nature of this clay, there was no need to mix it with water or store it. See figure (4-2)



Figure 4-2 Clay obtained from the Al-Aali Company

4.2 CARRYING OUT THE EXPERIMENTS

To evaluate the behaviour of clay buildings under seismic effects, the mechanical properties of clay wall sections must be determined. These include:

1. Compressive strength
2. Tensile strength
3. Elastic modulus
4. Shear strength

In addition, throughout this work flexural bending strength has been determined and clay shrinkage behaviour was observed and recorded.

4.2.1 Compressive strength

4.2.1.1 Clay obtained from Austria

The compression tests were carried out on clay cube in accordance with the relevant standards to determine the compressive strength and the stress-strain relations used to evaluate the elasticity modulus.

Test specimen preparation

The test specimen used in this experiment is a clay cube with dimensions of 100 x 100 x 100 mm (Figure 4-3). The formwork should be clean and lubricated with formwork oil in order to prevent clay sticking inside the module.

To prepare clay and incorporate it into the formwork, the clay was mixed with the necessary amounts of water. Before the incorporation of the clay inside the formwork, the slump test should be performed. 200 g of prepared clay is rolled into a ball and dropped from a height of 2 m onto a smooth flat surface. This process is defined by [25], Part 2, Section 2.2. The diameter of the flat compressed ball is then determined.



Figure 4-3 formwork preparation for the compression test

According to the standard, the ball diameter should be 50 mm. If the diameter is less than this value, the clay should be mixed with more water and *vice versa* (See figure 4-4).



Figure 4-4 Slump test for prepared clay

The prepared clay is then inserted into the formwork. The clay-water mixture is added to the form in layers. Each layer is then compressed. For compacting, a separate compression stamp was used (See Figure 4-5).



Figure 4-5 Prepared clay in the formwork for the compression test

After placing the clay mixture in the formwork, the drying time required to prepare the clay specimens for the test is 28 days. The drying and storage of the individual specimens was conducted according to [27] in a climate chamber or room with the following constant climate conditions:

- Temperature: 20 ° C
- Humidity: 65%

The specimens were dried to reach the equilibrium moisture content. Figure (4-6)



Figure 4-6 Prepared clay specimens for the compression test

Carrying out the tests

The compression tests were performed at the end of the drying time. The test device applies an increasing compression load to the top surface of the clay cube up to the point of failure (see figure 4-7).



Figure 4-7 Compression test carried out on the prepared clay specimens

The obtained compressive strength is 2.1 N/mm². Some of the specimen failed before it reached the ideal value. This might be due to insufficient compaction during specimen preparation.

The compressive strength was calculated using the following formula:

$$\sigma = \frac{F}{A} [N / mm^2] \quad 4-1$$

Where:

σ is the compressive strength in N/mm²

F is the maximum acting force in N

A is the loaded area in mm²

The results obtained for all five clay cubes are shown in Table 4-1 and represented in Figure 4-8.

Table 4-1 Compression test results

Cube[W]	A [mm ²]	Specimen thickness [mm]	Specimen width [mm]	σ [N/mm ²]	F _{Max} [N]	Date
1	10000	100	100	2.1	20443.64	7.8.2012
2	10000	100	100	1.96	19616.17	7.8.2012
3	10000	100	100	1.43	14257.05	7.8.2012
4	10000	100	100	1.8	17985.38	7.8.2012
5	10000	100	100	1.74	17420.47	7.8.2012

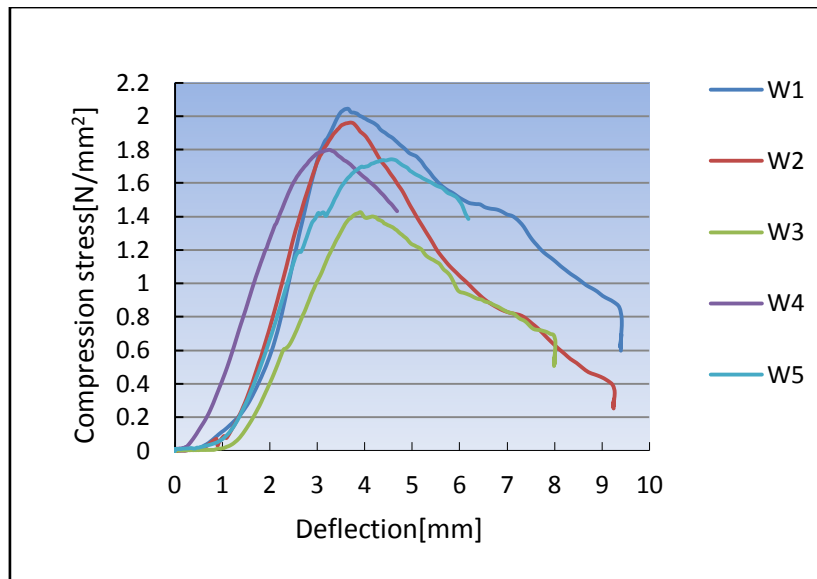


Figure 4-8 Compressive strength result

4.2.1.2 Clay obtained from the Dubai region

As mentioned above, two types of clay from different regions were tested. In this case the flexure bending stress test was carried out before the compression test.

Test specimen preparation

The specimens used for testing both flexure bending stress and compression stress was a series of prisms (S1-S16) each with dimensions 40 x 40 x 160 mm. Drying time and storage conditions were the same as in section 4.2.1.1. The shrinkage effect and the time required to reach equilibrium moisture content for the prisms were observed.

The clay-water mixing ratio was approximately 25%. The mixing was performed with the help of a HOBART mixer. Before pouring the specimens, the slump test was performed (see figure 4-9).



Figure 4-9 Clay specimen preparation

Flexural test

Figure 4-10 shows the flexural test being performed and Table 4-2 presents the compilation of the results. The distance between the two support rollers was set to 130 mm.



Figure 4-10 Flexural bending test on clay prisms

From the obtained fracture load, F , the flexural strength σ_{BZ} can be calculated using the general tension formula for single load (test load in the middle) directions.

$$\sigma_{BZ} = 1,5 \cdot \frac{F \cdot l}{b \cdot d^2} [N/mm^2]$$

4-2

Where:

b is the wide of the specimen in mm

d is the height of the specimen in mm

l is the distance between the mid axes of the support rollers in mm

The mean value of the flexural bending strength is 0.88 N/mm².

Table 4-2 Determination of flexural strength

Prism #	Max force	Length	Flex. And bending strength	Mean value (σ_{BZ})
	kN	mm	N/mm ²	N/mm ²
S	f	L	σ_{BZ}	σ_{BZ}
S1	0.27	138	0.87	0.91
S2	0.29	137	0.93	
S3	0.28	138	0.91	
S4	0.29	139	0.94	
S5	0.26	130	0.79	0.85
S7	0.28	130	0.85	
S8	0.3	130	0.91	
S9	0.26	130	0.79	0.78
S10	0.24	130	0.73	
S11	0.25	130	0.76	
S12	0.28	130	0.85	
S13	0.26	130	0.79	0.82
S14	0.28	130	0.85	
S15	0.27	130	0.82	
S16	0.27	130	0.82	

Compression test

Compressive strength is strength of the specimen under compressive forces and is the most important property of clay. Compressive strength, as described above, is calculated from the ratio between the maximum force at failure and the cross sectional area of the sample surface. The specimens were dried to a constant weight and then tested. The bending test was carrying out first to determine flexural strength and then the two resulting fraction parts of the prisms were used to determine the compressive strength (see figure 4-11).

The clay specimens were problematic to install into the testing machine for the compression test. The roughness and irregularity of the specimen surface can create a problem when the load is inserted above the specimen. To limit this source of error, the following options can be used:

- The surface can be abraded until smooth.
- The top and bottom of the test specimen can be adjusted using cement mortar or gypsum.
- Load-distributing insulation boards can be attached to the top of specimen and bottom of the testing machine.

In this series of experiments, the surface was smoothed by abrading (see figure 4-12).



Figure 4-11 Carrying out the compression test

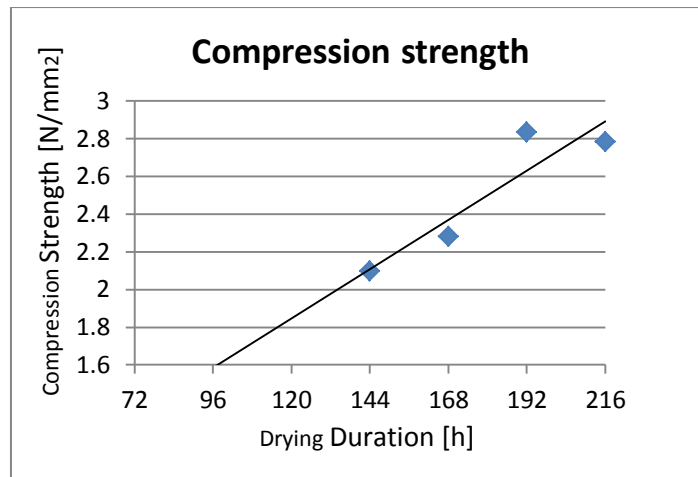


Figure 4-12 the relation between the drying time and compressive strength for series (S1-S16)

Table 4-3 Compressive strength results (S1-S16)

Specimen#	Max force	Surface Area	Compression stress	Mean Value	
	kN	mm ²	N/mm ²	N/mm ²	
S	F	A	σD	σD	
S1	5.1	1900	2.68	2.10	
	5.5	3400	1.62		
S2	5.4	2647	2.04		
	5.8	3120	1.86		
S3	5.9	3230	1.83		
	5.8	2730	2.12		
S4	5	2280	2.19		
	4.5	1850	2.43		
S5	5.6	1961	2.86		2.28
	5.9	3510	1.68		
S6	6.2	2730	2.27		
	6.4	3081	2.08		
S7	5.9	1961	3.01		2.83
	6.3	3510	1.79		
S8	6.1	2000	3.05		
	6.3	Failed	Failed		
S9	6.2	2400	2.58		
	6	1850	3.24		
S11	---	----	---		
S10	6.4	2660	2.41		
	6.1	2280	2.68		
S11	6.8	1900	3.58	2.78	
	7	3400	2.06		
S12	6.7	2730	2.45		
	6.9	3081	2.24		
S13	6.8	2280	2.98		
	6.6	1850	3.57		
S14	6.7	1961	3.42		
	6.9	3510	1.97		

The mean compressive strength that obtained for these specimens sierra is 2.7 N/mm^2
See table (4-3) above.

4.2.2 Tensile strength

The tensile strength of clay is very low compared to its compressive strength. This property can be measured in a variety of ways. The fundamental test method is to subject a sample to controlled tension until failure.

The most common testing machine used in tensile testing is the universal testing machine. This type of machine has two crossheads: one is adjusted for the length of the specimen and the other is driven to apply tension to the test specimen. There are two types of machine: hydraulic powered and electromagnetically powered (see Figure 4-13).

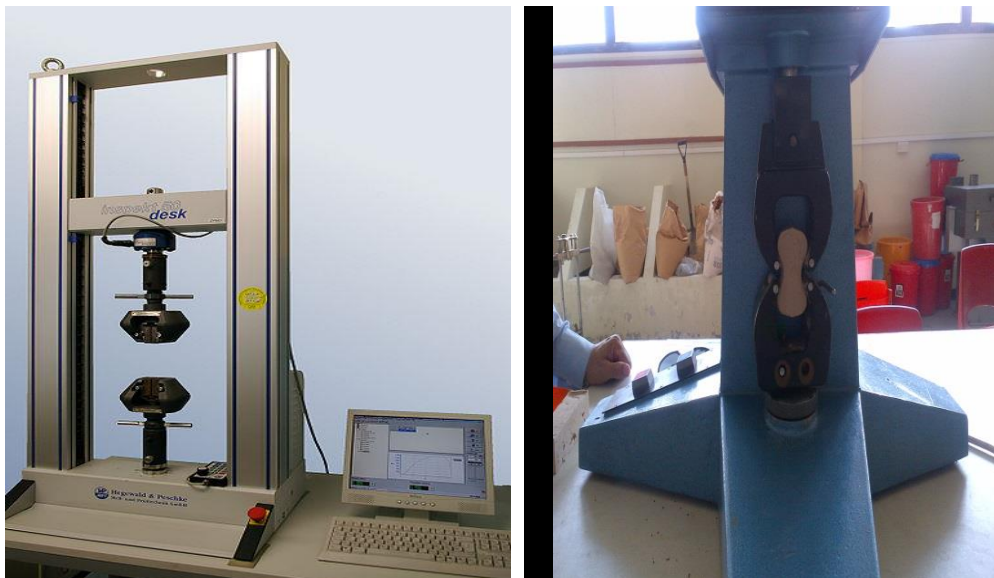


Figure 4-13 (right) A mechanical tensile test machine. (left) A universal tensile testing machine (Hegewald & Peschke)

The test process involves placing the test specimen in the testing machine and applying tension to it until it fractures. During the application of tension, the elongation of the gauge section is recorded against the applied force.

Test specimen preparation

Two types of clay were tested in both electrical and mechanical devices. The specimens both types of clay and test machine have the same dimensions (see the figure 4-14).

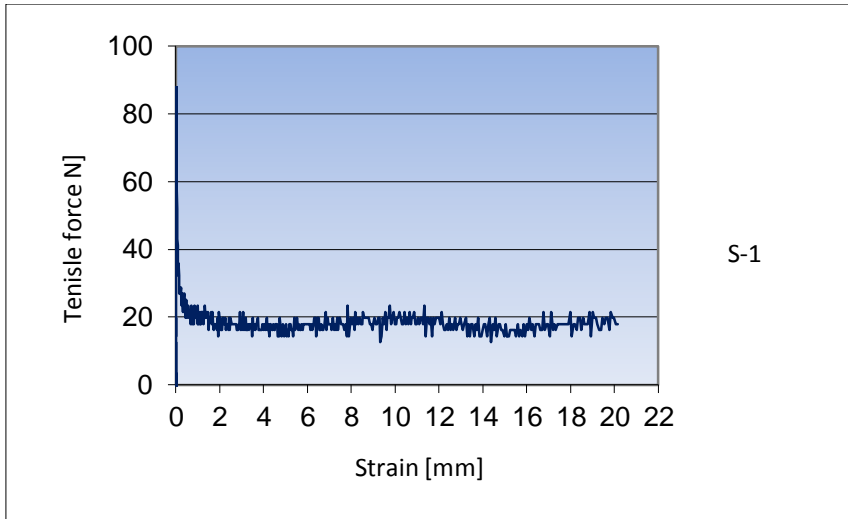


Figure 4-14 Tensile test specimens

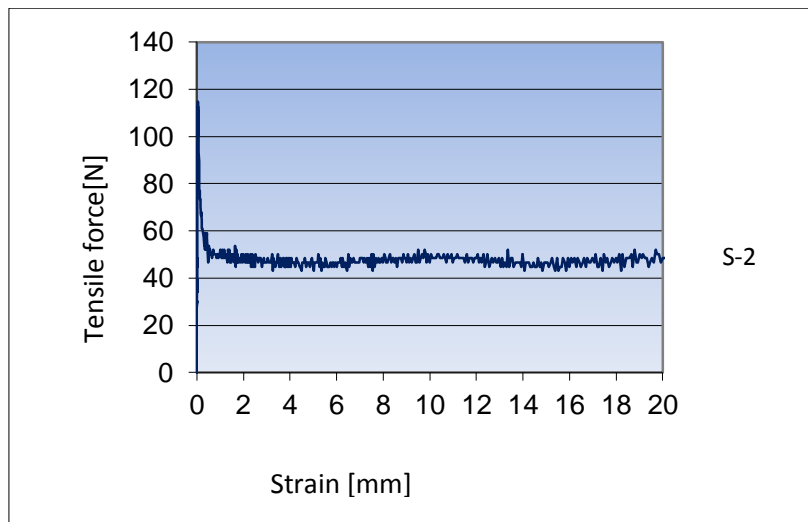
Test procedure

The tensile tests on the clay specimens were carried out to determine their tensile strength and maximum tensile force.

The test was performed on a series of clay specimens, and the results showed an average tensile force of 90 N for both types of clay and with both test devices (see Figure 4-15).



(a)



(b)



(c)

Figure 4-15 Tensile test results. (a&b) Using the electrical machine. (c) The test performed using a mechanical machine

4.2.3 Elastic modulus

The elastic modulus was determined using cyclic compressive stress. Young's modulus was determined from the stress-strain curve at a value of 3000 - 4000 N/mm².

Test specimen preparation

The clay specimens used to determine the elasticity modulus were prisms with dimensions of 100 x 100 x 400 mm.

The formwork used for preparing the specimens is a wooden formwork which needs to be lubricated with formwork oil in order to remove the specimens easily without any sticking problems.



Figure 4-16 Preparation of clay prisms for the elasticity modulus test

Before pouring the clay into the formwork, the slump test was repeated to ensure the plasticity of the prepared clay. The clay was poured into the formwork in layers. After adding each layer, with the clay should be compacted with a small wooden stick to ensure a clay prism without any gap (see Figure 4-16).

The specimens should be dried until there is no further change in weight. This takes approximately 28 days.

Carrying out the test

The test has been carried out according to the section 3.2.1.5. See figure (4-17)



Figure 4-17 Test setup for determining the elasticity modulus

The elasticity modulus E can be evaluated using the following general formula:

$$E = \frac{\sigma}{\varepsilon} [N/mm^2] \quad 4-3$$

Where:

σ is the compression stress value [N/mm²]

ε is the strain obtained from the relation of the length deformation over 170 mm (distance between the two sensors).

σ represents compression stress, which is recorded against the length deformation that appears in the middle part of the specimen where the strain sensor is fixed. It was recommended that the compression and strain values for the last cycle of three or four loading and unloading cycles would be optimal for calculating the elasticity modulus.

From the last data cycle for prism 1, figure (4-18), Table 4-4, the modulus of elasticity can be calculated as follows:

$$E\text{-Modulus} = 5.39E-01 \text{ N/mm}^2 \div (3.00E-02\text{mm}/170\text{mm})$$

$$E\text{-Modulus} = 3054.33 \text{ N/mm}^2$$

Table 4-4 Elasticity modulus results – Prism 1

Length deflection [mm]	Compression strength[N/mm2]
5.00E-02	6.00E-01
2.00E-02	6.10E-02
3.00E-02	5.39E-01
E-Modulus =	σ/ξ
E-Modulus =	3054.33

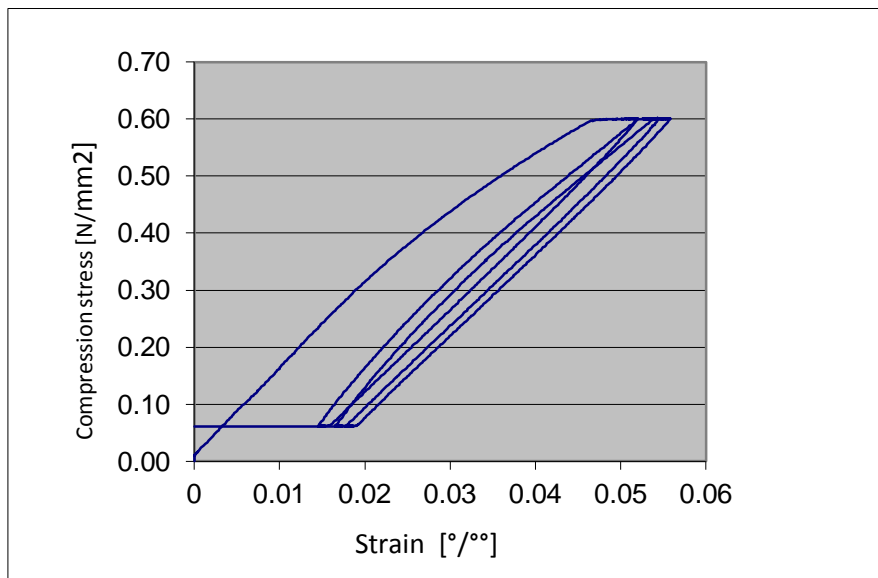


Figure 4-18 Elasticity modulus results for Prism 1

Similarly for Prism 2, Table 4-5, the modulus of elasticity can be calculated from the last data cycle as follows:

$$E\text{-Modulus} = 5.40E-01 \text{ N/mm}^2 \div (2.36E-02\text{mm}/170\text{mm})$$

$$E \text{ Modulus} = 3900 \text{ N/mm}^2$$

Table 4-5 Elasticity modulus results for Prism 2

Length deflection [mm]	Compression strength[N/mm ²]
2.70E-02	6.00E-01
3.40E-03	6.00E-02
2.36E-02	5.40E-01
E-Modulus =	σ/ξ
E-Modulus =	3900

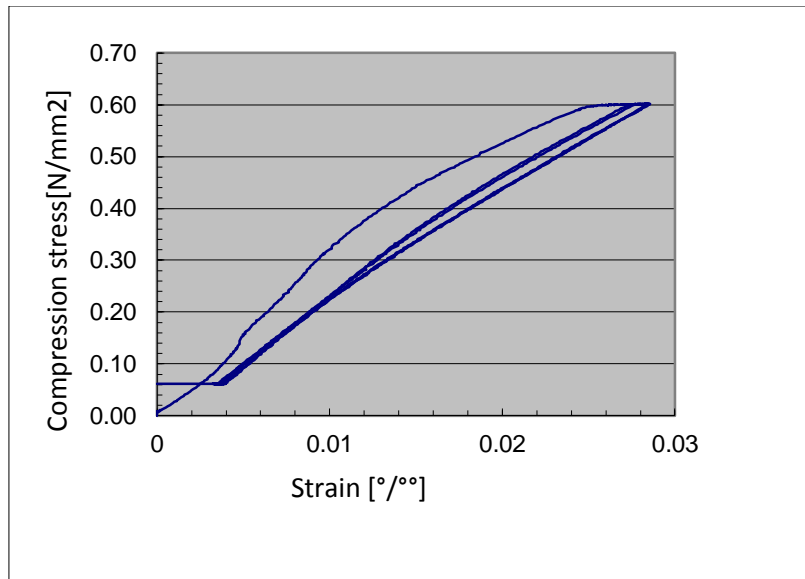


Figure 4-19 Elasticity modulus results for Prism 2

4.2.4 Shear strength

The stability of structures which are subjected to a horizontal loads caused by earthquakes events depends on the structural behaviour of all components in the load direction. Walls are considered in this case as slices which depend on its shear strength. In order to investigate the real value for clay shear strength, shear tests were performed with clay wall sections.

The experimental setup was prepared using the following (Figure 4-20):

1. Hydraulic device
2. Later force device (force piston)
3. Steel structure

4. Two displacement sensors
5. Laptop
6. PC monitoring station



Figure 4-20 Shear test setup

The shear test was performed on six clay wall sections and two wood frames (Table 4-6). A 6000 N constant vertical load has been implemented using the hydraulic device in order to simulate the roof load on the wall sections. The test was performed at the Vienna University of Technology at the Institute of Material Engineering.

Table 4-6 Shear test specimen

Specimens	Symbols	Dimensions[m]
Wood Frame	A1, A2	1.2 x 0.9 x 0.1
Clay wall section strength with wood Frame and iron grid	B1, B2	1.2 x 0.9 x 0.1
Clay wall section	C1, C2	1.2 x 0.9 x 0.15
Clay wall section strength with wood frame	D1	1.2 x 0.9 x 0.1
Clay wall section strength with wood frame and X-wood diagonal	E1	1.2 x 0.9 x 0.1

Shear test results

The shear test results were compared with the simulation using finite element method. The results were very close.

The Europa codes state that a clay wall's shear strength values should lie in the range of 0.1-0.6 N/mm². The test results give values in this range and the wall sections which were strengthened with wood showed better shear strength capacity.

The shear strength capacity and the finite element simulation results are described as follows:

1) Wood Frame (A1 & A2)

The wooden frames have been prepared from spruce wood with the dimensions showed in the table (4-6). The benefit of testing the wooden frame is to show the shear capacity that they will carry by it during testing the wooden clay specimens.



Figure 4-21 Shear strength test for wood frame A1 and A2

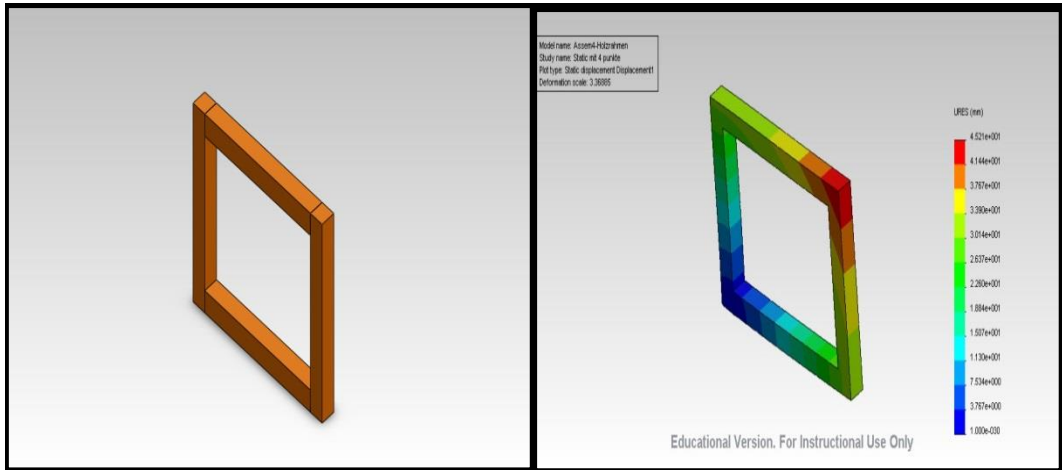
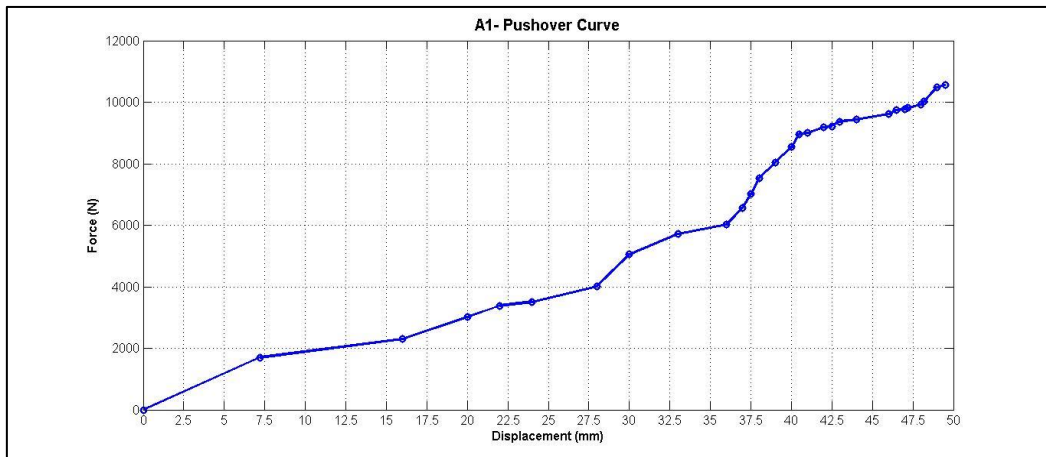
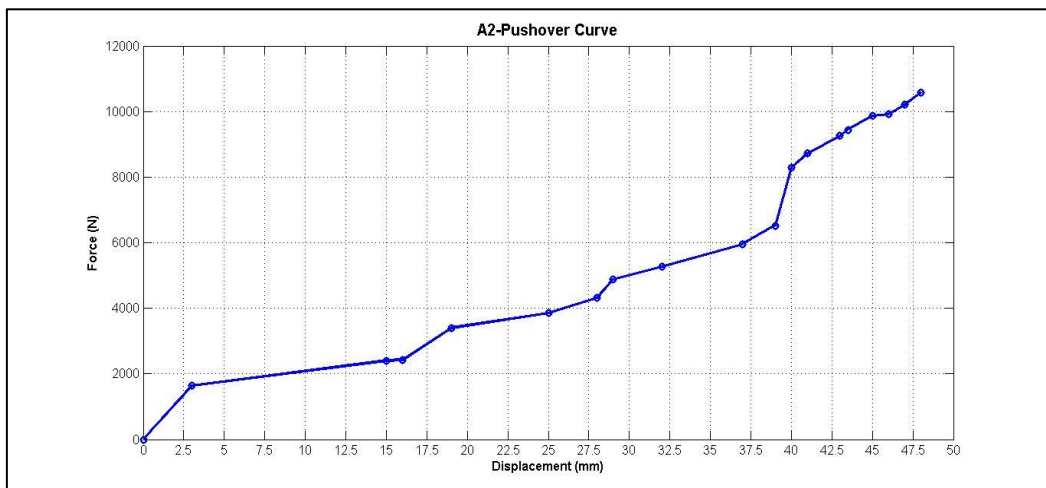


Figure 4-22 Shear strength test simulation for wood frame A1 and A2



(a)



(b)

Figure 4-23 (a) and (b) Force –Top displacement test results for wood frame A1 and A2

The results showed that; the maximum shear force which before the wooden frame breaks is up to 11000 N. The comparison between test results and simulation results for top displacement is as follows:

Table 4-7 Test and simulation results comparison for Wood Frame

Top Displacement (mm)	Test Result	Simulation result
A1	49	45.2
A2	48	45.2

2) Clay wall section strength with Wood Frame and iron mesh grid (B1 & B2)

The specimens here have been tested to investigate the shear capacity of clay wall section that is reinforced with iron mesh grid. (Figure 4-24 & 25)



Figure 4-24 Shear strength test for wall section B1



Figure 4-25 Shear strength test for wall section B2

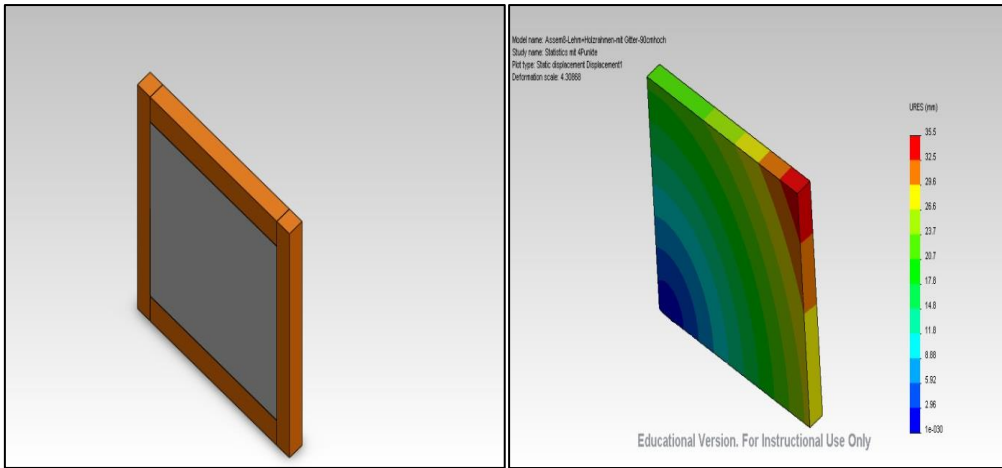
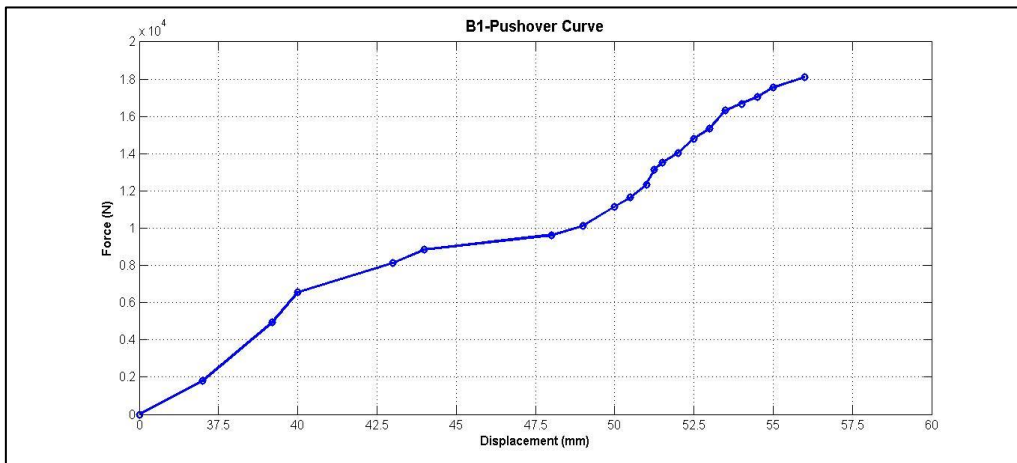
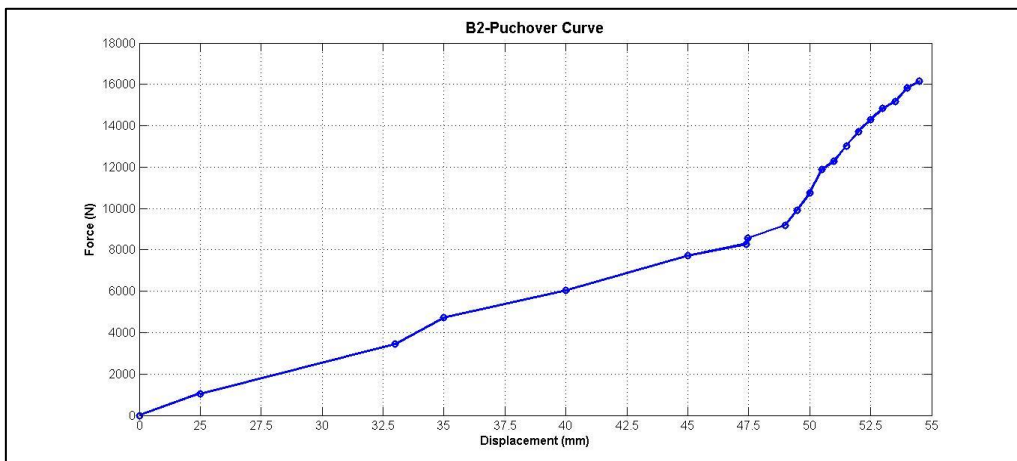


Figure 4-26 Shear strength test simulation for wall section B



(a)



(b)

Figure 4-27 (a) and (b) Force –Top displacement test results for wall sections B1 and B2

The results showed an increasing in shear capacity. The specimen failed by a 17000 N. which in small calculation to find the shear stress in the clay wall section only through the subtraction of 10000 N that the wood frame can carry, the left 7000 N is the strength value that refers to the clay wall section. See figure (4-27)

The comparison between test results and simulation results for top displacement is as follows:

Table 4-8 Test and simulation results comparison for wall sections B1 and B2

Top Displacement (mm)	Test Result	Simulation result
B1	56	36
B2	54.5	36

3) Clay wall section (C1 & C2)

The specimen in this test has a clay material without any strengthen by which the shear strength can be recognised with a clay wall section of 150mm. see figure (4-28&29)



Figure 4-28 Shear strength test for wall section C1



Figure 4-29 Shear strength test for wall section C2

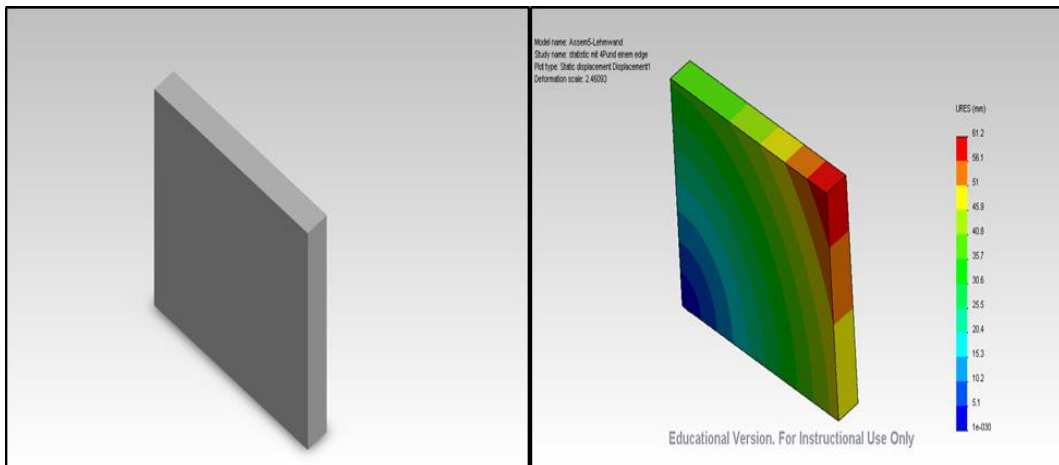


Figure 4-30 Shear strength test simulation wall section C

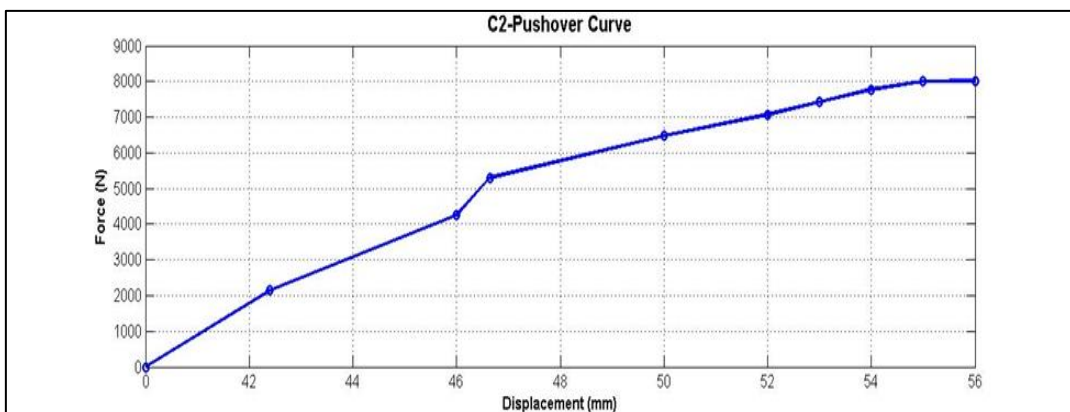


Figure 4-31 Force –Top displacement test results for wall section C2

The maximum shear force that the clay wall section showed is 8000 N which indicate an incensement in shear capacity up to 1000 N due to the extra wall section width. See figure (4-31).

The comparison between test results and simulation results for top displacement (figure 4-30) is as follows:

Table 4-9 Test and simulation results comparison for wall sections C1 and C2

Top Displacement (mm)	Test Result	Simulation result
C1	56	61.2
C2	54.5	61.2

4) Clay wall section strength with wood frame (D1)

The specimen here is a clay wall section with a wooden frame without any strengthens. The result showed a maximum shear force of 12800 N. see figure (4-32,33&34).



Figure 4-32 Shear strength test for wall section D1

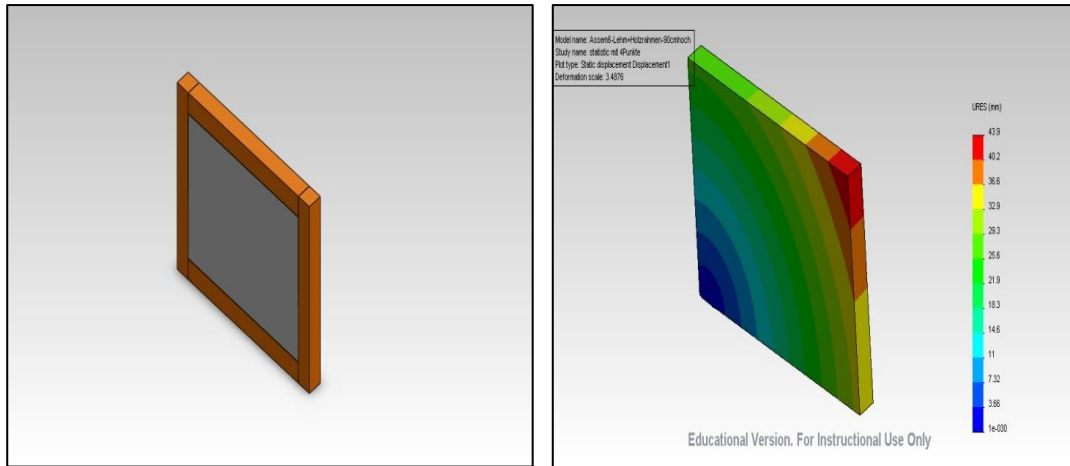


Figure 4-33 Shear strength test simulation wall section D

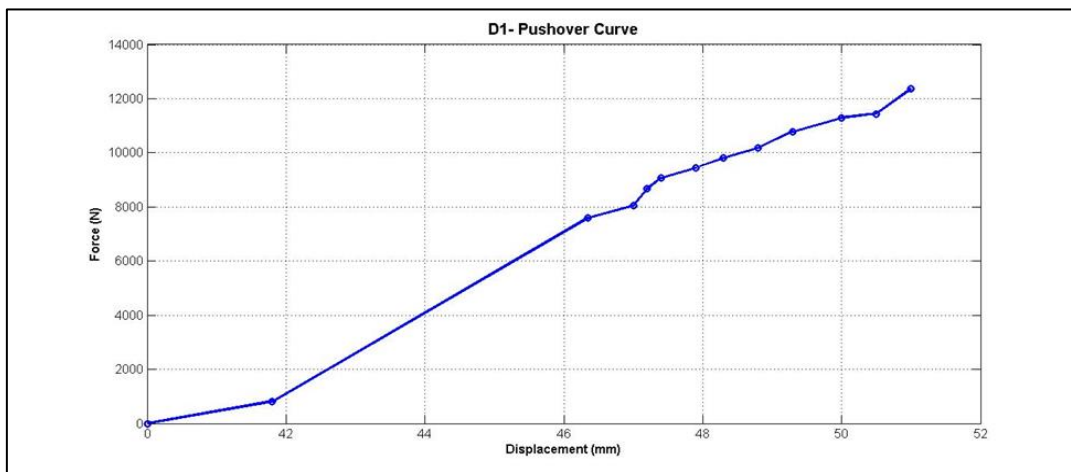


Figure 4-34 Force –Top displacement test results for wall section D1

The comparison between test results and simulation results for top displacement is as follows:

Table 4-10 Test and simulation results comparison for wall section D1

Top Displacement (mm)	Test Result	Simulation result
D1	51	44

5) Clay wall section strengthened with wood frame and X-wood diagonal (E1)

The last clay wall section in this test, is a specimen with wooden cross bracing that increased the shear strength up to 13700 N. See figure (4-35,36&37)



Figure 4-35 Shear strength test for wall section E1

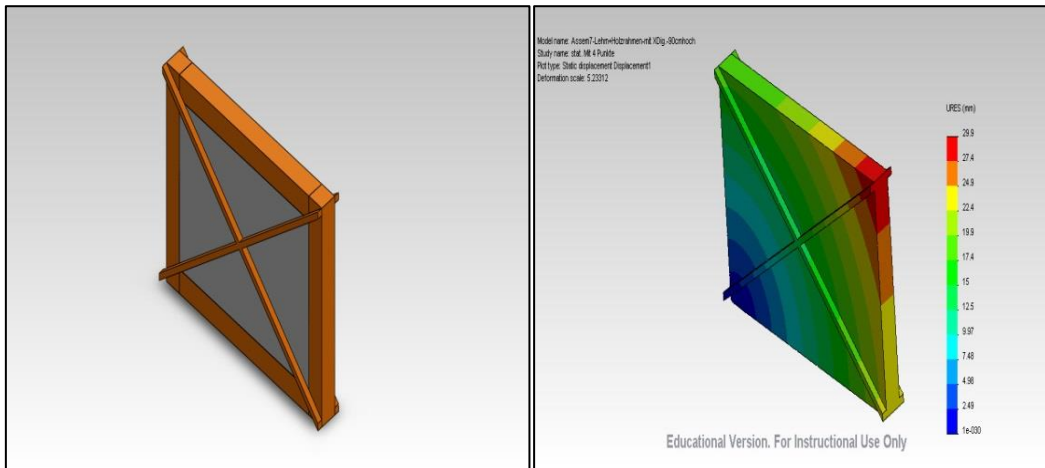


Figure 4-36 Shear strength test simulation wall section E

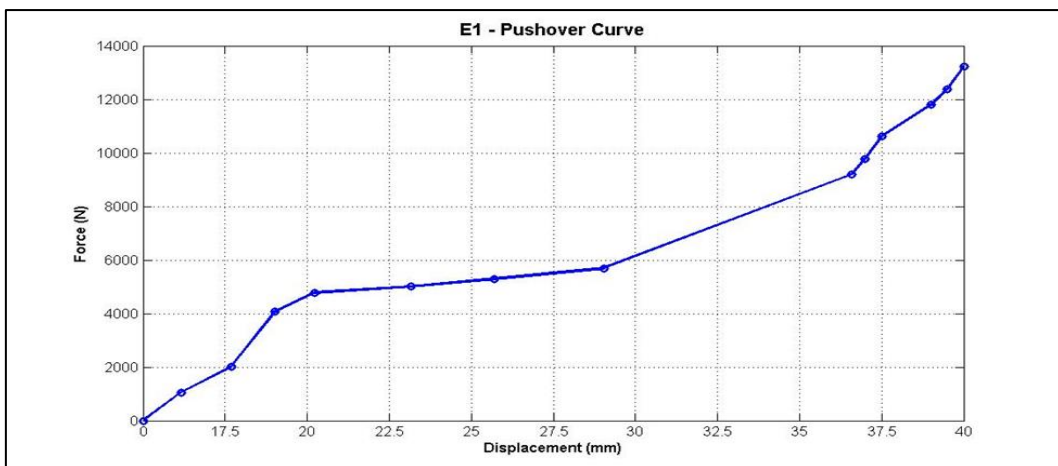


Figure 4-37 Force –Top displacement test results for wall section E1

The comparison between test results and simulation results for top displacement is as follows:

Table 4-11 Test and simulation results comparison for wall section E1

Top Displacement (mm)	Test Result	Simulation result
E1	40	30

4.3 EVALUATION OF TEST RESULTS

The results of the tests into the important mechanical properties of clay showed a good approximation to the values recommended in the standards and guidelines.

A summary of the results obtained during this work is given in Table 4-12.

Table 4-12 Summary of the obtained results

Mechanical properties	Unit	Obtained value Austria Clay	Obtained value Dubai Region Clay
Compressive strength	N/mm ²	2	2.7
Flexural strength	N/mm ²	----	0.9
Binding force	N	90	120
Elasticity modulus	N/mm ²	3000 - 4000	----
Shear strength	N/mm ²	0.01-0.05	----

5. DEVELOPMENT OF THE ANALYTICAL AND NUMERICAL MODEL FOR SEISMIC LOADS

This chapter describes the principal methods used to calculate the internal shear forces and deformations in structures due to earthquake effects.

In order to evaluate the linear and non-linear methods of application and detection used in the real world for real structures, a historical clay mosque was investigated using the four calculation methods. The EN 1998 standard codes have been used for implementing the methods and comparing the results. The EN 1998 standard codes were chosen because they are commonly used in the Arab world.

The aim of the variant study is to identify possible means by which the non-linear load capacity reserves, which are demonstrated by the deformation-based assay, can be made available for linear detection methods. It will investigate and evaluate the margins between the different detection methods and compared to fully non-linear deformation-based calculation in practice and whether it is possible and useful to develop simplified factors for non-linear reserves.

The building chosen for implementing the theories is a historical mosque in Dubai and consists of three separate rooms. The prayer room has been chosen for the analysis procedure.

The load-bearing walls are made entirely of clay unreinforced masonry, with a thin layer of clay for the roof and a wood balcony.

Part of this chapter is the implementation of the Solid Works program used for evaluating the different methods.

The building is located on strong stone ground at Hatta village in Dubai. According to the EC8, the ground condition is to be considered as Type A-1, and according to the national seismic network in Dubai [34], the reference peak ground acceleration (PGA) in this Zone is 1.66 m/s^2 (see Figure 5-1).

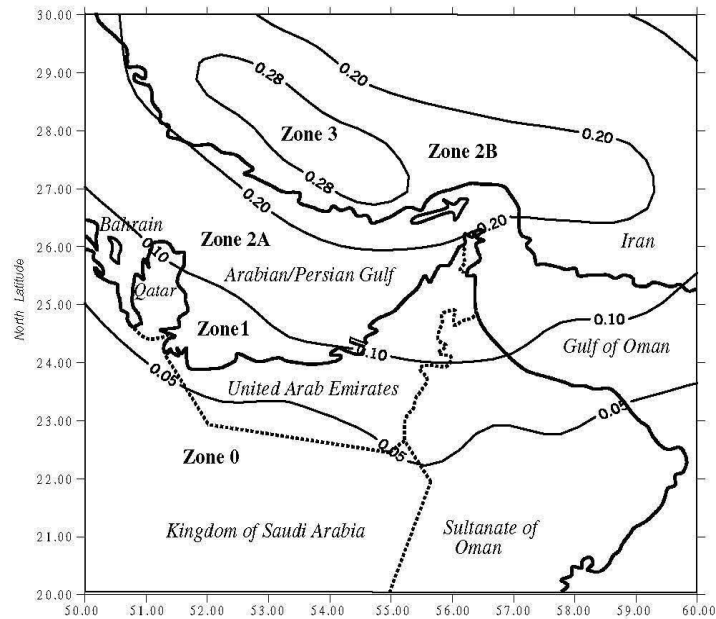


Figure 5-1 Dubai seismic zones [35]

In practice, there are four main calculating methods:

1. Equivalent lateral force method
2. Response spectrum method
3. Pushover-curve method
4. Time history method

The following is a brief overview of some points where the EN 1998 differs from the United States of America Standards for implementation of earthquake methods.

Analysed Standards

Comparing texts that has various seismic standards that have been analysed portrays the basic accord concerning the principle elements of a framework of seismic resistant; for instance, simplicity, equilibrium, homogeny and redundancies among others.

ASCE (2006) [36] states that the established principles for seismic plan of building various structures that are used in the comparative evaluation include the Euro code 8 – EN 1998-1:2004 and American Standard – ASCE. This paper has effectively discussed various details regarding the application of the two standards.

Comparative Analysis

1. Defining Recurrence Periods that are used in defining Seismic Input

Researchers have advanced various criteria in various codes in trying to define the periods of recurrence (ASCE, 2006). American Public Transport Association (1999) [37] states that for the framework of non-collapse requirements, Euro code 8 propose four hundred and seventy five year's recurrence period consideration. This matches to a likelihood of ten percent of seismic contribution being surpassed in fifty years. It should be noted that the basic accelerations incorporated for this plan range from 0.025g to around 0.15g. Scholars argue that the American benchmark known as ASCE describes a period of recurrence of around 2475 years. This matches with a possibility of about two percent of the seismic contributions that surpass in fifty years; however, economic factors makes this principles to make room for a cutback factor of about two thirds which is used in the ensuing values for the seismic plan forces. Scholars contend that in the territory of the Americans, the design's Design ground accelerations range from 0.024g to 0.80g.

2. Defining Seismic Zonation and Seismic Ground Motion Values

The definition of seismic zonation for every national authority is a responsibility that is transferred by the Euro code 8. In this principle, only one parameter gives the definition for local seismicity. This is a value that is referred to as ZPA (Zero Period Acceleration), which is used for positioning peak ground acceleration to the rock ground (a_g). Scholars contend that in ASCE standard, experts defines seismic input through three fundamental parameters, that is, using peak ground accelerations which is often meant for spectral periods of around 0.2s and 1.0s. The other parameter is the period T_D which often defines the disarticulation which is the managed spectrum region. It is important to note that in the standards, these constraints are defined through various detailed maps.

3. Definition of Horizontal Elastic Response Spectra Shape

In the elastic response range of the Euro code 8 and in other analysed standard's elastic ranges, the pseudo-accelerations which are denoted by (S_e) are taken to be structural periods' (T) function. The range diverge from the peak ground acceleration (a_g) in a proportional manner, multiplied by a coefficient of soil (S), linked to the amplification of soil and then one makes consideration of the parameter η ; this is the damping values'

correction factor that is diverse from 5%. Other analysed principles usually consider the normal structural damping while defining the spectra [38]. See figure (5-2).

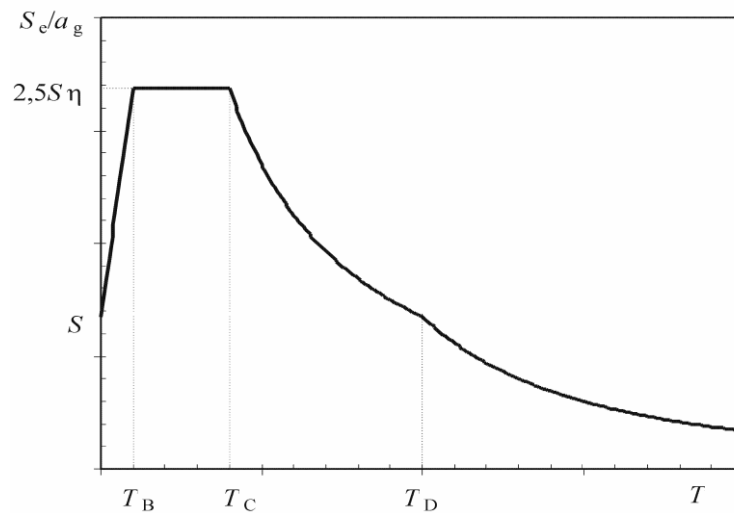


Figure 5-2 the elastic response spectrum's shape of 5%

There is a constant acceleration (acceleration controlled) which is explained in the region that is between T_B and T_C reference periods. This region represent the periods that are superior to T_D and it is the displacement governed (that is, accelerations changing was T_2 inverse changes).

The changeover region which is between the utmost spectral accelerations and the peak ground acceleration is the one which is between 0 (referred to as ZPA or the zero period acceleration) and T_B . It is worth mentioning that S , T_B , T_C and T_D values are considered a function of the subsoil type which is in the two types of spectra as defined in the code. Type 2 and type 1, are respectively linked to lower and higher regions of seismicity respectively.

Cardone, and Dolce [39] state that in ASCE and Euro code 8, the relationship (denoted by β) between the structure's maximum acceleration and the upper limit ground acceleration need to be 2.5. ASCE (2006) defines the peak ground accelerations' (a_g) specific values, parameters β , as well as the period T_C and T_D via the maps.

4. Specific Soil Conditions Consideration

Scholars contend that the conditions of the grounds are classified by the entire analysed standards in accordance to the cut off wave proliferation velocities (v_s) as well as to the blows' number in the pattern Penetration Test. In case of the sites that are non-homogeneous, the perimeters' averaging criteria in various exterior subsoil layers (characteristically in the initial 30m) are projected in the principles. The classes of soil, ranging from very rigid to deposits that are soft, are in the classes of Euro code 8 classes that start from A to E and S1 versus S2. It should be noted that in ASCE, they often range from A to F. ASCE (2006) contend that the amplification of seismic soil either more or fewer stiff layers determines the response spectra shape's definition. Experts note that in fewer stiff soil deposits, there is higher amplification and this leads to superior soil coefficient (S) values. Scholars agree that every analysed standard describe a separate liquefiable soils' class (for instance, Class S2 which is in the Euro code 8). ASCE is the only standard that considers interaction of Soil-structure.

5. Classification of Structures in various Vital Levels

The entire analysed standards acknowledge the importance of categorizing the structures in vital Classes. Agarwal and Shrikhande [38] argue that this is helpful in the reliability differentiation in accordance with the estimated uncertainties and costs associated with a failure. The reliability differentiation in the standards can be defined basically through the multiplying factor application to the assessed seismic forces. The standard also defines 3 or 4 vital Classes. Scholars argue that in these classes, the $\gamma = 1$ is a factor that is assigned to common frameworks, for instance the residential and business buildings. Euro code 8 defines four paramount Classes and usually factor γ changes in both principles that range from $\gamma = 0.8$ to $\gamma = 1.4$. There are also uncertainty Categories which are I to IV especially in case of ASCE. Basically factor γ ranges between $\gamma = 1.0$ and $\gamma = 1.5$.

6. Seismic Force-resisting Systems and Subsequent Response Modification Coefficients

Cardone, and Dolce [39] agree that analysed standards acknowledge the impracticality of expecting the frameworks to behave in a simply elastic manner. In the seismic excitation, various frameworks are anticipated to be in a range that is non-linear, thus creating large twists and scattering a huge energy amount. Therefore, the structures need to be planned

and comprehensive in the verge of ensuring that the essential energy dissipation capacity ensures. So long as the essential extent of ductility prevails, elastic spectra's transformation in the spectra design can be considered; in this case the ductility that has been considered should be implied. The entire principles consider the aspects of the reduction as a structural systems' function as well as a function of the structural materials. Generally, the reduction aspects ('R' in the ASCE code and 'q' in Euro code 8) are significantly considered a function of classes of ductility (such as the medium and elevated ductility that is in Euro code 8 as well as a regular, transitional and particular detailing especially in the ASCE). Both, Dubinsky and Hil [40] state that the coefficients' numerical value is normally can be defined empirically in the principles based on the past experience and on the basis of good engineering judgments. It should be mentioned that the behaviour factor range in the Euro code should be between 1 and 3.5.

7. Structural Irregularities and the legitimate seismic analysis's Procedures

It is acknowledged that the analysed principles strictly recommends various fundamental standards in the construction's conceptual plan as stipulated in Euro code 8's item 4.2.1. these principles include structural straightforwardness, homogeneity and design's and evaluation's regularity, bi-directional shiftiness and torsional resistance, sufficient foundation, and floor plain's diaphragmatic. Sonja [41] states that Irregularity in the design or elevation are not favoured by the principles, which calls for additional elaborated analysis approaches, extra rigorous criteria that puts design forces into among others. For simple and standard structures, various analyzed standards make it possible for a creative force (static correspondent) analysis approach especially when the fundamental mode's contribution in every horizontal course becomes preponderant in forceful reaction. The analyzed standards offer various formulas that approximate assessment of basic structure's periods. For the structures that are regular, it is allowed to have two planar methods, one for every horizontal direction.

Cardone, and Dolce [39] state that all evaluated standards make it possible to use modal reaction spectrum evaluation. Moreover, in every analysed principle, the accepted numbers of measured modes warrants that not less than 90% of the entire structure's mass can be considered in every direction considered as orthogonal horizontal. For the modal

components' arrangement, the rule of Complete Quadratic Combination (CQC) is the most preferred one in approximately all the principles. ASCE has a restriction in those structural periods that are achieved methodically, through contrasting them with obtained periods as well as the estimated pragmatic appraisal formulas.

Scholars contend that the standards enables the linear time-history evaluation and this uses recorded as well as simulated time-histories that matches with the design reaction spectra, which is applied concurrently in at least to the two directions that are horizontal (Agarwal and Shrikhande). There are codes (such as Euro code 8) that utilize the non-linear evaluation in the domain of time; however, they need to be validated with respect to extra conventional approaches. There are some codes (such as the Euro code 8) that make it possible for static analysis that is non-linear (pushover). The ASCE standards accept the association between the outcomes attained with the evaluation of time history and with those achieved while using the spectral analysis.

5.1 MODIFICATION OF EQUIVALENT LATERAL FORCE METHOD FOR CLAY BUILDING

5.1.1 Material Characteristics

All the material characteristics used in the analytical evaluation are mean values obtained through the experiments of this work.

a) Load-bearing walls:

Clay density: $\rho = 2000 \text{ kg/m}^3$

Clay compressive strength: $f = 2.1 \text{ N/mm}^2$

Elasticity modulus is:

$E = 4000 \text{ N/mm}^2$

Shear modulus G according to EC8-1 as follows:

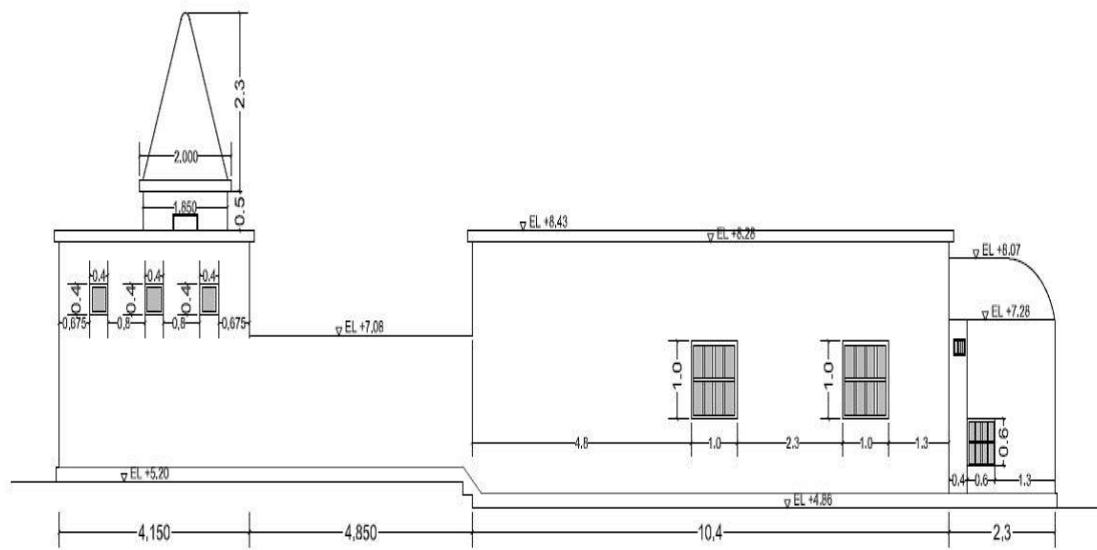
$G = 0.21 * E$

$G = 0.21 * 4000 = 840 \text{ N/mm}^2$

b) Ceiling:

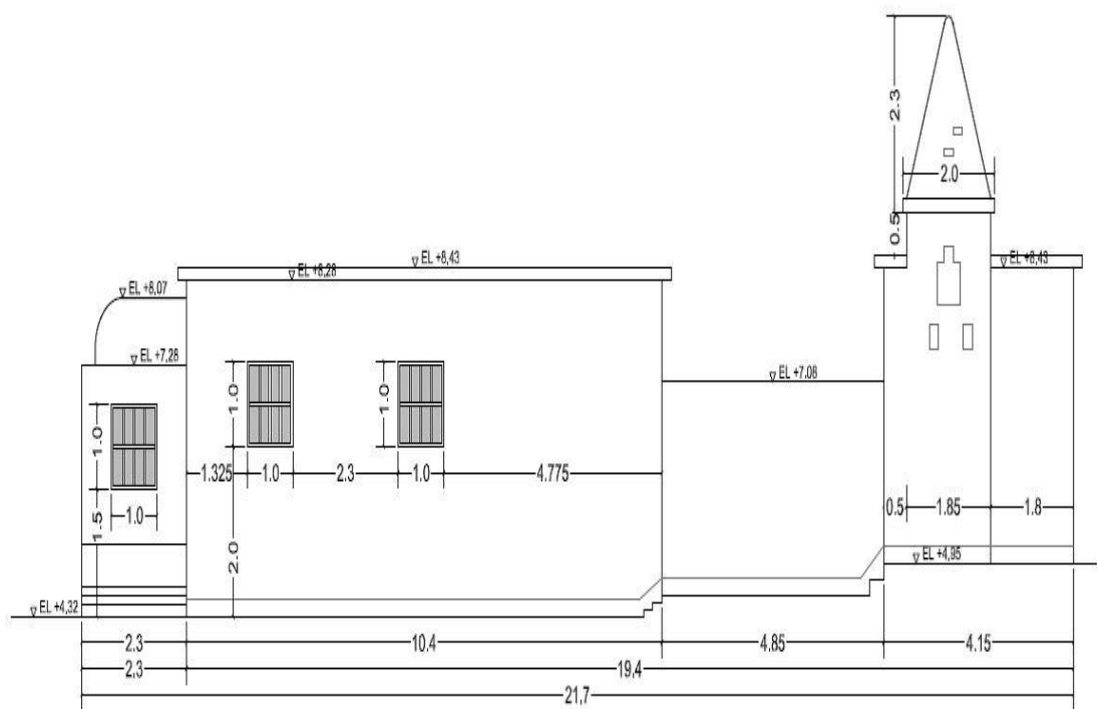
Clay layer density: $\rho = 2000 \text{ kg/m}^3$

Wooden stick density: $\rho = 500 \text{ kg/m}^3$



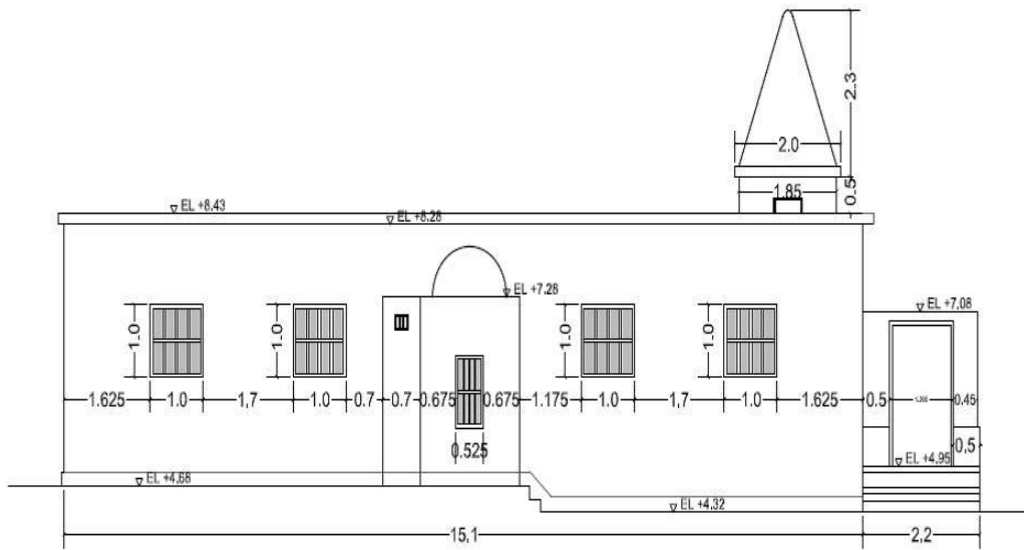
NORTH ELEVATION

Figure 5-4 North View



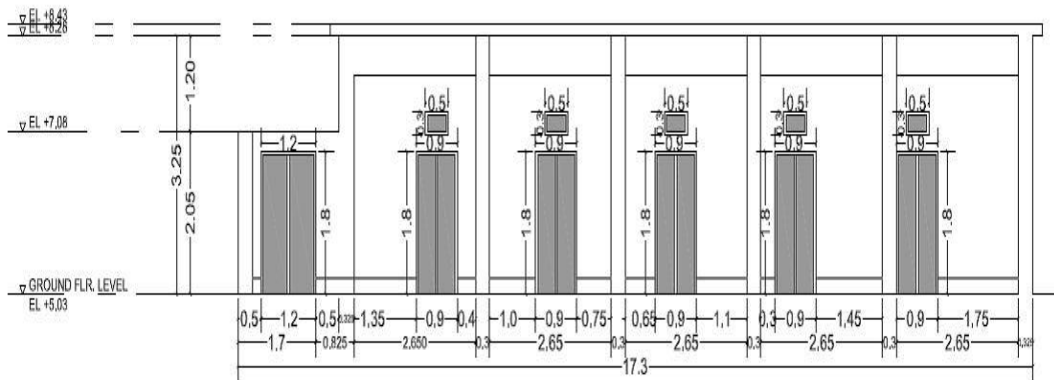
SOUTH ELEVATION

Figure 5-5 South View



WEST ELEVATION

Figure 5-6 West View

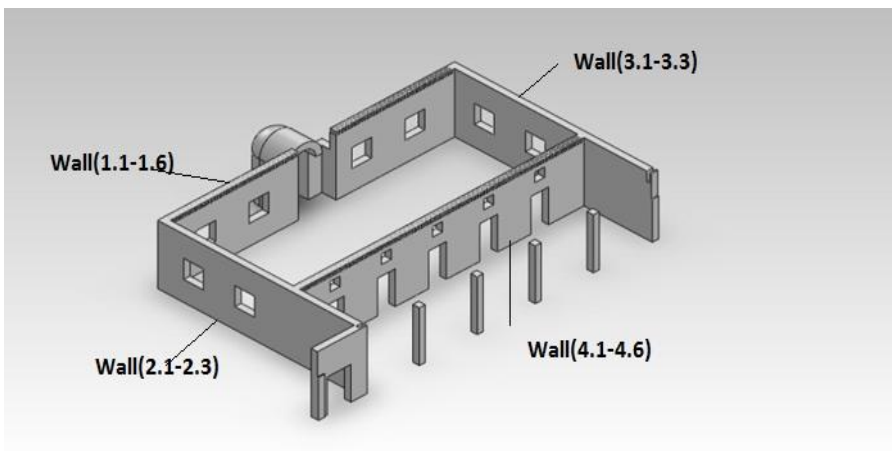


SECTION ELEVATION

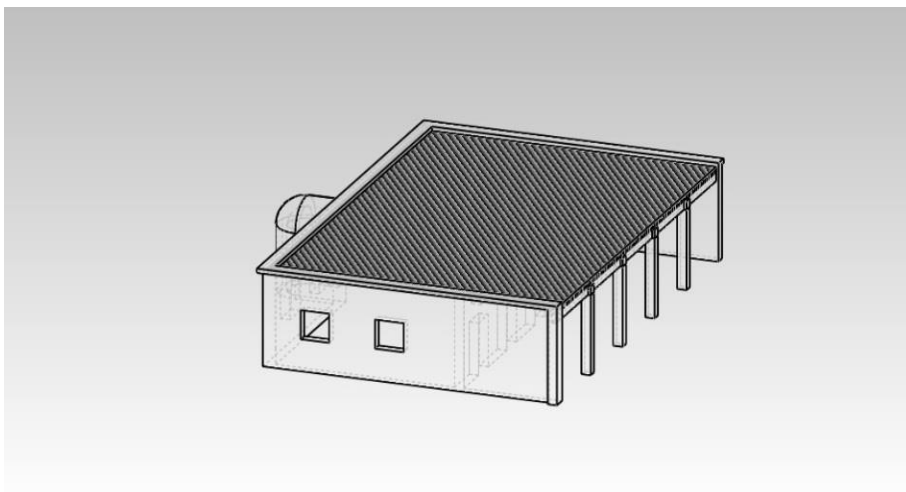
Figure 5-7 Door View Section



(a)



(b)



(c)

Figure 5-8 (a, b and c) Prayer Hall

5.1.3 Loads

The load distribution for the building, figure (5-9) has been calculated as follows:

a) Ceiling and roof

For wood ceilings with a thickness of $d = 0.13 \text{ m}$ ($= 0.105 \text{ m} + 0.025 \text{ m}$) and for the roof's clay layer with a mean thickness of $d = 0.02 \text{ m}$, the loads may be taken as:

i. Dead loads:

Construction loads: 1 kN/m^2

Clay layer loads: $g_k = 0.02 \cdot 19.62 = 0.392 \text{ kN/m}^2$

Wooden ceiling loads: $g_k = 0.025 \cdot 4.9 = 0.1225 \text{ kN/m}^2$

ii. Wooden beams

Wooden beams loads: $g_k = 0.105 \cdot 4.9 = 0.5145 \text{ kN/m}^2$

Number of wooden beams: 90 pcs

Beam thickness = 0.105 m (as a mean value for the wooden beam)

Beam width = 0.08 m

Beam Length = 9.75 m

iii. Wood base

Wood base loads (above the four clay column):

Number of wooden bases: 4 pcs

Wood base thickness = 0.3 m

Wood base area = 0.0975 m^2

iv. Horizontal wooden beams

Horizontal wooden beam loads (between the columns): 5 pcs

Horizontal wooden beam thickness = 0.3 m

Horizontal wooden beam width = 0.15 m

Horizontal wooden beam length = 2.65 m

v. Life loads:

Because the mosque is constructed in an arid desert where the wind effect should be taken in consideration, the live load value considered here is the live load plus the wind load. $q_k = 2 \text{ kN/m}^2$

b) Walls

Wall thickness is 0.325m.

Wall dead load: $g_k = 19.62 \cdot 0.325 = 6.38 \text{ kN/m}$

c) Columns

Column thickness is 0.325 m.

Number of columns: 4 pcs

Column height = 2.8 m

The column dead load is : $g_k = 19.62 \cdot 0.325 = 6.38 \text{ kN/m}^2$

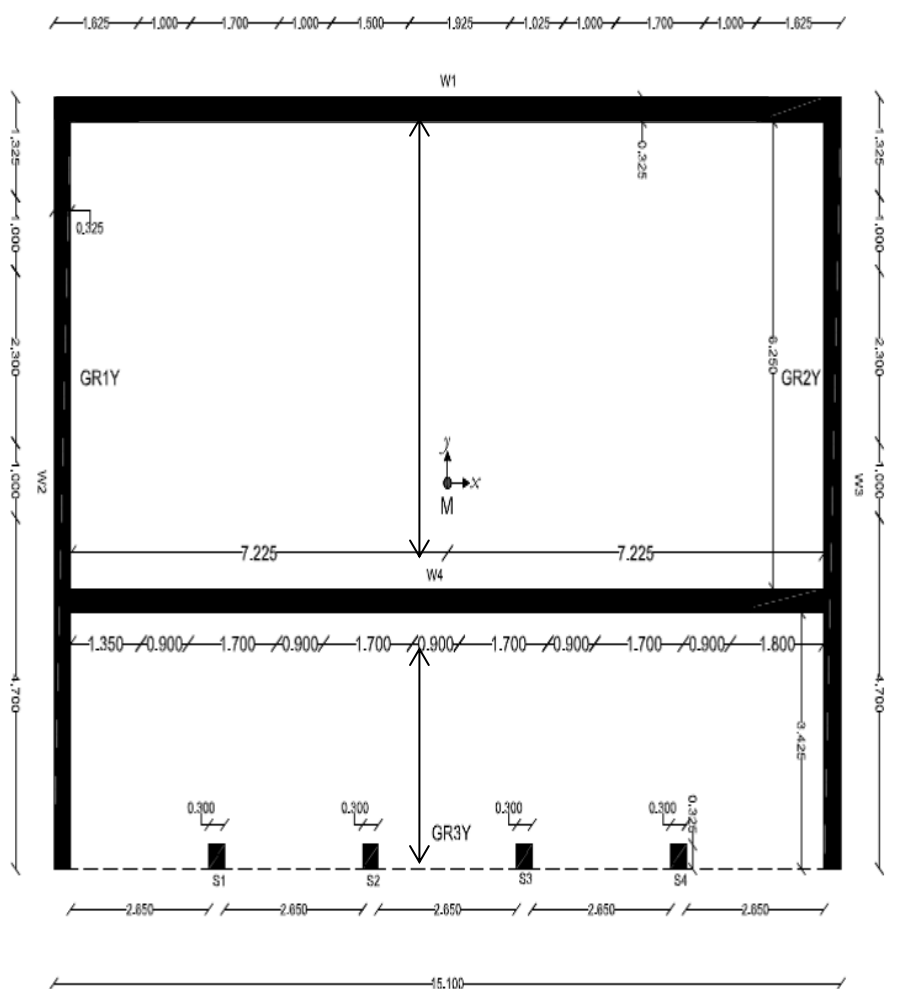


Figure 5-9 Ceiling and roof overloaded distribution

5.1.4 Mass Calculation

Table 5-1 Mass calculation

		Roof & ceiling					Walls						Column					Σ Mass	
	H	A	$\psi E_i q_k$	$Q_{roof(ceiling)}$	Σg_k	$G=$	l_w	A_w	W_{DB}	A_{ow}	V_w	G_w	H	A_{ST}	$\psi E_i q_k$	$Q_{roof(ceiling)}$	g_k	$G_{ceiling=}$	$\Sigma G + \Sigma \psi E_i Q$
			$\psi E_i q_k A$	$g_k A$															
	m	m ²	kN/m ²	kg	kN/m ²	kg	m	m ²	m ²	m ²	m ³	kg	m	m ²	kN/m ²	kg	kN/m ²	kg	kg
EG	3.1	145.95	0.6	8926.299694	1.5475	27884.5	50.25	155.78	19.88	135.9	44.166	94982.2	2.8	0.84	0	0	6.5	556.5749	132349.5375

Where:

- H Height of the building
- A Floor Area
- ψE_i Combination factor for live loads
- q_k Live loads
- g_k Dead loads
- A_{ST} Column area
- l_w Wall length, $l_w = (2 \times 14.45) + (2 \times 10.075) (0.3 \times 4) + = 50.25m$
- A_w Wall area (wall length x height of influence)
- W_{DB} Wall opening area
- A_{OW} Net wall area (wall area less W_{DB})
- V_w Wall volume

5.1.5 Geometric characteristic data

The geometrical cross-section data of the building can be determined in the direction of the coordinate system represented in Figure (5-9).

The moment of inertia, I_y , about the y-axis is as follows:

$$I_y = \sum (I_{y,i} + A_i \cdot x_{is}^2) \quad 5-1$$

The moment of inertia, I_x , about the x-axis is as follows:

$$I_x = \sum (I_{x,i} + A_i \cdot y_{is}^2) \quad 5-2$$

Where:

- I_y Geometrical moment of inertia about the y-axis of ith part

A_i Surface area of i th part

x_{is} Distance from the center of gravity of the i th part to the center of gravity of the building

$I_{x,i}$ Moment of inertia about the x-axis of the i th part

y_{is} Distance from the center of gravity of the i th part to the center of gravity of the building

The equivalent moment of inertia I_e is given by:

$$I_e = \left(\frac{1}{I} + \frac{27 \cdot E}{4 \cdot G \cdot A_c \cdot H^2} \right)^{-1} \quad 5-3$$

The stiffness center x_s, y_s has the following coordinates:

$$x_s = \frac{\sum (I_{x,i} \cdot x_i)}{\sum I_{x,i}} \quad 5-4$$

$$y_s = \frac{\sum (I_{y,i} \cdot y_i)}{\sum I_{y,i}} \quad 5-5$$

The polar moment of inertia I_{pm} at a constant height, h , and constant density, ρ , gives the polar moment of inertia for walls with:

$$I_{pm} = \int (x^2 + y^2) dm = \int (x^2 + y^2) \rho \cdot dV = \int (x^2 + y^2) \rho \cdot h \cdot dA = \rho \cdot h (I_x + I_y) \quad 5-6$$

This expression can also be used to calculate the polar moment of inertia of ceilings, but instead of h the ceiling thickness, d , must be used.

The torsion radii r_x, r_y are:

$$r_x = \sqrt{\frac{\sum (I_{x,i} \cdot x_i^2) + \sum (I_{y,i} \cdot y_i^2)}{\sum I_{y,i}}} \quad 5-7$$

$$r_y = \sqrt{\frac{\sum (I_{x,i} \cdot x_i^2) + \sum (I_{y,i} \cdot y_i^2)}{\sum I_{x,i}}} \quad 5-8$$

The radius of gyration I_s of the floor mass is given by:

$$l_s = \sqrt{\frac{I_{pm}}{m}}$$

5-9

5.1.6 Building Geometric characteristic data

Geometric data for earthquake loads in the x-direction

Clay walls E-modulus: $E_{\text{clay wall}} = 4000 \text{ N/mm}^2$

Clay walls shear modulus: $G_{\text{clay wall}} = 840 \text{ N/mm}^2$

Wall height: $H = 3.1 \text{ m}$

Wall thickness: $d = 0.325 \text{ m}$

For further calculation, table (5-2) and (5-3) the coordinate origin is assumed to be at the center of mass.

Table 5-2 Determination of geometric data for earthquake loads in the x-direction

Wall G.Date		Wall number																							
		1.1	1.2	1.3	1.4	1.5	1.6	2.1	2.2	2.3	3.1	3.2	3.3	4.1	4.2	4.3	4.4	4.5	4.6	S1	S2	S3	S4	Σ	
b	m	0.325	0.325	0.325	0.325	0.325	0.325	1.325	2.3	4.375	1.325	2.3	4.375	0.325	0.325	0.325	0.325	0.325	0.325	0.325	0.325	0.325	0.325		
h	m	1.300	1.7	1.5	1.025	1.7	1.3	0.325	0.325	0.325	0.325	0.325	0.325	1.350	1.7	1.7	1.7	1.7	1.8	0.300	0.300	0.300	0.300		
lwi	m																								
&																									
Ac	m2	11.594																							
Ai=b.h	m2	0.423	0.553	0.4875	0.3331	0.553	0.423	0.431	0.7475	1.4219	0.431	0.7475	1.422	0.439	0.553	0.553	0.553	0.553	0.585	0.098	0.098	0.098	0.098	11.594	
loy	m4	0.060	0.133	0.0914	0.0292	0.133	0.06	0.004	0.0066	0.0125	0.004	0.0066	0.013	0.067	0.133	0.133	0.133	0.133	0.158	0.001	0.001	0.001	0.001	1.311	
xsi	m	-6.600	-4.08	-1.64	1.64	4.08	6.6	-7.400	-7.400	-7.400	7.400	7.400	7.400	-6.550	-4.125	-1.53	1.525	4.125	6.33	-4.425	-1.475	1.475	4.425		
ysi	m	5.030	5.030	5.030	5.030	5.030	5.030	4.500	1.725	-3	4.500	1.725	-3	-1.540	-1.540	-1.540	-1.540	-1.540	-1.540	-5.030	-5.030	-5.030	-5.030		
Ai.xsi	m3	-2.789	-2.254	-0.8	0.5463	2.254	2.789	-3.187	-5.532	-10.52	3.187	5.5315	10.52	-2.874	-2.279	-0.84	0.843	2.279	3.7031	-0.431	-0.144	0.144	0.431	0.576	
Ai.ysi	m3	2.125	2.779	2.4521	1.6756	2.779	2.125	1.938	1.2894	-4.266	1.938	1.2894	-4.27	-0.676	-0.851	-0.85	-0.85	-0.85	-0.901	-0.490	-0.490	-0.490	-0.490	4.918	
Ai.xsi^2	m4	18.404	9.197	1.3112	0.896	9.197	18.4	23.581	40.933	77.862	23.581	40.933	77.86	18.823	9.401	1.285	1.285	9.401	23.44	1.909	0.212	0.212	1.909	410.040	
xs	m																							0.050	
ys	m																							0.424	
(xsi-xs)^2.Ai	m4	18.682	9.422	1.392	0.843	8.975	18.128	23.899	41.485	78.911	23.265	40.385	76.820	19.110	9.629	1.370	1.203	9.176	23.074	1.952	0.227	0.198	1.866	122.825	
Isy	m4	18.742	9.556	1.483	0.872	9.108	18.188	23.903	41.491	78.923	23.269	40.392	76.832	19.177	9.762	1.503	1.336	9.309	23.232	1.953	0.227	0.199	1.867	411.323	
loy.ysi	m5	0.299	0.669	0.4598	0.1467	0.669	0.299	0.017	0.0113	-0.038	0.017	0.0113	-0.04	-0.103	-0.205	-0.2	-0.2	-0.2	-0.243	-0.004	-0.004	-0.004	-0.004	1.345	
y shear	m																							1.026	
Isye	m4	0.125	0.162	0.133	0.089	0.162	0.125	0.128	0.222	0.423	0.128	0.222	0.423	0.130	0.162	0.149	0.147	0.162	0.174	0.029	0.026	0.025	0.029	3.377	
Isye.yshear	m5	0.129	0.167	0.136	0.092	0.166	0.129	0.131	0.228	0.434	0.131	0.228	0.434	0.134	0.167	0.153	0.151	0.167	0.178	0.029	0.027	0.026	0.029	3.464	

Where:

h, b	Dimensions of the wall
A_i	Wall area
I_{oy}, I_{ox}	Wall moment of inertia
X_{si}, Y_{si}	Coordinates of the centroid of the wall i
X_s, Y_s	Coordinates of the centre
I_{sy}, I_{sx}	Moment area of inertia
Y_{shear}	Shear centre
I_{sye}	Equivalent moment of inertia

Table 5-3 Determination of geometric data for earthquake loads in the y-direction

Wall G.Date		Wall number																							
		1.1	1.2	1.3	1.4	1.5	1.6	2.1	2.2	2.3	3.1	3.2	3.3	4.1	4.2	4.3	4.4	4.5	4.6	S1	S2	S3	S4	Σ	
b	m	0.325	0.325	0.325	0.325	0.325	0.325	1.325	2.3	4.375	1.325	2.3	4.375	0.325	0.325	0.325	0.325	0.325	0.325	0.325	0.325	0.325	0.325		
h	m	1.300	1.7	1.5	1.025	1.7	1.3	0.325	0.325	0.325	0.325	0.325	0.325	1.350	1.7	1.7	1.7	1.7	1.8	0.300	0.300	0.300	0.300		
lwi	m																								
&																									
Ac	m2																								
Ai=b.h	m2	0.423	0.553	0.488	0.333	0.553	0.423	0.431	0.748	1.422	0.431	0.748	1.422	0.439	0.553	0.553	0.553	0.553	0.585	0.098	0.098	0.098	0.098	11.594	
lox	m4	0.004	0.005	0.004	0.003	0.005	0.004	0.063	0.330	2.268	0.063	0.330	2.268	0.004	0.005	0.005	0.005	0.005	0.005	0.001	0.001	0.001	0.001	5.377	
xsi	m	-6.600	-4.08	-1.64	1.64	4.08	6.6	-7.400	-7.400	-7.400	7.400	7.400	7.400	-6.550	-4.125	-1.53	1.525	4.125	6.33	-4.425	-1.475	1.475	4.425		
ysi	m	5.030	5.030	5.030	5.030	5.030	5.030	4.500	1.725	-3	4.500	1.725	-3	-1.540	-1.540	-1.540	-1.540	-1.540	-1.540	-5.030	-5.030	-5.030	-5.030		
Ai.xsi	m3	-2.789	-2.254	-0.800	0.546	2.254	2.789	-3.187	-5.532	-10.522	3.187	5.532	10.522	-2.874	-2.279	-0.843	0.843	2.279	3.703	-0.431	-0.144	0.144	0.431	0.576	
Ai.ysi	m3	2.125	2.779	2.452	1.676	2.779	2.125	1.938	1.289	-4.266	1.938	1.289	-4.266	-0.676	-0.851	-0.851	-0.851	-0.851	-0.901	-0.490	-0.490	-0.490	-0.490	4.918	
Ai.ysi^2	m4	10.690	13.979	12.334	8.428	13.979	10.690	8.720	2.224	12.797	8.720	2.224	12.797	1.041	1.310	1.310	1.310	1.310	1.387	2.467	2.467	2.467	2.467	135.118	
xs	m																							0.050	
ys	m																							0.424	
(ysi-ys)^2.Ai	m4	8.963	11.721	10.342	7.067	11.721	8.963	7.154	1.265	16.671	7.154	1.265	16.671	1.693	2.131	2.131	2.131	2.131	2.257	2.900	2.900	2.900	2.900	133.033	
lsx	m4	8.967	11.725	10.346	7.070	11.725	8.967	7.217	1.594	18.939	7.217	1.594	18.939	1.697	2.136	2.136	2.136	2.136	2.262	2.901	2.901	2.901	2.901	138.410	
lox.xsi	m5	-0.025	-0.020	-0.007	0.005	0.020	0.025	-0.466	-2.438	-16.783	0.466	2.438	16.783	-0.025	-0.020	-0.007	0.007	0.020	0.033	-0.004	-0.001	0.001	0.004	0.005	
x shear	m																							0.001	
lsxe	m4	0.125	0.163	0.144	0.098	0.163	0.125	0.126	0.196	0.416	0.126	0.196	0.416	0.122	0.153	0.153	0.153	0.153	0.162	0.029	0.029	0.029	0.029	3.306	
lsxe.x shear	m5	0.000	0.000	0.000	0.000	0.000	0.000	0.000	0.000	0.000	0.000	0.000	0.000	0.000	0.000	0.000	0.000	0.000	0.000	0.000	0.000	0.000	0.000	0.000	

Where:

h, b	Dimensions of the wall
A_i	Wall area
I_{oy}, I_{ox}	Wall moment of inertia
X_{si}, Y_{si}	Coordinates of the centroid of the wall i
X_s, Y_s	Coordinates of the centre
I_{sy}, I_{sx}	Moment area of inertia
X_{shear}	Shear centre I_{sxe}
I_{sxe}	Equivalent moment of inertia

The Determination of the shear areas and moments of inertia is in table (5-4) below.

Table 5-4 Determination of the shear areas and moments of inertia

Prayers Hall			H =	3.1								
	b	H	A	I_{oy}	I_{ox}	X_{sm}	Y_{sm}	I_{ym}	I_{xm}	$A_{c,x}$	$A_{c,y}$	
Wall #	m	M	m^2	m^4	m^4	m	m	m^4	m^4	m^2	m^2	
w1	1.1	0.325	1.3	0.4225	0.0595	0.0037	-6.6497	4.606	18.742	8.96655	0.42	
	1.2	0.325	1.7	0.5525	0.1331	0.0049	-4.1297	4.606	9.5556	11.7255	0.55	
	1.3	0.325	1.5	0.4875	0.0914	0.0043	-1.6897	4.606	1.4832	10.346	0.49	
	1.4	0.325	1.025	0.33313	0.0292	0.0029	1.5903	4.606	0.8717	7.06978	0.33	
	1.5	0.325	1.7	0.5525	0.1331	0.0049	4.0303	4.606	9.1076	11.7255	0.55	
	1.6	0.325	1.3	0.4225	0.0595	0.0037	6.5503	4.606	18.188	8.96655	0.42	
w2	2.1	1.325	0.325	0.43063	0.0038	0.063	-7.4497	4.076	23.903	7.21676		0.431
	2.2	2.3	0.325	0.7475	0.0066	0.3295	-7.4497	1.301	41.491	1.59444		0.748
	2.3	4.375	0.325	1.42188	0.0125	2.268	-7.4497	-3.424	78.923	18.9392		1.422
w3	3.1	1.325	0.325	0.43063	0.0038	0.063	7.3503	4.076	23.269	7.21676		0.431
	3.2	2.3	0.325	0.7475	0.0066	0.3295	7.3503	1.301	40.392	1.59444		0.748
	3.3	4.375	0.325	1.42188	0.0125	2.268	7.3503	-3.424	76.832	18.9392		1.422
w4	4.1	0.325	1.35	0.43875	0.0666	0.0039	-6.5997	-1.964	19.177	1.69652	0.44	
	4.2	0.325	1.7	0.5525	0.1331	0.0049	-4.1747	-1.964	9.762	2.13636	0.55	
	4.3	0.325	1.7	0.5525	0.1331	0.0049	-1.5747	-1.964	1.5031	2.13636	0.55	
	4.4	0.325	1.7	0.5525	0.1331	0.0049	1.4753	-1.964	1.3356	2.13636	0.55	
	4.5	0.325	1.7	0.5525	0.1331	0.0049	4.0753	-1.026	9.3091	0.58633	0.55	
	4.6	0.325	1.8	0.585	0.158	0.0051	6.2803	-1.964	23.232	2.26202	0.59	
S1	0.325	0.3	0.0975	0.0007	0.0009	-4.4747	-5.454	1.953	2.90127		0.098	
S2	0.325	0.3	0.0975	0.0007	0.0009	-1.5247	-5.454	0.2274	2.90127		0.098	
S3	0.325	0.3	0.0975	0.0007	0.0009	1.4253	-5.454	0.1988	2.90127		0.098	
S4	0.325	0.3	0.0975	0.0007	0.0009	4.3753	-5.454	1.8672	2.90127		0.098	
Σ					1.3112	5.3773			411.32	136.86	6	5.59

Where:

h, b Dimensions of the wall

A Wall surface area

I_{oy}, I_{ox} Wall moment of inertia

I_{ym}, I_{xm} Moment of inertia about the centre of mass

A_{cx}, A_{cy} Effective area

As a consequence, the following quantities are necessary for the assessment of the structural regularity in plan.

Equivalent moment of inertia:

$$\sum I_{sxe} = 3.31 \text{ m}^4$$

$$\sum I_{sye} = 3.38 \text{ m}^4$$

Shear effective cross-section area for the replacement bar:

$$A_{cx} = 6.0 \text{ m}^2$$

$$A_{cy} = 5.59 \text{ m}^2$$

Moments of inertia around the center of mass for the equivalent bar:

$$\sum I_{xm} = 136.86 \text{ m}^4$$

$$\sum I_{ym} = 411.32 \text{ m}^4$$

The coordinates of the center of stiffness according to the equivalent moments of inertia:

$$x_s = 0.049 \text{ m} \quad e_{0x} = 0.0487 \text{ m}$$

$$y_s = 0.42 \text{ m} \quad e_{0y} = 0.601 \text{ m}$$

Torsion radii with equivalent moments of inertia are given as follows:

$$r_x = \sqrt{\frac{\sum (I_{ex,i} \cdot x_i^2) + \sum (I_{ey,i} \cdot y_i^2)}{\sum I_{ey,i}}}$$

5-10

$$r_y = \sqrt{\frac{\sum (I_{ex,i} \cdot x_i'^2) + \sum (I_{ey,i} \cdot y_i'^2)}{\sum I_{ex,i}}}$$

5-11

Torsion radii with equivalent moments of inertia presented in table (5-5):

Table 5-5 Determine of the Torsion radii according to the stiffness center

Determination of torsion radii:							
Wall #	x _i '	y _i '	I _{sxe}	I _{syx}	I _{sxe} ·x _i ' ²	I _{syx} ·y _i ' ²	
	m	m	m ⁴	m ⁴	m ⁶	m ⁶	
w1	1.1	-6.600943	4.004123	0.12456	0.1255	5.4275	2.0117
	1.2	-4.080943	4.004123	0.16289	0.1624	2.7128	2.6034
	1.3	-1.640943	4.004123	0.14373	0.1327	0.387	2.1278
	1.4	1.639057	4.004123	0.09821	0.0894	0.2639	1.4331
	1.5	4.079057	4.004123	0.16289	0.1622	2.7103	2.6012
	1.6	6.599057	4.004123	0.12456	0.1254	5.4244	2.0113
w2	2.1	-7.400943	3.474123	0.12649	0.1281	6.9284	1.5456
	2.2	-7.400943	0.699123	0.19601	0.2223	10.736	0.1086
	2.3	-7.400943	-4.02588	0.41578	0.4228	22.774	6.8531
w3	3.1	7.399057	3.474123	0.12649	0.128	6.9249	1.5454
	3.2	7.399057	0.699123	0.19601	0.2223	10.731	0.1086
	3.3	7.399057	-4.02588	0.41578	0.4228	22.762	6.8521
w4	4.1	-6.550943	-2.56588	0.12176	0.1303	5.2254	0.8578
	4.2	-4.125943	-2.56588	0.15333	0.1624	2.6102	1.0694
	4.3	-1.525943	-2.56588	0.15333	0.1488	0.357	0.9798
	4.4	1.524057	-2.56588	0.15333	0.147	0.3561	0.9678
	4.5	4.124057	-2.56588	0.15333	0.1623	2.6078	1.0686
	4.6	6.329057	-2.56588	0.16235	0.1736	6.5032	1.1429
S1	-4.425943	-6.05588	0.02886	0.0287	0.5653	1.0533	
S2	-1.475943	-6.05588	0.02886	0.0258	0.0629	0.9476	
S3	1.474057	-6.05588	0.02886	0.0254	0.0627	0.9323	
S4	4.424057	-6.05588	0.02886	0.0287	0.5649	1.0526	
Σ							
			3.30628	3.377	116.7	39.874	

$$r_x = \sqrt{\frac{116.7 + 39.874}{3.377}} = 6.81m$$

$$r_y = \sqrt{\frac{116.7 + 39.874}{3.306}} = 6.88m$$

To calculate the radius of gyration of the mass floor plan, walls, floor and ceilings polar moment of inertia should be calculated as well. See tables (5-6) and (5-7)

Table 5-6 Calculating the ceiling moments of inertia

Ceiling Moment of Inertia									
Position	b	h	A	loy	lox	xi	yi	Ai·xi ²	Ai·yi ²
	m	m	m ²	m ⁴	m ⁴	m	m	m ⁴	m ⁴
Ceiling	10.1	14.45	145.945	2539.5	1240.7	-0.0497	-0.424	0.3603	26.2567
Σ			145.945	2539.5	1240.7			0.3603	26.2567

Table 5-7 Calculating the Column moments of inertia

Columns Moment of Inertia							H =	2.8m		
Position	b	h	A	loy	lox	xi	yi	Ai·xi ²	Ai·yi ²	
	m	m	m ²	m ⁴	m ⁴	m	m	m ⁴	m ⁴	
S1	0.325	0.3	0.0975	0.0007	0.0009	-4.425	-5.04	1.9091	2.47666	
S2	0.325	0.3	0.0975	0.0007	0.0009	-1.475	-5.04	0.2121	2.47666	
S3	0.325	0.3	0.0975	0.0007	0.0009	1.475	-5.04	0.2121	2.47666	
S4	0.325	0.3	0.0975	0.0007	0.0009	4.425	-5.04	1.9091	2.47666	
Σ				0.0007	0.0009			1.9091	2.47666	

The total polar mass moment of inertia:

$$I_{pm} = (I_{sx} + I_{sy}) \cdot \rho \cdot h$$

$$\text{Total } I_{pm} = I_{pm} \text{ Ceiling} + I_{pm} \text{ Walls} + I_{pm} \text{ Columns}$$

$$I_{pm} \text{ Ceiling} = 11340.38 \text{ m}^4$$

$$I_{pm} \text{ Walls} = 33987.3 \text{ m}^4$$

$$I_{pm} \text{ Columns} = 245.69 \text{ m}^4$$

$$\Sigma \text{ Sum} = 4645604.219 \text{ m}^4$$

Radius of gyration of the Floor mass:

$$l_s = \sqrt{\frac{I_{pm}}{m}}$$

$$l_s = 6.14 \text{ m}$$

Where m refers to the mass of the building.

5.1.7 Criteria for structural regularity

Constructive regularity is evaluated according to EC8-1.

Criteria for regularity:

$$l_s = 6.14 \text{ m}$$

$$e_{0x} = 0.048 \text{ m}$$

$$e_{0y} = 0.6 \text{ m}$$

$$r_x = 6.81 \text{ m}$$

$$r_y = 6.88 \text{ m}$$

$$\lambda = l_{\max}/l_{\min} = 1.45$$

- | | | | | |
|----|---------------------|----------|------|---------------|
| 1. | $\lambda < 4$ | 1.4519 < | 4 | satisfied |
| 2. | $e_{0x} < 0.3r_x$ | 0.048 < | 2.04 | satisfied |
| | $e_{0y} < 0.3r_y$ | 0.6 < | 2.06 | satisfied |
| 3. | $r_x > l_s$ | 6.81 < | 6.13 | not satisfied |
| | $r_y > l_s$ | 6.88 < | 6.13 | not satisfied |
| 4. | $e_0 < 0.1 \cdot l$ | | | |
| | $e_{0x} < 0.1l_x$ | 0.048 < | 1.51 | satisfied |
| | $e_{0y} < 0.1l_y$ | 0.6 < | 1.04 | satisfied |

Due to the regularity criteria in plan and in elevation that are fulfilled according to EC8-1, the simplified response spectrum method can be used for evaluating the earthquake effectiveness.

Seismic action

According to the seismic classification for EC8-1, the importance category for this type of building is 2, and the horizontal ground acceleration will be:

$$a_g = \gamma_1 \cdot a_{gR}$$

$$a_{gR} = 1.7 \text{ m/s}^2$$

$$a_{vg} = (2/3) \cdot a_{gR} = 1.13 \text{ m/s}^2$$

Where $\gamma_1 = 1$ for the importance category factor and a_{gR} and a_{vg} represent the calculated vertical and horizontal ground acceleration.

According to condition of the EC8-1, if the vertical ground acceleration $a_{vg} < 2.45 \text{ m/s}^2$, vertical ground acceleration should not be considered.

The soil conditions in Dubai will be considered as Zone 2, Type A 1 for the analysis.

For the horizontal component of the seismic action, the design spectrum $S_d(T)$ is defined by EC8-1 using the following equations:

$$0 \leq T \leq T_B \quad S_d(T) = a_g \cdot S \cdot \left[\frac{2}{3} + \frac{T}{T_B} \cdot \left(\frac{2.5}{q} - \frac{2}{3} \right) \right] \quad 5-12$$

$$T_B \leq T \leq T_C \quad S_d(T) = a_g \cdot S \cdot \frac{2.5}{q} \quad 5-13$$

$$T_C \leq T \leq T_D \quad S_d(T) = \begin{cases} a_g \cdot S \cdot \frac{2.5}{q} \cdot \left[\frac{T_C}{T} \right] \\ \geq \beta \cdot a_g \end{cases} \quad 5-14$$

$$T_D \leq T \quad S_d(T) = \begin{cases} a_g \cdot S \cdot \frac{2.5}{q} \cdot \left[\frac{T_C T_D}{T^2} \right] \\ \geq \beta \cdot a_g \end{cases} \quad 5-15$$

With a_g, S, T_B, T_C and T_D defined by EC8, see figure (5-10):

$S_d(T)$ Ordinate of the design spectrum.

q Behaviour coefficient for unreinforced masonry is = 1.5

β Factor for the lower limit of the design spectrum.

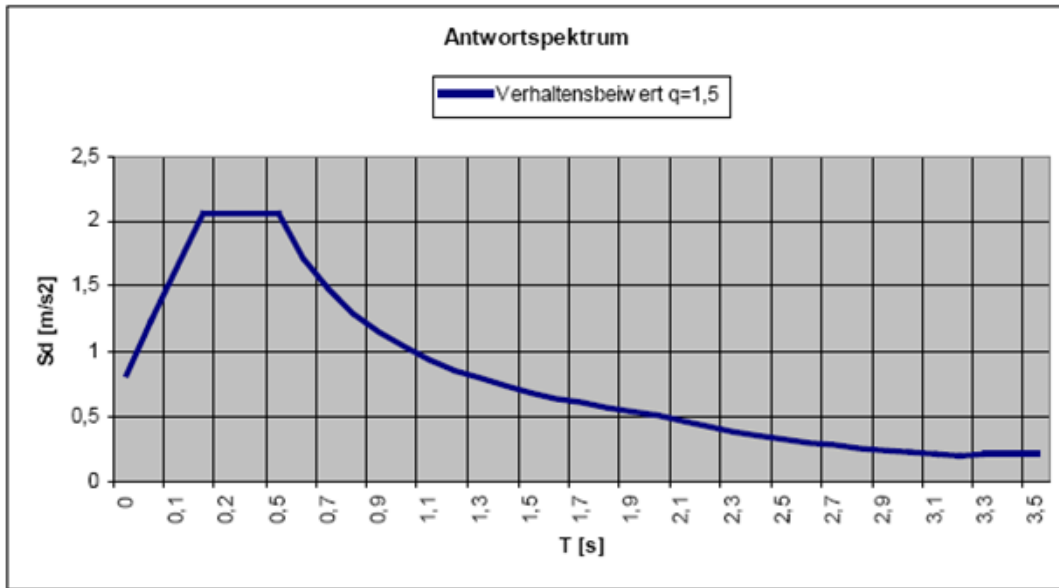


Figure 5-10 General design spectrum according to EC-8

5.1.8 Simplified response spectrum method

The simplified response spectrum method is performed according to EC8-1. The natural vibration period T_1 may be determined by the following expression as approximately:

$$T_1 \text{ is the natural vibration period} = C_t * (H)^{0.75}$$

$$C_t = 0.075 / (A_{cx,y})^{0.5}$$

$$C_{tx} = 0.030607465$$

$$C_{ty} = 0.03172162$$

$$T_{1x} = 0.072 \text{ s}$$

$$T_{1y} = 0.074 \text{ s}$$

Before determining the total seismic force using the simplified response spectrum, the following requirements must be checked:

$$T_{1x}, T_1 < \begin{cases} 4T_C & = 4 * 0.4 = 1.6 \text{ s} \\ \text{or:} \\ 2.0 \text{ s} \end{cases}$$

Both checks are satisfied.

According to EC-8, to determine the total seismic force, the correction coefficient λ still needs to be calculated:

Because of the earthquake, factors are equal to $S = 1$, $T_B = 0.15$, $T_C = 0.4$, $T_D = 2$, $a_g = 1.7$, $q = 1.5$

This gives the following result:

$$S_d(T_{1x}) = 1.944 \text{ m/s}^2 \geq 1 \Rightarrow \lambda = 1$$

$$S_d(T_{1y}) = 1.973 \text{ m/s}^2 \geq 1 \Rightarrow \lambda = 1$$

The total seismic force F_{bx}, F_{by} can now be calculated using the following formula:

$$F_{bx} = S_d(T_{1x}) * m * \lambda \quad 5-16$$

$$F_{bx} = (1.944 * 132349.54 * 1) / 1000 = 257.254 \text{ kN}$$

$$F_{by} = S_d(T_{1y}) * m * \lambda \quad 5-17$$

$$F_{by} = (1.973 * 132349.54 * 1) / 1000 = 261.1583 \text{ kN}$$

$$F_b = \sqrt{257 * 254^2 + 261 * 158^2} = 366.583 \text{ kN}$$

The earthquake force corresponds in the x-direction to approximately 19%, and the y-direction to 20% of the total weight of the structure.

5.1.9 Earthquake forces due to the torsional effect

In this example, the regularities and symmetry in plan predominant.

Calculating the torsional effect

It is also possible to determine the torsional stress according to EC8-1. Using the following formulas, the total seismic forces are calculated on individual wall sections under consideration of torsional effects:

Earthquakes in the x-direction:

Stress in the x-direction:

$$F_r = F_{b,x} \cdot \frac{I_{y,r}}{\sum I_{y,i}} + F_{b,x} \cdot e_{\max,y} (bz_w \cdot e_{\min,y}) \frac{I_{y,r} \cdot y'_r}{\sum (I_{x,i} \cdot x_i'^2) + \sum (I_{y,i} \cdot y_i'^2)} \quad 5-18$$

Stress in the y-direction:

$$F_k = -F_{b,x} \cdot e_{\max,y} (bz_w \cdot e_{\min,y}) \frac{I_{x,k} \cdot x'_k}{\sum (I_{x,i} \cdot x_i'^2) + \sum (I_{y,i} \cdot y_i'^2)} \quad 5-19$$

Earthquakes in the y-direction:

Stress in the y-direction:

$$F_k = F_{b,y} \cdot \frac{I_{x,k}}{\sum I_{x,i}} + F_{b,y} \cdot e_{\max,x} (bz_w \cdot e_{\min,x}) \frac{I_{x,k} \cdot x'_k}{\sum (I_{x,i} \cdot x_i'^2) + \sum (I_{y,i} \cdot y_i'^2)} \quad 5-20$$

Stress in the x-direction:

$$F_r = -F_{b,y} \cdot e_{\max,x} (bz_w \cdot e_{\min,x}) \frac{I_{y,r} \cdot y'_r}{\sum (I_{x,i} \cdot x_i'^2) + \sum (I_{y,i} \cdot y_i'^2)} \quad 5-21$$

For earthquakes in the x-direction:

The following values for eccentricity are given:

$$l_y = 10.4 \text{ m}, b_x = 15.1 \text{ m} \text{ , (length and width of the prayer hall)}$$

$$e_{0y} = 0.6$$

$$e_{1y} = 0.1 \cdot (l+b) \cdot (10 \cdot (e_{0y}/l))^{0.5} < 0.1 \cdot (l+b)$$

$$e_{1y} = 1.94 < 2.55$$

$$e_{2y} = 0.05 \times l_y$$

$$e_{2y} = 0.52$$

This results in:

$$e_{\max,y} = e_{0y} + e_{1y} + e_{2y} = 3.1 \text{ m}$$

$$e_{\min,y} = e_{0y} - e_{2y} = 0.1 \text{ m}$$

The earthquake in the x-direction produces stress in two directions (X and Y). Stresses in both the X and Y directions are illustrated in Tables 5-8 and 5-9 respectively.

Table 5-8 Stress in X direction

Wall #	Isye	yi'	Fr _{x,trans}	Isye-yi' ²	Fr _{x,rot} (T _{max})	Fr _{x,rot} (T _{min})	Fr _x (Ed _x)	
	m ⁴	M	kN	m ⁶	kN	kN	kN	
w1	1.1	0.125472	4.00412	9.55822	2.0117	2.527076896	0.067459085	12.08529737
	1.2	0.162378	4.00412	12.3696	2.60341	3.270377645	0.087301136	15.64000146
	1.3	0.132711	4.00412	10.1096	2.127751	2.672859361	0.071350676	12.78247617
	1.4	0.089384	4.00412	6.80908	1.433094	1.800237934	0.048056473	8.609318856
	1.5	0.162243	4.00412	12.3593	2.601236	3.267646283	0.087228223	15.62693921
	1.6	0.125447	4.00412	9.55627	2.011289	2.526561493	0.067445326	12.08283255
W2	2.1	0.128058	3.47412	9.75515	1.545594	2.237757779	0.059735852	11.99290626
	2.2	0.222289	0.69912	16.9335	0.108649	0.781687849	0.020866776	17.71515314
	2.3	0.422832	-4.0259	32.2104	6.853121	-8.56230315	-0.22856650	23.64809278
W3	3.1	0.128039	3.47412	9.75373	1.545369	2.237431535	0.059727143	11.99115781
	3.2	0.222256	0.69912	16.931	0.108633	0.781573886	0.020863734	17.71257043
	3.3	0.42277	-4.0259	32.2057	6.852122	-8.56105485	-0.22853318	23.64464511
W4	4.1	0.130285	-2.5659	9.92485	0.857763	-1.6814889	-0.04488652	8.243365128
	4.2	0.162437	-2.5659	12.3741	1.069438	-2.09644023	-0.05596344	10.27763088
	4.3	0.148829	-2.5659	11.3375	0.979849	-1.92081761	-0.05127528	9.416654999
	4.4	0.147004	-2.5659	11.1985	0.967834	-1.89726464	-0.05064655	9.30118846
	4.5	0.162305	-2.5659	12.3641	1.068573	-2.09474431	-0.05591817	10.26931675
	4.6	0.173595	-2.5659	13.2241	1.142902	-2.24045382	-0.05980782	10.98364599
S1	0.028722	-6.0559	2.18795	1.053327	-0.87488067	0.015441915	1.313071114	
S2	0.025838	-6.0559	1.96828	0.947573	-0.78704242	0.013891542	1.181238421	
S3	0.025423	-6.0559	1.93664	0.932342	-0.77439192	0.011859078	1.162251831	
S4	0.028702	-6.0559	2.18648	1.052616	-0.87429023	0.00269435	1.312184941	
Σ	3.377017		257.254	39.87418	-10.2619621	-0.14167619	246.9919397	

Table 5-9 Stress in the Y direction

	Wall #	Isxe	xi'	F _{kx,trans}	Isxe·xi' ²	F _{ky,rot(Tmax)}	F _{ky,rot(Tmin)}	F _{ky(Edx)}
		m4	M	kN	m6	kN	kN	kN
W1	1.1	0.1	-6.6		5.428	4.13579328	0.11040298	4.13579
	1.2	0.2	-4.1		2.713	3.34363557	0.08925672	3.34364
	1.3	0.1	-1.6		0.387	1.18629919	0.03166768	1.1863
	1.4	0.1	1.64		0.264	-0.80970612	-0.0216147	-0.8097
	1.5	0.2	4.08		2.71	-3.34209038	-0.0892155	-3.3421
	1.6	0.1	6.6		5.424	-4.13461166	-0.1103714	-4.1346
W2	2.1	0.1	-7.4		6.928	4.70878015	0.12569859	4.70878
	2.2	0.2	-7.4		10.74	7.29679078	0.19478427	7.29679
	2.3	0.4	-7.4		22.77	15.4778189	0.41317282	15.4778
W3	3.1	0.1	7.4		6.925	-4.70758025	-0.1256666	-4.7076
	3.2	0.2	7.4		10.73	-7.2949314	-0.1947346	-7.2949
	3.3	0.4	7.4		22.76	-15.4738748	-0.4130675	-15.474
W4	4.1	0.1	-6.6		5.225	4.01215288	0.10710246	4.01215
	4.2	0.2	-4.1		2.61	3.18208684	0.08494426	3.18209
	4.3	0.2	-1.5		0.357	1.17686625	0.03141587	1.17687
	4.4	0.2	1.52		0.356	-1.17541175	-0.031377	-1.1754
	4.5	0.2	4.12		2.608	-3.18063235	-0.0849054	-3.1806
	4.6	0.2	6.33		6.503	-5.16834387	-0.1379664	-5.1683
	S1	0	-4.4		0.565	0.64249582	0.02284353	0.6425
	S2	0	-1.5		0.063	0.21425653	0.00761775	0.21426
	S3	0	1.47		0.063	-0.21398276	-0.007608	-0.214
	S4	0	4.42		0.565	-0.64222204	-0.0228338	-0.6422
	Σ	3.3			116.7	-0.7664112	-0.0204541	-0.7664

Where:

$F_{rx,trans}$ Translational part of the earthquake force in the x-direction

$F_{kx,trans}$ Translational part of the earthquake force in the x-direction

$F_{rx,rot(T_{max},T_{min})}$ Rotational part of the earthquake force in the x-direction, according to T_{max} and T_{min}

$F_{ky,rot(T_{max},T_{min})}$ Rotational part of the earthquake force in the y-direction, according to T_{max} and T_{min}

$F_{rx}(Edx)$ Translational and rotational portion of the seismic force in the x-direction

$F_{ky}(Edx)$ Translational and rotational portion of the seismic force in the y-direction

For earthquakes in the y-direction:

The following values for eccentricity are given:

$$l_y = 10.4 \text{ m}, b_x = 15.1 \text{ m}$$

$$e_{0x} = 0.049$$

$$e_{1x} = 0.1 \cdot (l + b) \cdot (10 \cdot (e_{0x}/b))^{0.5} < 0.1 \cdot (l + b)$$

$$e_{1x} = 0.049 < 2.55$$

$$e_{2x} = 0.05 b$$

$$e_{2x} = 0.755$$

This results in:

$$e_{\max,x} = e_{0x} + e_{1x} + e_{2x} = 1.262$$

$$e_{\min,x} = e_{0x} - e_{2x} = -0.71$$

The earthquake in the y-direction produces stress in two directions (Y and X). Both stresses in the Y and X directions are illustrated in tables 5-10 and 5-11 respectively.

Table 5-10 Stress in the Y direction

	Wall #	lsxe	xi'	Fky,trans	lsye·xi'2	Fky,rot(Tmax)	Fky,rot(Tmin)	Fky(Edy)
		m4	m	kN	m6	kN	kN	kN
w1	1.1	0.1	-6.6	9.839084	5.428	-1.73063652	3.80339644	13.6425
	1.2	0.2	-4.1	12.86649	2.713	-1.39915548	0.78308613	13.6496
	1.3	0.1	-1.6	11.35279	0.387	-0.49641086	0.27783364	11.6306
	1.4	0.1	1.64	7.757739	0.264	0.33882423	-0.1896348	8.09656
	1.5	0.2	4.08	12.86649	2.71	1.39850889	-0.7827242	14.265
	1.6	0.1	6.6	9.839084	5.424	1.73014206	-0.9683343	11.5692
w2	2.1	0.1	-7.4	9.991327	6.928	-1.97040478	1.10280571	11.0941
	2.2	0.2	-7.4	15.4827	10.74	-3.05336648	1.70892297	17.1916
	2.3	0.4	-7.4	32.84162	22.77	-6.47674501	3.62493607	36.4666
w3	3.1	0.1	7.4	9.991327	6.925	1.96990268	-1.1025247	11.9612
	3.2	0.2	7.4	15.4827	10.73	3.05258842	-1.7084875	18.5353
	3.3	0.4	7.4	32.84162	22.76	6.4750946	-3.6240124	39.3167
w4	4.1	0.1	-6.6	9.617794	5.225	-1.67889878	0.93965421	10.5574
	4.2	0.2	-4.1	12.1113	2.61	-1.33155487	0.74525109	12.8565
	4.3	0.2	-1.5	12.1113	0.357	-0.49246361	0.27562443	12.3869
	4.4	0.2	1.52	12.1113	0.356	0.49185498	-0.2752838	12.6032
	4.5	0.2	4.12	12.1113	2.608	1.33094623	-0.7449104	13.4422
	4.6	0.2	6.33	12.82373	6.503	2.16271076	-1.2104365	14.9864
	S1	0	-4.4	2.27964	0.565	-0.26885452	0.1504738	2.43011
	S2	0	-1.5	2.27964	0.063	-0.08965636	0.05017931	2.32982
	S3	0	1.47	2.27964	0.063	0.0895418	-0.0501152	2.36918
	S4	0	4.42	2.27964	0.565	0.26873996	-0.1504097	2.54838
	Σ	3.3		261.1582	116.7	0.32070733	2.65529036	293.929

Table 5-11 Stress in the X direction

	Wall #	Isye	yi'	Fry,trans	Isye-yi'2	Fr _{x,rot} (Tmax)	Fr _{x,rot} (Tmin)	Fr _x (Edy)
		m4	M	kN	m6	kN	kN	kN
W1	1.1	0.125	4.004		2.012	-1.057	0.592	-1.057
	1.2	0.162	4.004		2.603	-1.369	0.766	-1.369
	1.3	0.133	4.004		2.128	-1.118	0.626	-1.118
	1.4	0.089	4.004		1.433	-0.753	0.422	-0.753
	1.5	0.162	4.004		2.601	-1.367	0.765	-1.367
	1.6	0.125	4.004		2.011	-1.057	0.592	-1.057
W2	2.1	0.128	3.474		1.546	-0.936	0.524	-0.936
	2.2	0.222	0.699		0.109	-0.327	0.183	-0.327
	2.3	0.423	-4.026		6.853	3.583	-2.005	3.583
W3	3.1	0.128	3.474		1.545	-0.936	0.524	-0.936
	3.2	0.222	0.699		0.109	-0.327	0.183	-0.327
	3.3	0.423	-4.026		6.852	3.582	-2.005	3.582
W4	4.1	0.130	-2.566		0.858	0.704	-0.394	0.704
	4.2	0.162	-2.566		1.069	0.877	-0.491	0.877
	4.3	0.149	-2.566		0.980	0.804	-0.450	0.804
	4.4	0.147	-2.566		0.968	0.794	-0.444	0.794
	4.5	0.162	-2.566		1.069	0.877	-0.491	0.877
	4.6	0.174	-2.566		1.143	0.938	-0.525	0.938
S1	0.029	-6.056	1.053		0.366	-0.205	0.366	
S2	0.026	-6.056	0.948		0.329	-0.184	0.329	
S3	0.025	-6.056	0.932	0.324	-0.181	0.324		
S4	0.029	-6.056	1.053	0.366	-0.205	0.366		
Σ	3.377			39.874	4.294	-2.403	4.294	

Where:

- $F_{ky,trans}$ Translational part of the earthquake force in the y-direction
- $F_{ry,trans}$ Translational part of the earthquake force in the y-direction
- $F_{ky,rot(T_{max},T_{min})}$ Rotational part of the earthquake force in the y-direction, according to T_{max} and T_{min}
- $F_{rx,rot(T_{max},T_{min})}$ Rotational part of the earthquake force in the x-direction, according to T_{max} and T_{min}
- $F_{ky}(Edy)$ Translational and rotational portion of the seismic force in the y-direction
- $F_{rx}(Edy)$ Translational and rotational portion of the seismic force in the x-direction

Earthquake forces with torsional effect for each wall section are illustrated in the table (5-12) below:

Table 5-12 Seismic forces with torsional effect

Wall Number	Earthquake in x-Direction		Earthquake in y-Direction		x and y - superimposed		H[Wall height] = 3.1	
	$F_{rx}(Edx)$	$F_{ky}(Edx)$	$F_{rx}(Edy)$	$F_{ky}(Edy)$	$Edy+0.3*Edx$	$Edx+0.3*Edy$	MED	
	kN	kN	kN	kN	kN	kN	kNm	
W1	1.1	12.085		-1.057		2.56812544	11.7680582	36.481
	1.2	15.64		-1.369		3.32349999	15.2294513	47.2113
	1.3	12.782		-1.118		2.71627592	12.4469361	38.5855
	1.4	8.6093		-0.753		1.82948008	8.38332418	25.9883
	1.5	15.627		-1.367		3.32072426	15.216732	47.1719
	1.6	12.083		-1.057		2.56760167	11.7656581	36.4735
W2	2.1		4.709		11.094	12.5067669	8.03702001	38.771
	2.2		7.297		17.192	19.3806589	12.4542773	60.08
	2.3		15.48		36.467	41.1098984	26.4177847	127.441
W3	3.1		-4.708		11.961	10.5489558	-1.1192113	32.7018
	3.2		-7.295		18.535	16.3468077	-1.7343453	50.6751
	3.3		-15.47		39.317	34.6745488	-3.6788614	107.491
W4	4.1	8.2434		0.704		3.177	8.45445252	26.2088
	4.2	10.278		0.877		3.961	10.5408096	32.6765
	4.3	9.4167		0.804		3.629	9.65778676	29.9391
	4.4	9.3012		0.794		3.584	9.53936348	29.572
	4.5	10.269		0.877		3.957	10.5322826	32.6501
	4.6	10.984		0.938		4.233	11.2649036	34.9212

Table 5-13 Shear forces due to the earthquake of an individual wall

Wall Number	L	t	Vd
	[m]	[m]	[kN]
1.1	1.3	0.325	11.76806
1.2	1.7	0.325	15.22945
1.3	1.5	0.325	12.44694
1.4	1.025	0.325	8.383324
1.5	1.7	0.325	15.21673
1.6	1.3	0.325	11.76566
2.1	1.325	0.325	12.50677
2.2	2.3	0.325	19.38066
2.3	4.375	0.325	41.1099
3.1	1.325	0.325	10.54896
3.2	2.3	0.325	16.34681
3.3	4.375	0.325	34.67455
4.1	1.35	0.325	8.454453
4.2	1.7	0.325	10.54081
4.3	1.7	0.325	9.657787
4.4	1.7	0.325	9.539363
4.5	1.7	0.325	10.53228
4.6	1.8	0.325	11.2649

The shear forces due to the earthquake according to the equivalent lateral force method are summarized in table 5-13:

5.2 MODIFICATION OF RESPONSE SPECTRUM METHOD FOR CLAY BUILDING

Response spectrum analysis is very useful for analysing the performance of structures during earthquakes. A modal analysis should be carried out to determine the 3D mode shapes and the natural frequencies of vibration. The peak response of the building can then be estimated by reading the value from the ground response spectrum for the appropriate frequency. In most building codes in seismic regions, this value forms the basis for calculating the forces that a structure must be designed to resist.

The response spectrum method calculations have been performed using the computer simulation program SolidWorks version 2013.

a) Model specification

In the response spectrum method, the model represents a 3-dimensional model with the following material characteristics (Table 5-14):

Table 5-14 Model material specification

Material specification	Clay Wall (Lab tests +Literature)	Roof and ceiling Wood
Density[Kg/m ³]	2000	600
E-Module [N/mm ²]	4000	10500
Shear modulus G[N/mm ²]	850	500
Compressive strength [N/mm ²]	2.1	11
Shear strength [N/mm ²]	0.05	0.9
Tension strength [N/mm ²]	0.01	9
coefficient behaviour q[-]	1.5	1.5

b) Frequency and mode shape

The frequency simulation test is performed in order to find the real model frequency and its mode shape. The frequency simulation showed that the maximum participation mass ratio at the sixth mode in the x-direction and the seventh mode in the y-direction (Table 5-15).

Table 5-15 Model mass participation factor

Mode No.	Frequency (Hertz)	Effective Mass in X-direction	Effective Mass in Y-direction	Effective Mass in Z-direction
1	13.103	2.85E-06	0.042108	5.82E-06
2	14.08	2.28E-06	0.00092927	2.53E-09
3	14.997	0.00011181	0.013857	4.38E-09
4	16.71	8.77E-06	3.23E-05	0.00023345
5	18.764	0.0018631	0.0026189	0.001285
6	19.282	0.00012604	3.63E-06	0.65742
7	19.69	0.57084	5.28E-08	0.0001333
8	21.801	2.09E-06	1.13E-06	0.0040873
9	24.735	6.23E-05	0.0019362	0.0001585
10	28.69	8.56E-06	8.92E-06	0.012307
11	28.879	2.56E-05	7.60E-05	2.40E-05
12	29.974	0.0010686	0.012677	1.28E-06
13	30.144	0.001896	1.92E-05	4.35E-06
14	30.494	5.27E-06	0.00015062	0.0013884
15	31.548	0.0052749	0.0029499	1.85E-06
16	31.816	2.47E-05	2.99E-06	0.0013516
17	33.123	1.44E-06	5.77E-05	9.01E-05
18	33.336	0.0010512	0.0042854	1.43E-06
19	34.39	8.12E-05	0.00077516	0.00033593
20	34.465	3.80E-05	0.0050977	4.02E-05
21	35.18	0.0025162	0.00061359	2.12E-05
22	36.057	0.00098708	4.14E-05	1.27E-07
23	36.375	0.026943	8.29E-05	0.00064562
24	37.512	0.0044886	0.00017176	0.00094681
25	38.148	2.84E-05	0.0014337	0.0001528
26	38.794	0.0034926	0.0023096	0.00027121
27	38.96	0.0071117	2.97E-06	0.00049525
28	39.206	0.00069277	0.0011907	8.83E-05
29	39.675	0.0040043	0.00049269	0.00067515
30	40.445	0.0087102	2.92E-05	1.86E-05
31	41.049	0.0043006	7.73E-05	0.00032029
32	41.242	0.017073	1.06E-05	0.00049964
33	41.846	0.0019235	0.00010306	1.62E-05
34	42.15	0.005473	0.00011503	2.94E-06
35	42.967	4.65E-06	2.95E-05	0.00099982
36	43.412	0.00088835	0.00032646	0.0025889
37	43.612	0.0062374	0.0002696	0.0013115
38	44.541	0.00021166	0.0012309	2.03E-05
39	44.912	0.0014251	0.0016848	8.18E-05
40	45.112	0.00027226	3.95E-05	0.0036623
		Sum X = 0.67928	Sum Y = 0.097842	Sum Z = 0.69169

When using a 3-dimensional model, the more accurate method of calculating the maximum overlapping participation mass ratio and shear stress, as well as the horizontal shift displacement, is through Complete Quadratic Combination (CQC) theory [42]. This theory is the most conservative method used to estimate a peak value of displacement or force within a structure and uses the sum of the absolute of the modal response values. This approach assumes that the maximum modal values, for all modes, occur at the same point. The two main forms of the model mode shape are represented in Figures 5-11 and 5-12.

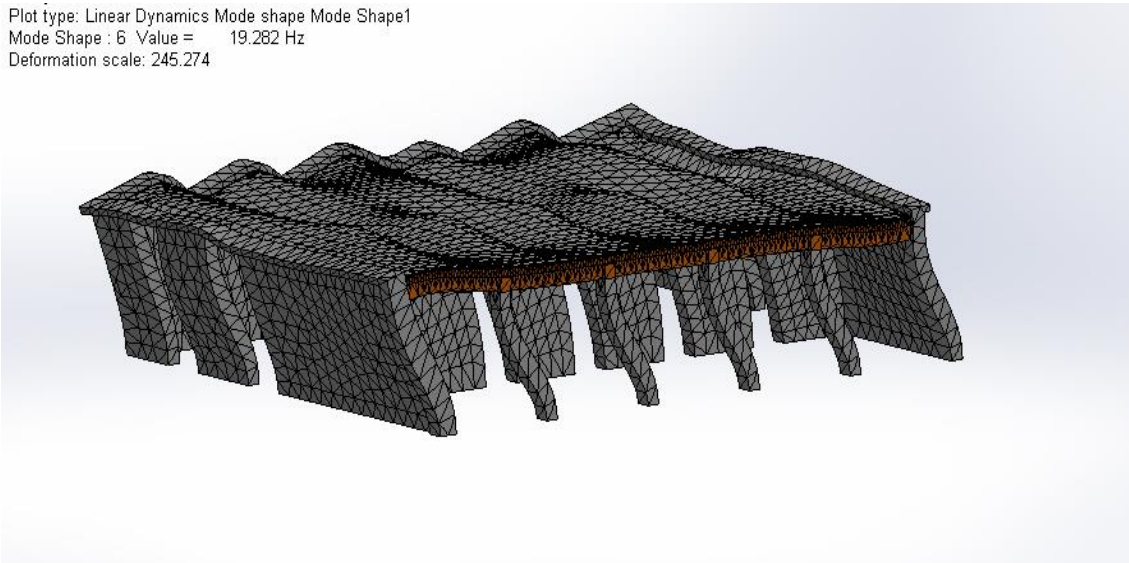


Figure 5-11 6th Model mode shape

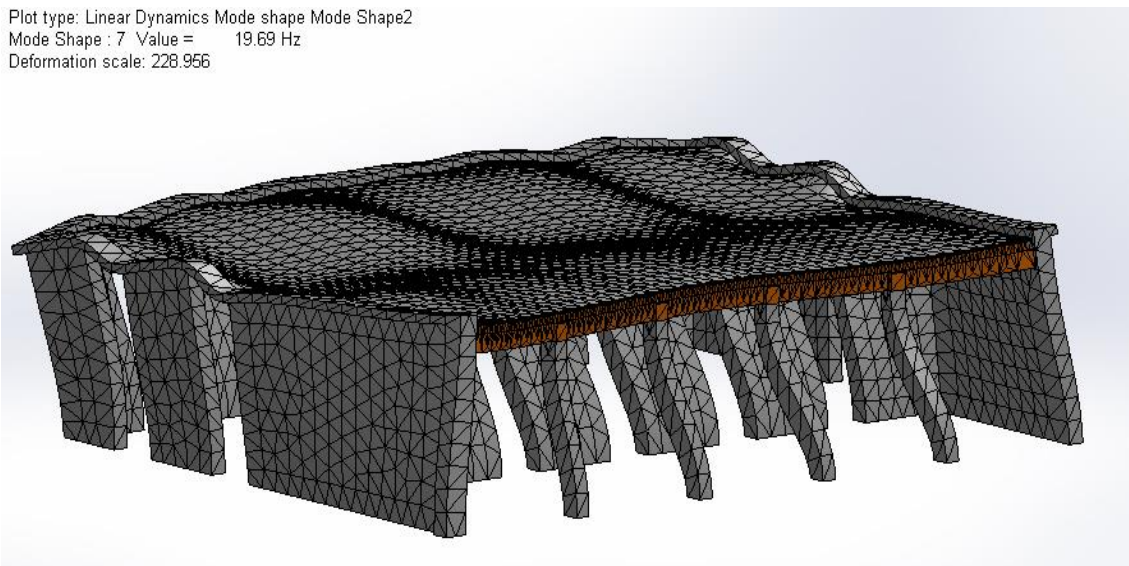


Figure 5-12 7th Model mode shape

c) Model analysis and simulation result

The simulation result has provided the frequency value with maximum effective mass participation in the x- and y-directions equal to 19.28 and 19.69 Hz respectively. These frequency values refer to the time period in seconds of the model vibration (Table 5-16).

Table 5-16 Frequency mode and its vibration time

Mode No.	Frequency(Rad/sec)	Frequency(Hertz)	Period(Seconds)
1	82.329	13.103	0.076318
2	88.465	14.08	0.071024
3	94.229	14.997	0.06668
4	104.99	16.71	0.059845
5	117.9	18.764	0.053293
6	121.15	19.282	0.051862
7	123.71	19.69	0.050788
8	136.98	21.801	0.045869
9	155.41	24.735	0.040429
10	180.27	28.69	0.034855
11	181.45	28.879	0.034628
12	188.33	29.974	0.033362
13	189.4	30.144	0.033174
14	191.6	30.494	0.032794
15	198.22	31.548	0.031698
16	199.91	31.816	0.031431
17	208.12	33.123	0.03019
18	209.46	33.336	0.029997
19	216.08	34.39	0.029078
20	216.55	34.465	0.029015
21	221.04	35.18	0.028425
22	226.55	36.057	0.027734
23	228.55	36.375	0.027492
24	235.7	37.512	0.026658
25	239.69	38.148	0.026214
26	243.75	38.794	0.025777
27	244.79	38.96	0.025667
28	246.34	39.206	0.025506
29	249.28	39.675	0.025205
30	254.12	40.445	0.024725
31	257.92	41.049	0.024361
32	259.13	41.242	0.024247
33	262.93	41.846	0.023897
34	264.84	42.15	0.023725
35	269.97	42.967	0.023273
36	272.76	43.412	0.023035
37	274.02	43.612	0.02293
38	279.86	44.541	0.022451
39	282.19	44.912	0.022266
40	283.45	45.112	0.022167

Shear stress and maximum wall deformation were calculated using this test in order to compare it with the other numerical and analytical methods (Figures 5-13, 5-14, 5-15 and 5-16). The maximum wall deformation shows a maximum value equal to 7 mm, while the shear force due to the earthquake varied between different walls.

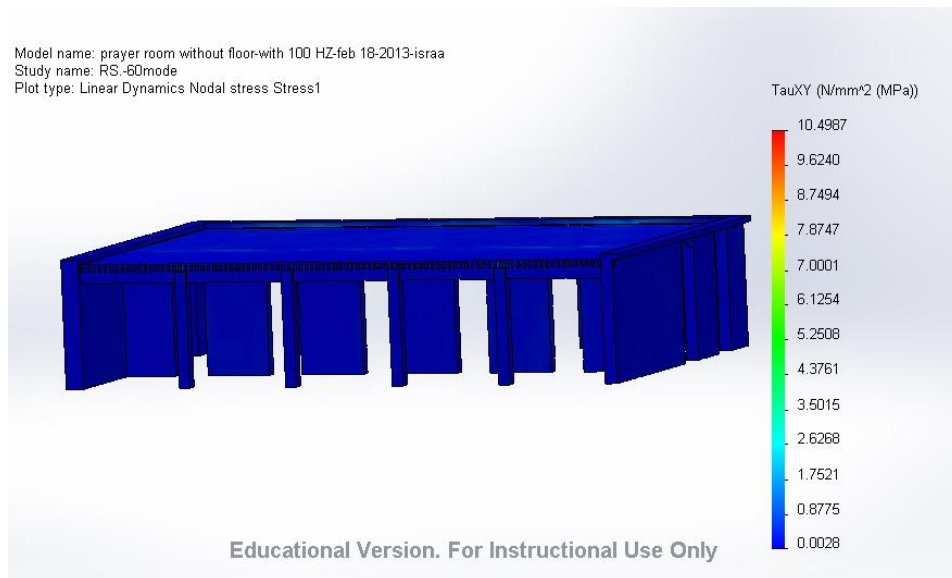


Figure 5-13 Shear stress in XY-direction

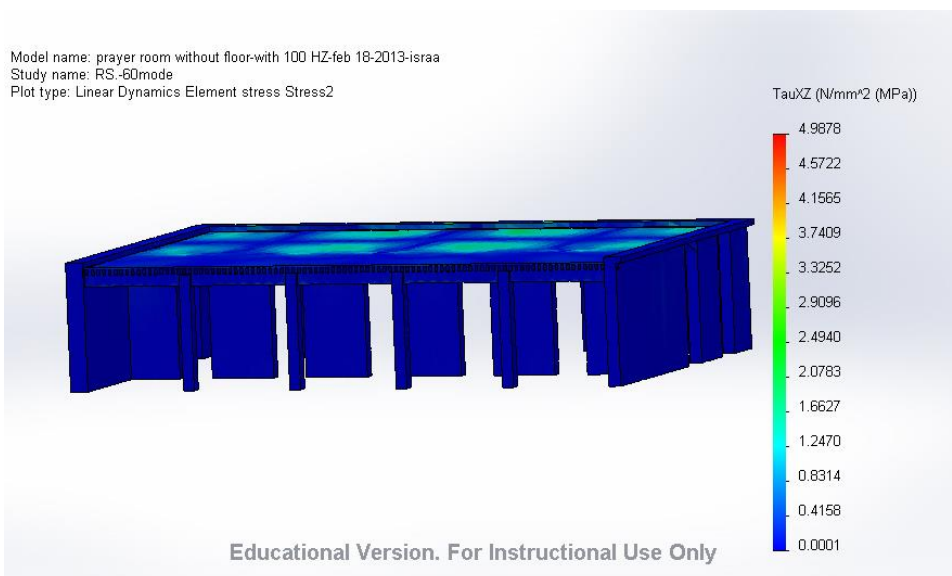


Figure 5-14 Shear stress in XZ-direction

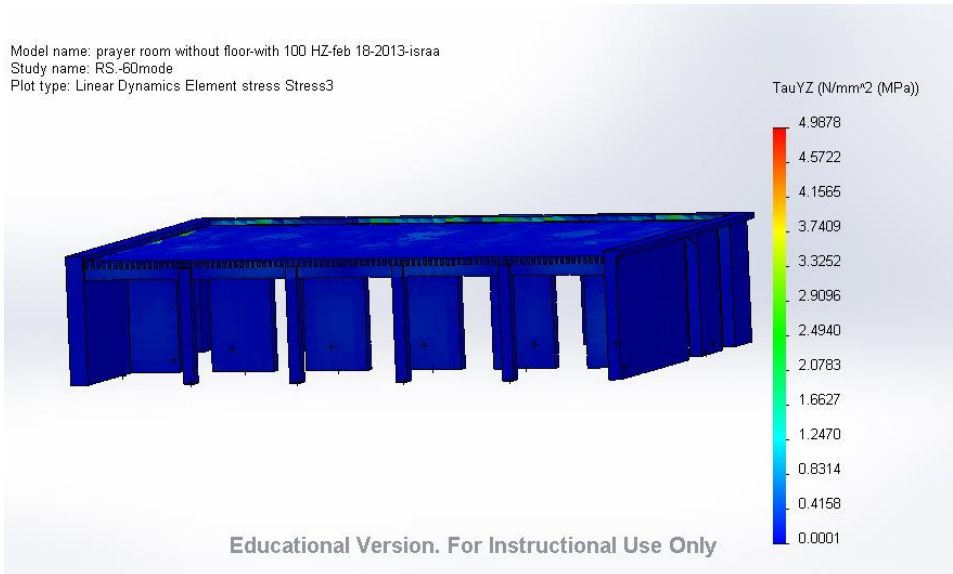


Figure 5-15 Shear stress in YZ-direction

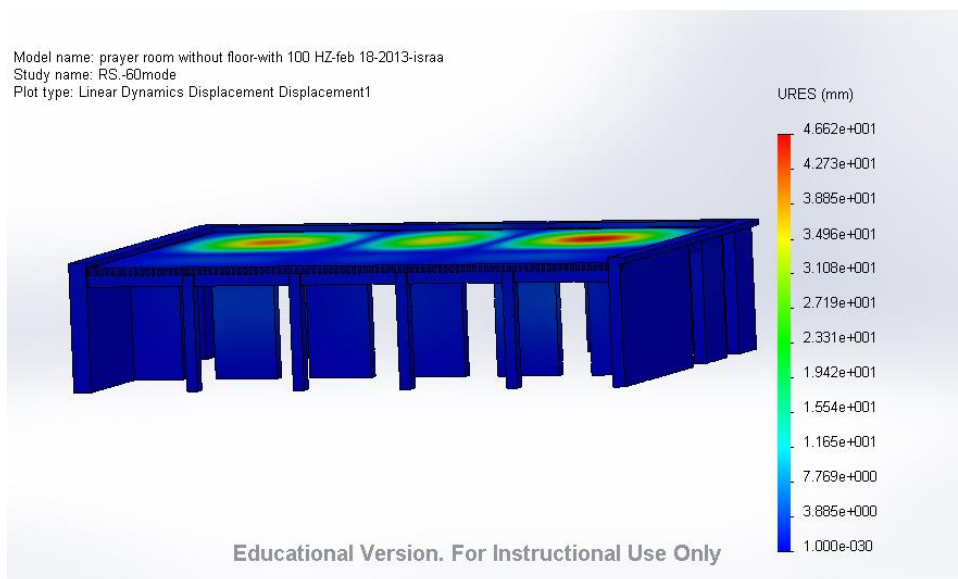


Figure 5-16 Resultant wall deformation

As a summary of the results according to this method, the walls' shear forces in two plane directions are presented in the following table (Table 5-17):

Table 5-17 Wall shear stress according to response spectrum analysis

Wall Number	L	t	Max. τ_{yz}	Max. τ_{yx}	V_{RS}
	M	m	N/mm ²	N/mm ²	KN
1.1	1.3	0.325	0.03	0.08	33.80
1.2	1.7	0.325	0.02	0.014	11.05
1.3	1.5	0.325	0.023	0.014	11.21
1.4	1.025	0.325	0.015	0.018	6.00
1.5	1.7	0.325	0.021	0.018	11.60
1.6	1.3	0.325	0.03	0.08	33.80
4.1	1.35	0.325	0.017	0.02	8.78
4.2	1.7	0.325	0.016	0.011	8.84
4.3	1.7	0.325	0.016	0.011	8.84
4.4	1.7	0.325	0.009	0.016	8.84
4.5	1.7	0.325	0.012	0.02	11.05
4.6	1.8	0.325	0.017	0.022	12.87

Where L, t are the wall dimensions, τ represents the shear stress in yz and yx plane directions and V_{RS} refers to the max shear force due to the earthquake according to the response spectrum method.

Theory advantages and disadvantages

The response spectrum method requires dynamic modelling of the structure and thus a much greater computational effort than the equivalent force method. The application of the response spectrum method is justified if the vibration behavior of the structure is substantial in addition to the fundamental frequency and higher natural vibrations. This is especially the case with irregular structures with significant stiffness variation in vertical and / or horizontal directions, and those with essentially torsion vibrations, which leads to considerable eccentricity between centres and stiffness centres.

Often it is sufficient to consider the first few natural vibration frequencies and the shape of a building. The number of vibration modes to be considered is indicated by the ratio of the sum of the modal masses to the total mass.

A major disadvantage of the response spectrum method is the "earthquake time lost". The duration of the earthquake, which is the most important factor for evaluating damages, has

no effect on the result. It also fails to provide any information about the vibration running. In addition, plastic deformation may only be considered as a relative value.

On the other hand, the method allows a good understanding of the vibration characteristics of a structure, which should be used for irregular structures in order to get a better conceptual understanding.

5.3 INELASTIC STATIC INVESTIGATION OF PUSHOVER METHODS

The original capacity spectrum method used graphical curves to compare the capacity of a structure with the demands of earthquake ground motion on the structure (Figure 5-17). The best visual evaluation for describing this method is the graphical presentation of how the structure will perform when subjected to earthquake ground motion. The method clearly shows the capacity of the structure, which is represented by a force-displacement curve, obtained via a non-linear static (pushover) experimental test or analytical calculation converted to the spectral accelerations and spectral displacements of an equivalent Single-Degree Of-Freedom (SDOF) system, respectively.

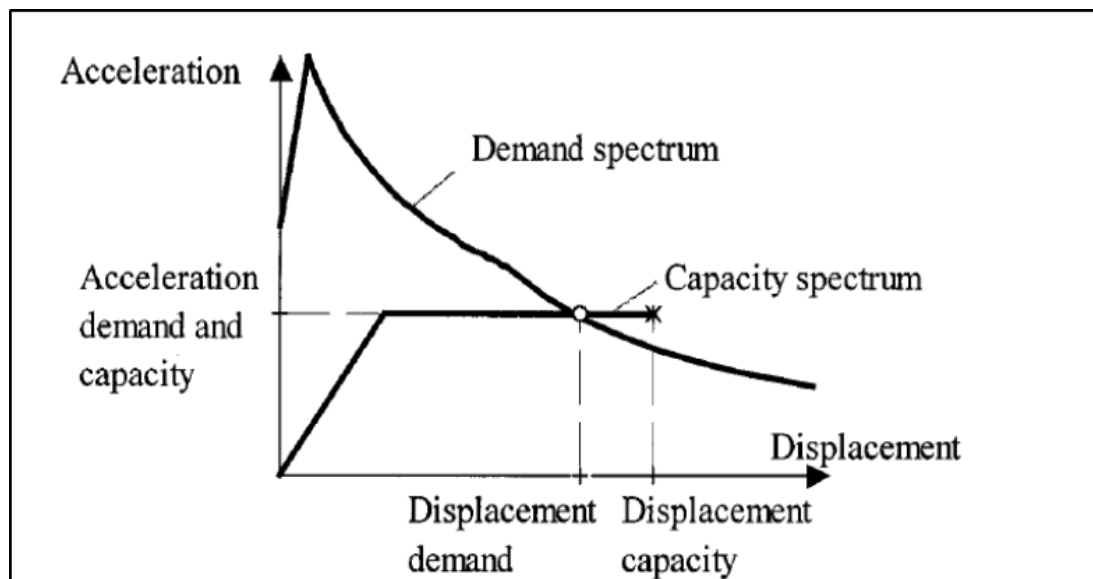


Figure 5-17 Capacity spectrum method [43]

These values define the capacity spectrum. The demands of the earthquake ground motion are defined by highly damped elastic spectra. The Acceleration-Displacement Response

Spectrum (ADRS) format is used, in which spectral accelerations are plotted against spectral displacements for periods T . The intersection of the capacity spectrum and the demand spectrum provides an estimate of the inelastic acceleration (strength) and displacement demand.

The basis of the proof is the non-linear load-deformation curve (capacity curve) of the structure, which is determined through static non-linear analysis by successive increase of the horizontal load due to earthquake. The calculation of the capacity curve of a building is made from the load-deformation curves of the individual walls, taking into account the load transfer to the successive failure of the shear walls [43].

For symmetric layouts with symmetric mass distribution, the capacity curve can be determined by simple superposition of the individual wall curves. In the case of irregular floor plans or unbalanced mass distributions, the load-deformation curve should be determined with a double-iterative calculation algorithm, with additional rotations and translations set perpendicular to the load direction. In the following section, the calculation steps are explained for the prayer hall in the mosque at Hatta Village in Dubai.

5.3.1 Determination of the elastic response spectrum

The response spectrum presented here refers to the response spectrum in Eurocode 8 for soil condition type 1, class A which is similar to the soil condition in Hatta Village in Dubai. The response spectrum, figure (5-18) used for this evaluation method should not take into account energy dissipation effects, which means the behaviour factor will be substituted as $q = 1$.

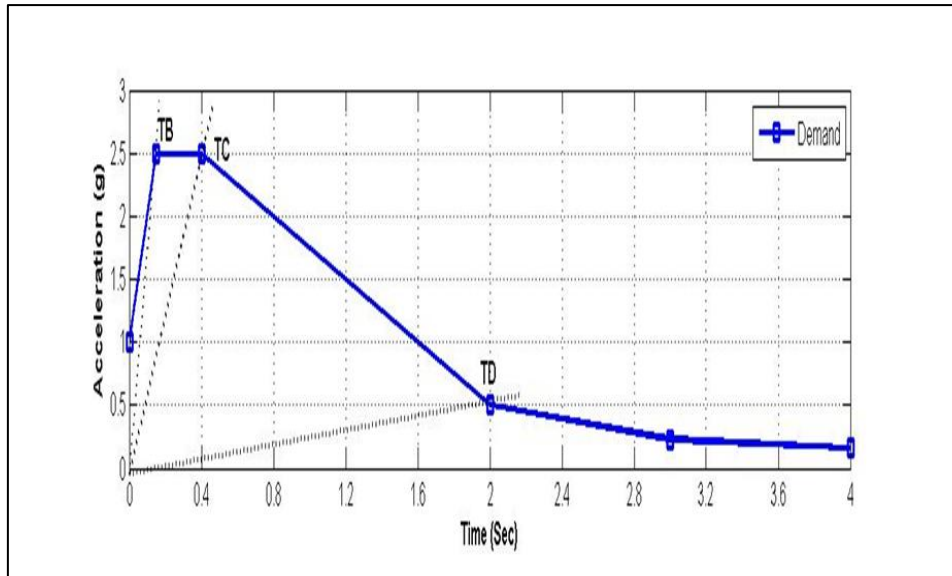


Figure 5-18 Normative response spectrum of soil type 1, class A according to the EC8

5.3.2 Determination of the building load-deformation curve

The interpolated load-deformation curves of the individual walls of the deformation detection is made by considering all normative value determined eccentricities in the principal directions of the structure.

The load-deformation curve is performed on the basis of two extreme constraints, the horizontal shear strength and the wall deformations.

A. Horizontal shear strength capacity

The determination of the horizontal capacity of single walls follows the differentiation in the contextual approach of EN 1998 [EC8]. The characteristic shear strength of masonry, f_k , is dependent on the type of wall, which is the case of this project is tamped clay walls. The code characteristic shear strength value is recommended as $f_k = 0.1 \text{ N/mm}^2$, and through the experiments performed at the Vienna University of Technology and University of Bahrain, the f_k values show an average of = 0.035 to 0.05 N/mm^2 .

The formulas presented here in order to determine the horizontal load capacities, have been used in accordance with EN 1998 Part 3 [44].

The maximum horizontal shear load capacity V_{BL} of a wall due to bending failure is determined by the following formula:

$$V_{BL} = \frac{L \cdot N_{SD}}{2 \cdot H_o} \left(1 - 1.15 \frac{\sigma_o}{f_d}\right) \quad 5-22$$

Where:

L is the length of the wall

N_{SD} is the centric compressive force

f_d , the mean compressive strength of the clay wall (which was considered here to be equal to 2.1, based on lab experiment values) and

σ_o is the calculated mean normal stress.

H_o is the distance between the cross-section in which the bending capacity is reached and the inflection point of the bending line (here assumed to be 1.8 m as a relative value based on the experimental results obtained in the lab).

The maximum horizontal shear load capacity due to the shear failure [45] is determined by:

$$V_{RD} = \frac{f_k \cdot l \cdot t}{\gamma_m} \quad 5-23$$

Where:

V_{RD} is the maximum shear force in the wall

f_k is the wall characteristic shear strength

t are the wall dimensions

γ_m is the safety factor (recommended here as value 2.1).

B. Deformation capacity

To develop an approach for determining the deformation shear capacity on stressed walls, the guidelines according to EN 1998 [EC8] were used. These recommended calculating the maximum deformation in displacement due to bending and due to the shear stress as equal to:

$$D_y = \begin{cases} 0.008(H_o/L) \cdot H_w & \text{Case of bending and force failure} \\ 0.004 \cdot H_w & \text{Case of shear failure} \end{cases} \quad 5-24$$

Where:

D_y is the Wall deformation displacement

H_w is the Wall height

L is the Wall length

The clay wall section experiment showed that wall length plays a large role in wall shear strength. This allows us to generate an approximate modified formula to calculate the maximum wall deformation due to the bending failure:

$$D_y = 0.0055 \cdot (H_w^2 / L) \cdot \alpha$$

Where:

D_y is the Wall deformation displacement

H_w is the Wall height

L is the Wall length

α is the Factor for full fixed ceiling with wall = 0.5

Which provides a shear failure of:

$$D_y = 0.0055 \cdot H_w$$

In order to generate the load-deformation curve for the prayer hall in the mosque, the shear capacities and maximum final deformations of shear walls will be taken only for those walls which lie in the x-direction, as shown in the following table (Table 5-18):

Table 5-18 Approximate shear strength and maximum final deformations of shear walls in x- direction

Wall #	L	t	N _{SD}	σ _d	V _{BL}	V _{Rd}	D _y
	m	m	kN	N/mm ²	[kN]	[kN]	[mm]
1.1	1.3	0.325	70.42	0.55	17.81	6.71	18.60
1.2	1.7	0.325	92.09	0.28	21.38	8.77	18.60
1.3	1.5	0.325	81.26	0.30	16.40	7.74	18.60
1.4	1.025	0.325	55.53	1.28	4.72	5.29	28.13
1.5	1.7	0.325	92.09	0.28	21.38	8.77	18.60
1.6	1.3	0.325	70.42	0.55	17.81	6.71	18.60
4.1	1.35	0.325	90.75	0.24	17.15	6.96	18.60
4.2	1.7	0.325	114.28	0.21	27.77	8.77	18.60
4.3	1.7	0.325	114.28	0.21	27.79	8.77	18.60
4.4	1.7	0.325	114.28	0.21	27.79	8.77	18.60
4.5	1.7	0.325	114.28	0.21	27.77	8.77	18.60
4.6	1.8	0.325	121.00	0.21	31.15	9.29	18.60

5.3.3 Creating the building load-deformation curve

After interpolating the max horizontal strength and deformation for each individual wall, the building pushover-curve can be obtained. As a first step, the maximum horizontal load capacity of each wall has been added, giving 94.75 kN. The load-deformation curve decreases gradually as a result of a gradual failure of each wall section (Figure 5-19). When the maximum deformation capacity of shear wall W (1.4) is achieved, horizontal load capacity of the structure is completely exhausted.

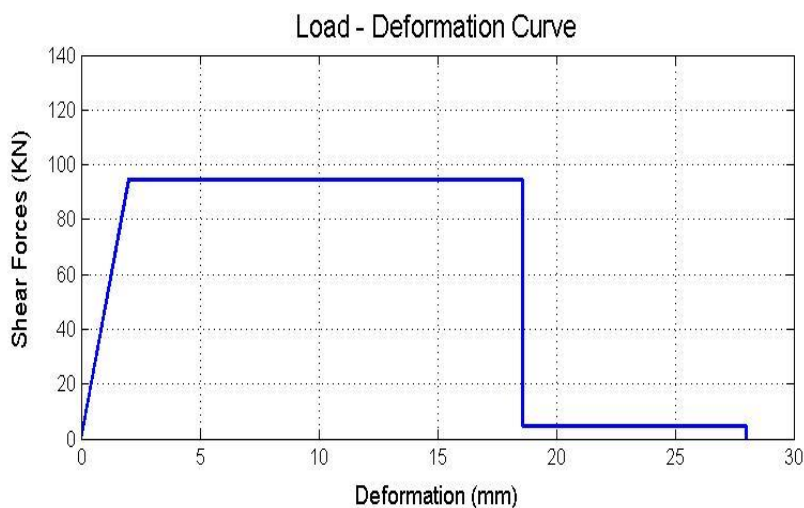


Figure 5-19 Load-deformation curve of the prayer hall for the mosque for walls in the x-direction

5.3.4 Creation of the building pushover-curve for an equivalent mass

The pushover-curve can be determined through three points: the maximum horizontal earthquake force on the specific direction, the calculated maximum wall deformation and the wall yield deformation. The idealization of the pushover-curve (Figure 5-20) can be determined by taking an approximate horizontal force equal to $0.6 F$ as recommended in the EN 1998, by idealizing the pushover curve to reduce maximum horizontal force.

The equivalent single mass system F^* , d^*_y and m^* can be obtained through transformation factor Γ which will be taken as 1 since the building has only one floor.

This produces the following values:

$$F^* = 0.6 * F$$

$$d^*_y = d_u : \text{which will be considered here as } 6 \text{ mm}$$

$$m^* = m$$

Where F and m represent the maximum horizontal shear force due to earthquake in the x-direction (257.3 kN calculated according to section 5.1.8) and the total mass respectively.

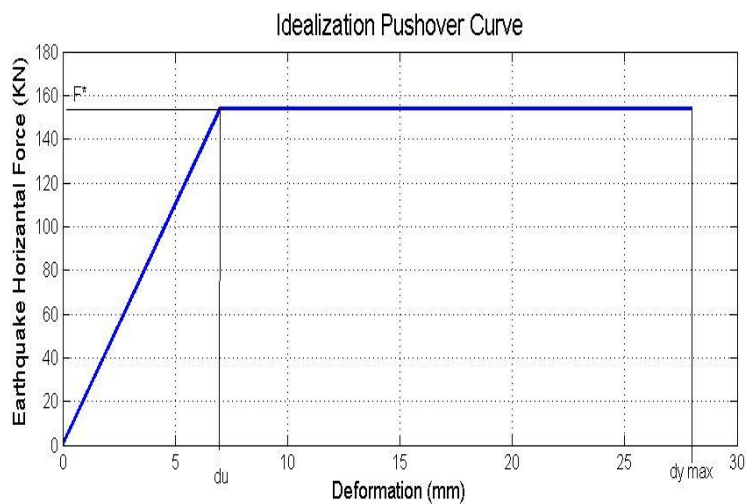


Figure 5-20 the idealization of the Pushover-curve

5.3.5 Determination of the period for an equivalent mass system

The period T^* for an equivalent mass system can be calculated using the following formula:

$$T^* = 2\pi \cdot \sqrt{\frac{m^* \cdot d_y^*}{F^*}} \quad 5-25$$

$$T^* = 2 \cdot 3.14 \cdot \sqrt{\frac{132349.53 \cdot 0.0063}{1000 \cdot 154}} = 0.5s$$

5.3.6 Determination of the maximum deformation for an equivalent mass system

The elastic maximum deformation d_{et}^* of the equivalent mass system through the period T^* can be determined using the following formula:

$$d_{et}^* = S_e(T^*) \cdot \left[\frac{T^*}{2 \cdot \pi} \right]^2 \quad 5-26$$

Where $S_e(T^*)$ represents the ordinate elastic response spectrum presented in section 5.3.1 according to the T^* period.

$$S_e(T^*) = ag \cdot s \cdot n \cdot 2.5 \cdot \left[\frac{T_c}{T^*} \right] \quad 5-27$$

$$S_e(T^*) = 1.66 \cdot 1 \cdot 1 \cdot 2.5 \cdot \left[\frac{0.4}{0.5} \right] = 3.3m/s^2$$

$$d_{et}^* = 3.3 \cdot \left[\frac{0.5}{2 \cdot \pi} \right]^2 \cdot 1000 = 20.9mm$$

In order to calculate d_t^* , which represents the desired target deformation, the following conditions must be followed:

$$1) \text{ If } T^* < T_c \text{ and } \frac{F_y^*}{m^*} \geq S_e(T^*)$$

It lies in the short period before the linear behaviour range.

In this case it will be considered that:

$$d_t^* = d_{et}^* \quad 5-28$$

$$2) \text{ If } T^* < T_c \text{ and } \frac{F_y^*}{m} < S_e(T^*)$$

Here the nonlinear behaviour appears within a short period range, which requires us to take into account the required ductility for determining the maximum deformation. This can be represented through:

$$d_t^* = \frac{d_{et}^*}{q_u} \left(1 + (q_u - 1) \frac{T_c}{T^*} \right) \geq d_{et}^* \quad 5-29$$

Where q_u is the relation between the system acceleration under elastic behaviour $S_e(T^*)$ and the acceleration through the limited system strength.

$$3) \text{ If } T^* \geq T_c$$

For a period equal or longer than T_c , the target deformation will be considered as:

$$d_t^* = d_{et}^* \quad 5-30$$

5.3.7 Determination of the target deformation for mass system

As mentioned in section 5.3.4, the transformation factor Γ is equal to 1, so the target deformation d_t for the system will be equal to:

$$d_t = \Gamma \cdot d_t^* \rightarrow d_t = 1 \cdot d_t^* = 20.9 \text{ mm}$$

5.3.8 Checking the allowable target deformation

The condition is met if the determined target deformation can be set using the guidelines from EN 1998-1 or EC8 as follows:

$$d_t \leq \frac{D_{y_{\max}}}{1,5}$$

So:

$$20.9 \text{ mm} \leq \frac{28 \text{ mm}}{1,5} \Rightarrow 20.9 \text{ mm} \leq 18.6 \text{ mm} \text{ which is not satisfied}$$

5.3.9 Determining the Ductility μ

By using the determined target deformation, the ductility factor can be calculated through the following mathematical expression:

$$\mu \leq \frac{d_t}{d_u}$$

$$\mu \leq \frac{21mm}{6mm} = 3.5$$

5.3.10 Determining the verified graph of the S_e - S_d Diagram

The determined target deformation can be represented and checked graphically with the help of the response spectrum and the building's pushover curve, which will be translated as a spectral acceleration spectral deformation diagram. The reduction factor R_{μ} , which depends on the calculated ductility, can be determined through:

$$R_u = \begin{cases} (\mu-1)\frac{T}{T_c} + 1 & \text{When } T \leq T_c \\ \mu & \text{When } T > T_c \end{cases} \quad 5-31$$

After combining all the diagrams, the performance point for the load-deformation curve and the pushover curve can be obtained by representing the curves with the reduced response spectrum as shown in Figures 5-21 and 5-22 respectively.

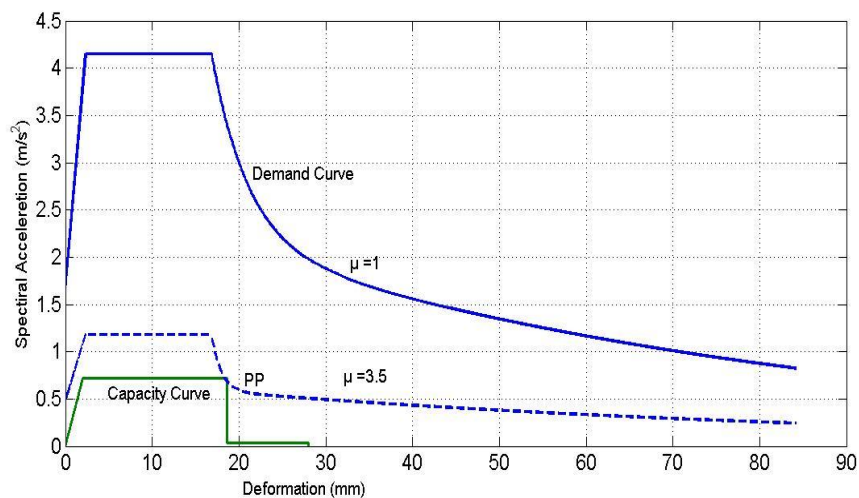


Figure 5-21 Determination of the performance point using the load deformation curve

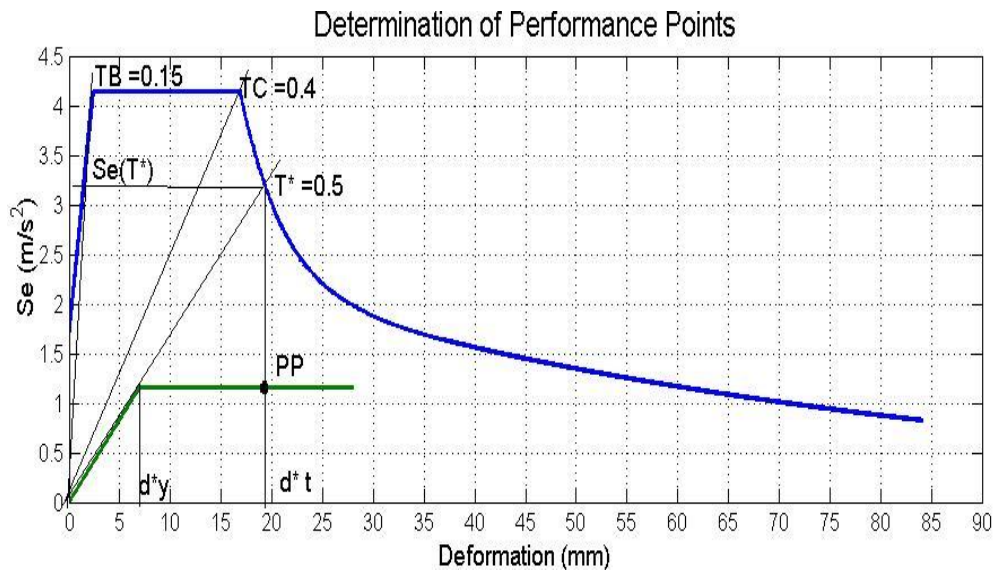


Figure 5-22 Determination of the performance point using the idealization of the pushover-curve

5.3.11 Pushover simulation Analysis

The response of the clay Mosque building to horizontal incremental static loads replicating the Earthquake is discussed in this section. Directions west-east and north-south are considered and the results obtained in the analysis are discussed. The incremental analysis continues until collapse is found, the so-called pushover analysis. Thus, it is possible to distinguish and identify the failure mechanisms. As expected, different behaviour is found for each main building direction. For this analysis the end point for the incremental horizontal load is the calculating earthquake force according to the section 5.1.8 for each relevant direction in order to compare it with results obtained from mathematical calculation of this method.

The interpretation of results from a pushover analysis is based mostly in the capacity curves, which give the relation between the static loads applied in horizontal direction and a displacement caused by these loads. Here, the seismic coefficient is used to quantify the horizontal load, which is defined as the ratio between the applied loads and the weight of the building.

For every step analysed several figures are shown, illustrating the deformed mesh, and the distribution of strains in the structure. These figures help to explain and understand the global structural behaviour.

5.3.11.1 W-E direction

The capacity curve for the west-east direction can be seen in the Figure 5-23.

The displacement increases in a proportional way to the applied load and no damage is observed in the model in this first steps. The first three steps in which figure 5-23 are shown represent the max Horizontal force that building can resist. The incremental horizontal load has been applied to 22% of the Building self-weight, in order to compare the maximum displacement that accrue according to the force calculating in this direction. All the steps are presented in the figure 5-24.

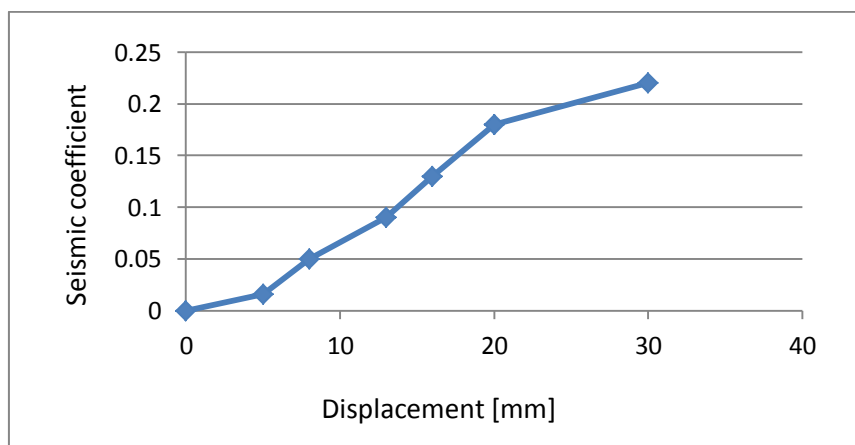


Figure 5-23 Capacity curve in W-E direction

5.3.11.1.1 Deformed mesh (displacements) W-E direction

The deformed mesh can be seen in Figure 5-24 and Figure 5-25 for all steps of the analysis for two perspective sides. The magnification factor has different values for every step. The deformation of the structure presents, undoubtedly, the consequence of applying horizontal loads in the direction perpendicular to the gable walls (from west to east). All the building is leaning to the east direction, being the largest displacements at the top of the structure. The windows are being deformed, losing their rectangularity; the corners are opening or closing. It is in these corners that the concentration of strains and stresses is larger, as can be seen in the Figure 5-24. The large deformation of the piers can also be observed.

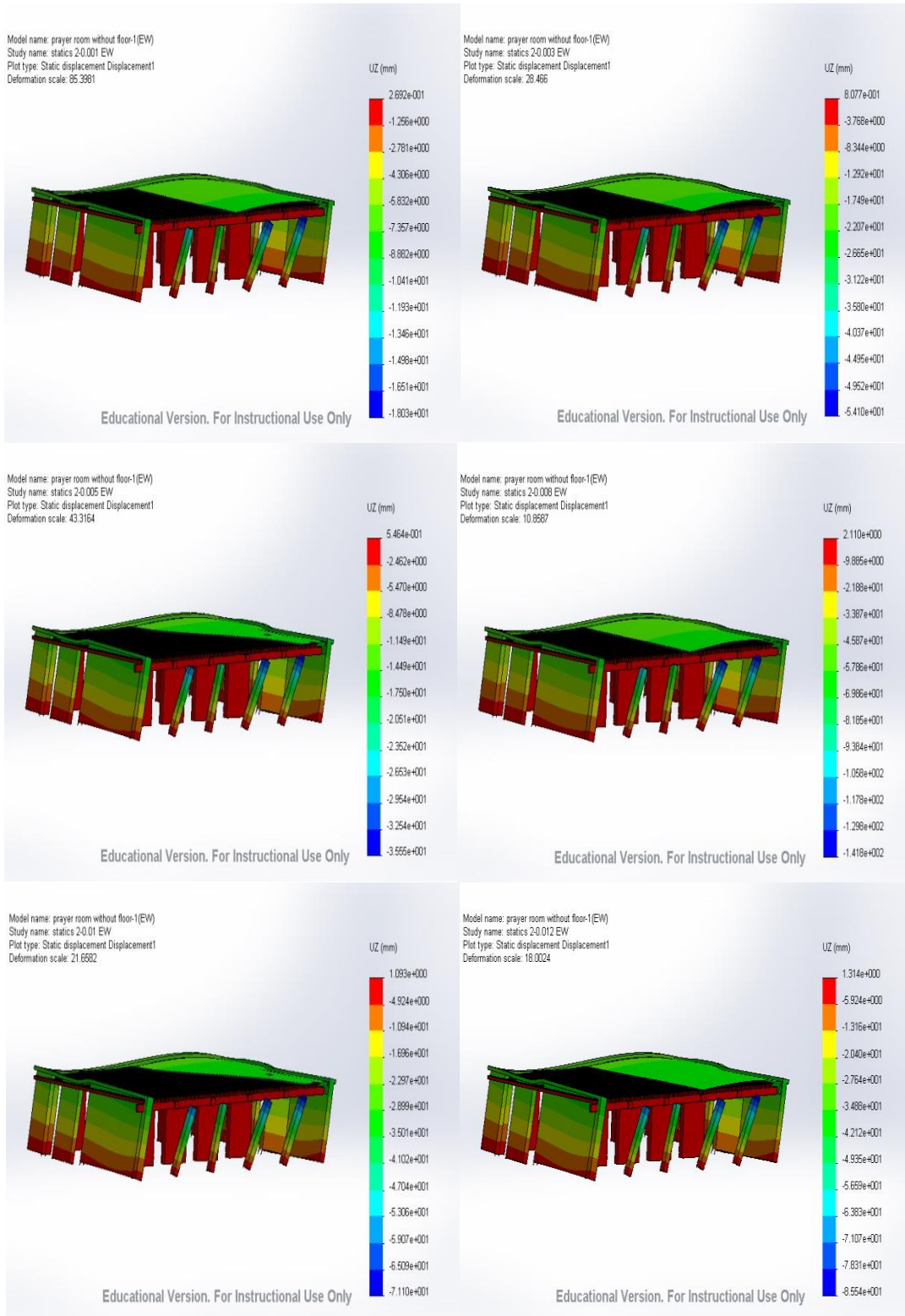


Figure 5-24 Deformed building in W-E direction (for the capacity curve steps - first perspective)

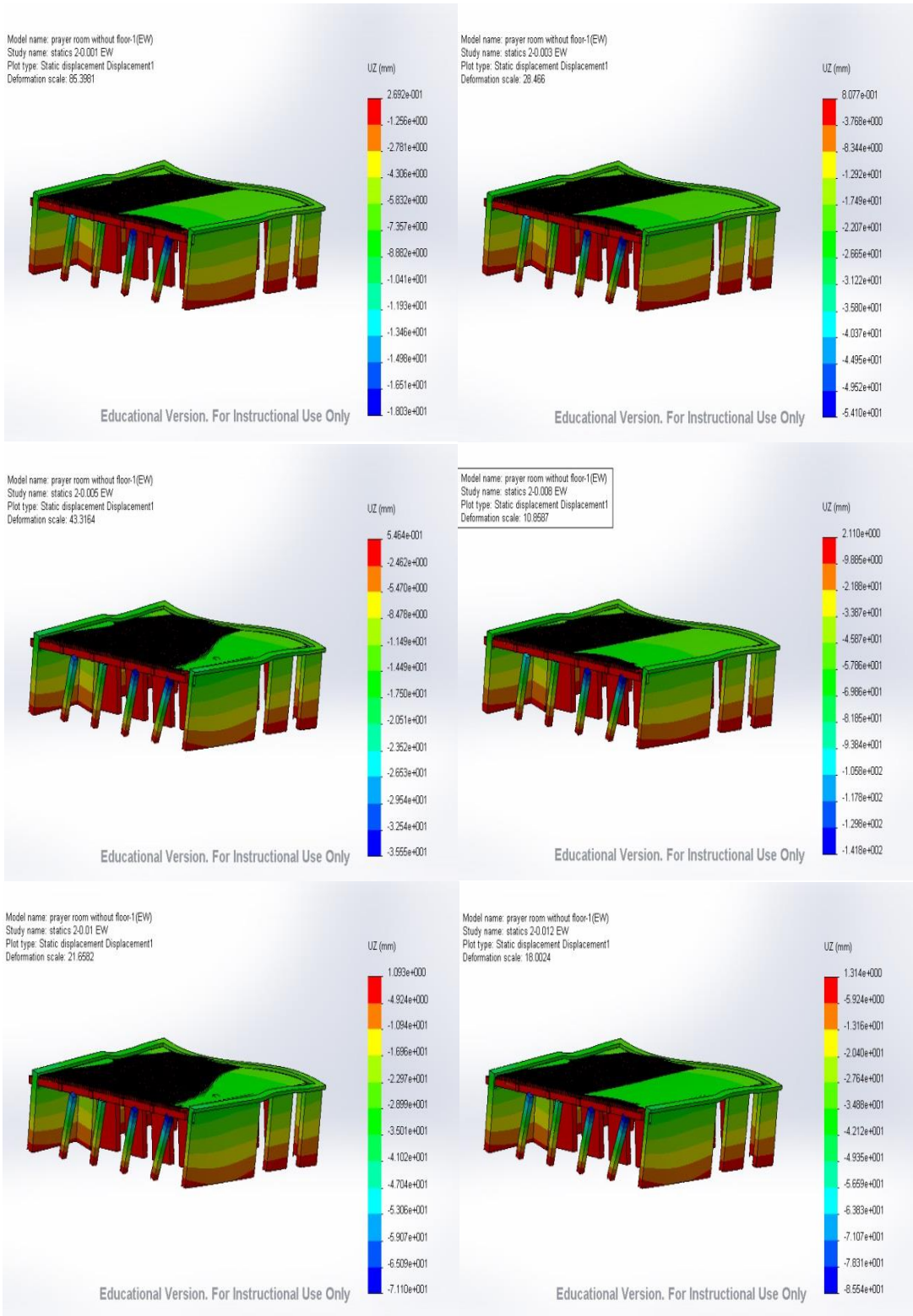


Figure 5-25 Deformed building in W-E direction (for the capacity curve steps - second perspective)

5.3.11.1.2 Principal tensile strains (maximum) W-E direction

The images shown here give an idea of the wall deformation. Figure 5-26 corresponding to all steps analysis. The tensile strains are rather large and the walls are starting to overturn through increasing the Horizontal load. Given the very large displacement attained, the building would be possibly already collapse and the damage concentration is excessive.

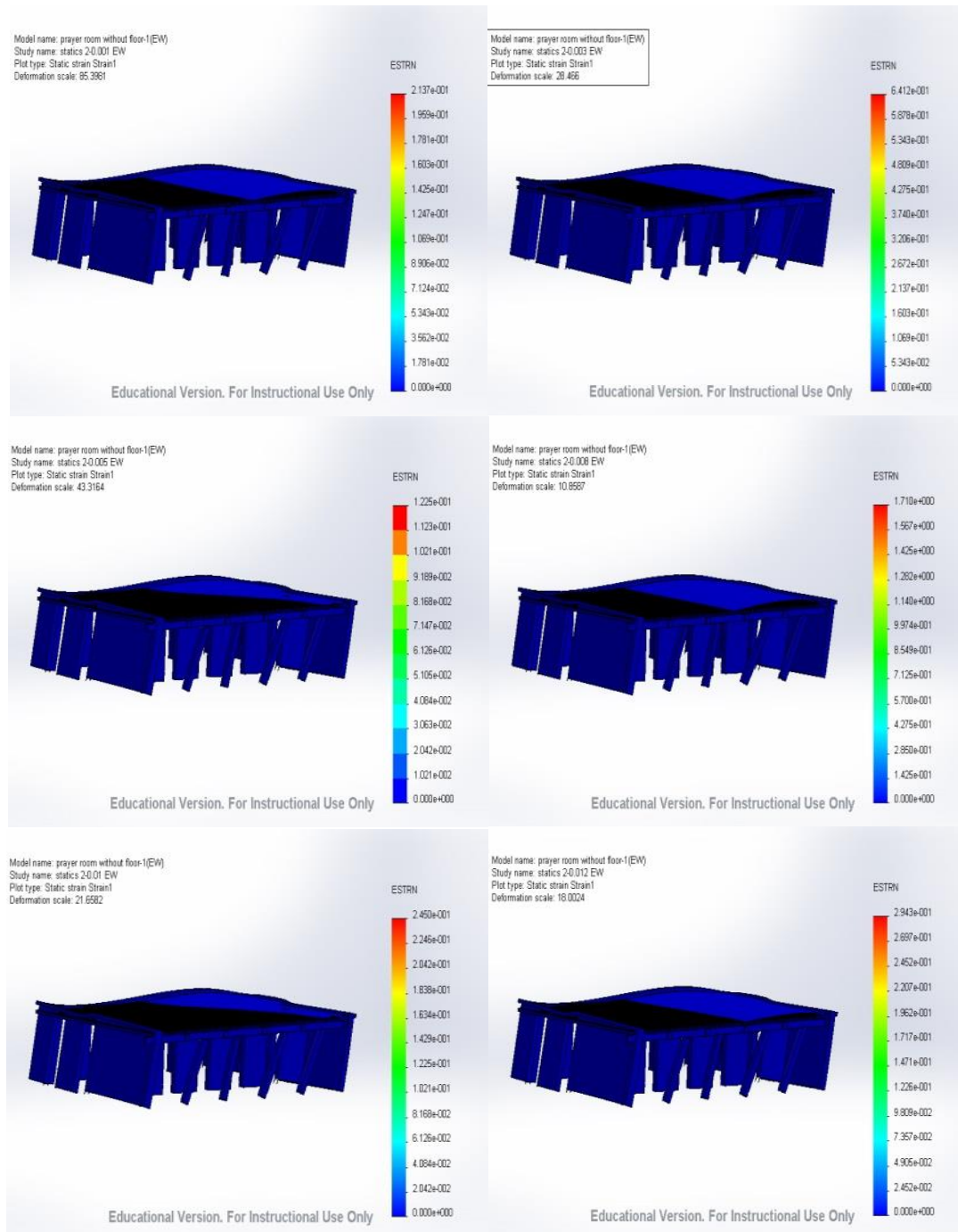


Figure 5-26 Tensile principal strain for all analysis steps of W-E direction

5.3.11.2 N-S direction

In the Figure 5-27 the capacity curve for the north-south direction can be seen. The curve has a similar shape to the one in the east-west direction. In the first steps it is seen that the stiffness in the north-south direction is lower than in the east-west direction. The difference of stiffness is due to the gable walls, which do not have many opening and their stiffness is higher than the global stiffness of the facades.

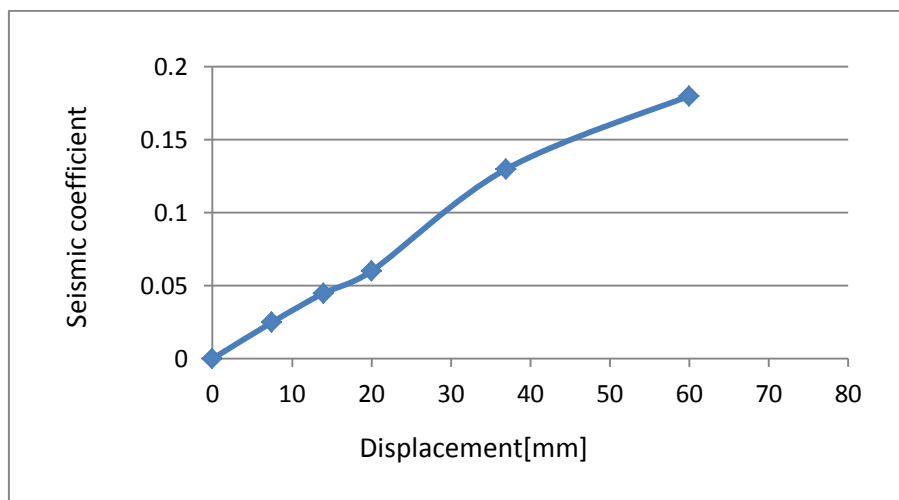


Figure 5-27 Capacity curve in N-S direction

5.3.11.2.1 Deformed mesh (displacements) N-S direction

In the Figure 5-28 the deformed mesh in all steps are shown. The magnification factors are different in every step. The behaviour of the structure is obvious. The whole building is leaning, tending to move to the south, since the load is applied in this direction. It is easy to notice that the facades' displacements are larger than those in the gable walls. Both two perspective sides for all steps are shown in the Figure 5-28 and Figure 5-29.

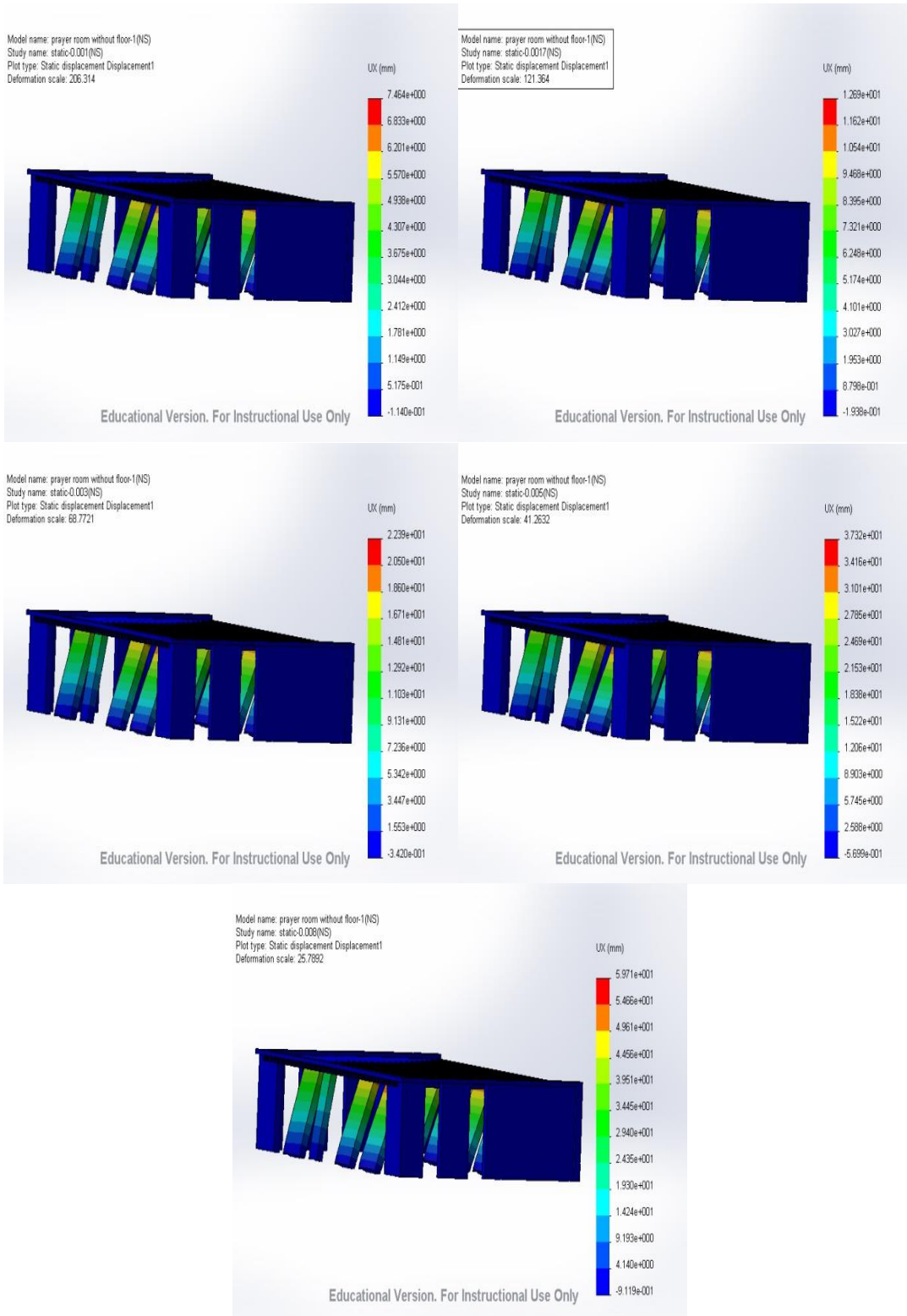


Figure 5-28 Deformed building in N-S direction (for the capacity curve steps - first perspective)

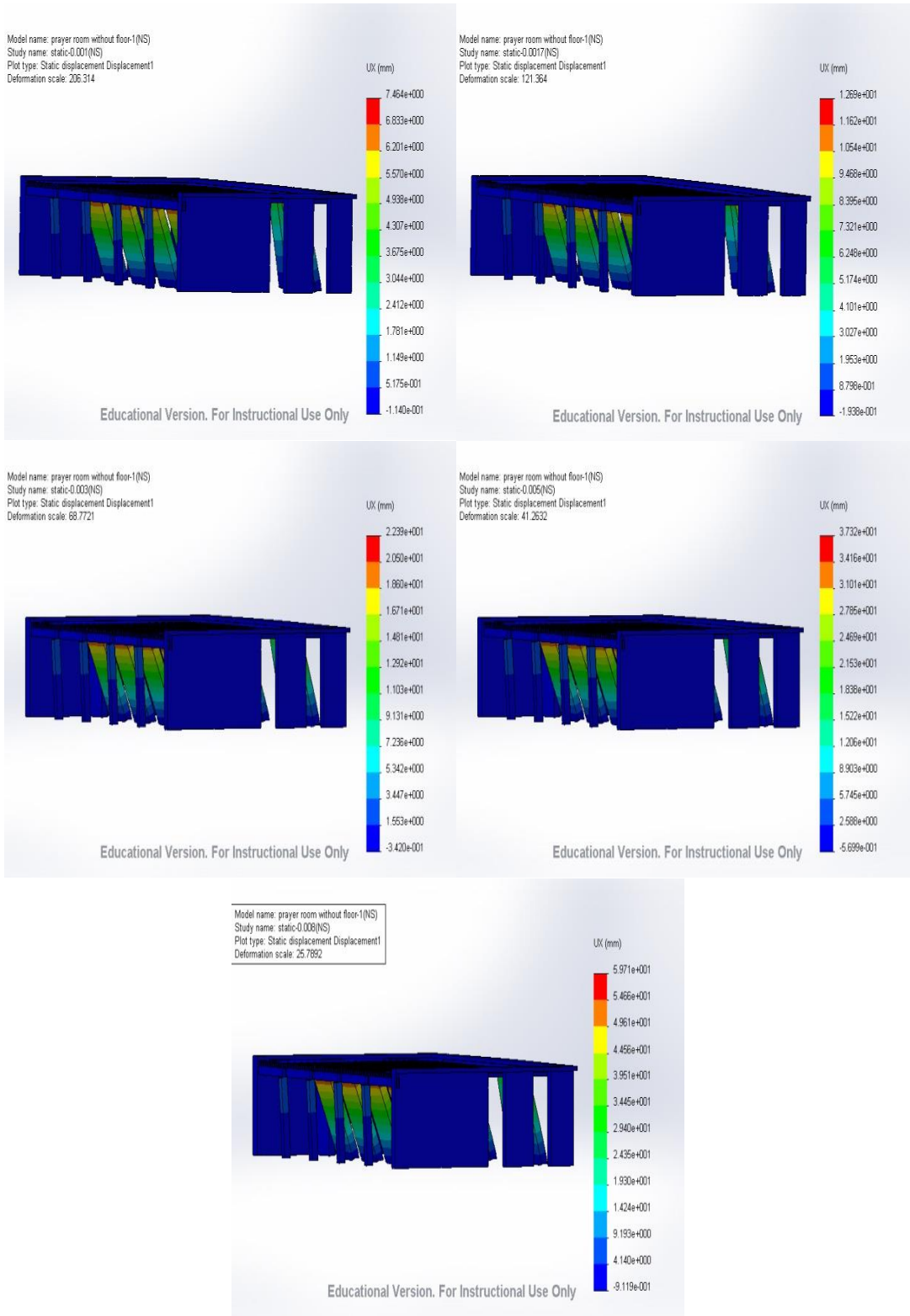


Figure 5-29 Deformed building in N-S direction (for the capacity curve steps - second perspective)

5.3.11.2.2 Principal tensile strains (maximum) N-S direction

Only one view is shown here for every step, namely the north-east view. The strains in the gable walls increased close to the edges with the north façade. This occurs because the north façade is trying to overturn more than the gable walls, so it is tending to detach from the building. Like for the east-west direction, the last step corresponds to a large displacement and the building could be already collapse in a real test. See Figure (5-30).

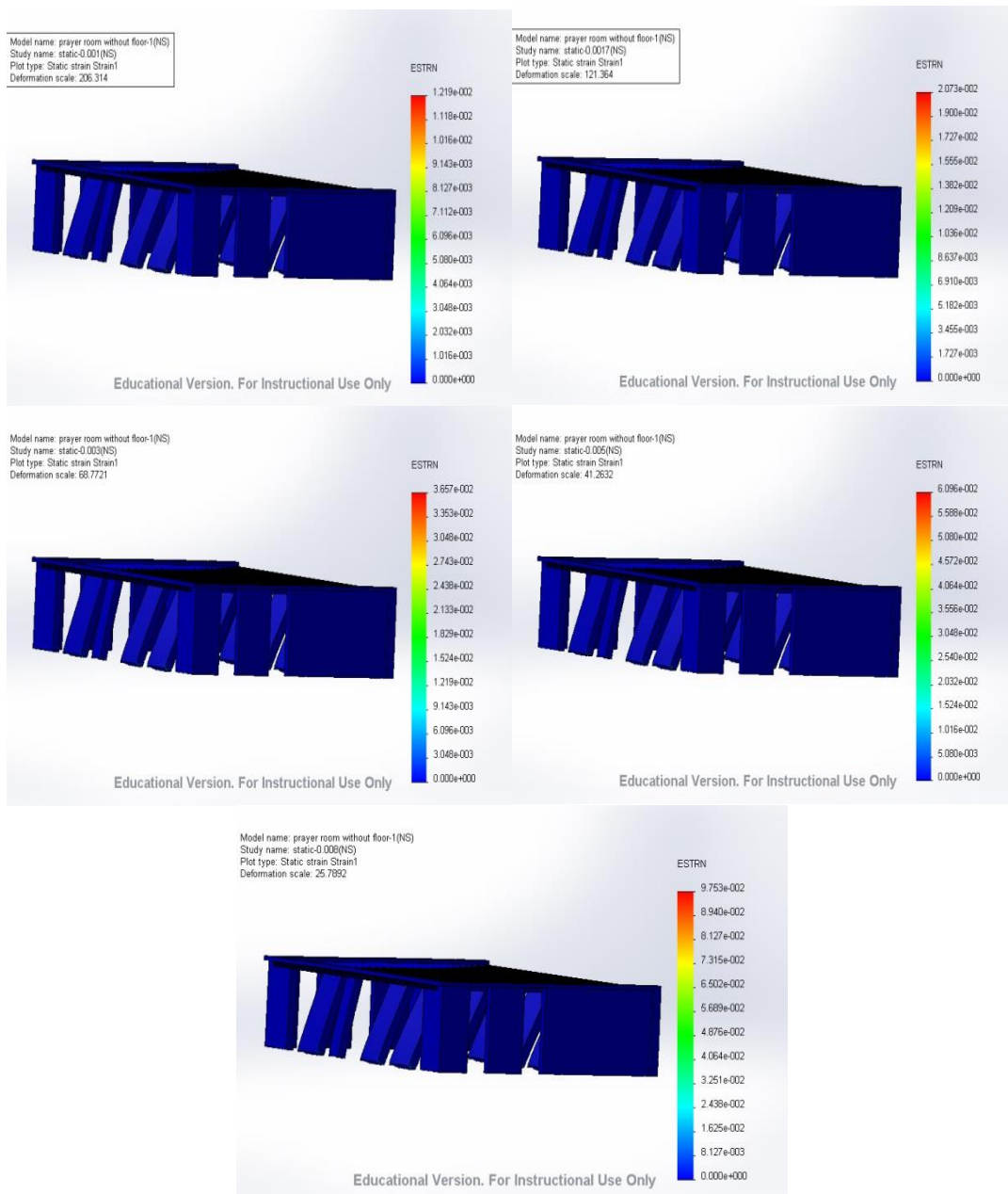


Figure 5-30 Tensile principal strain for all analysis steps of N-S direction

Theory disadvantages

The theoretical background of the method is difficult to defend. An important implicit assumption behind pushover analysis is that the response of a multi degree- of-freedom structure is directly related to an equivalent single-degree-of-freedom system. However, as seen in dynamic time-history analysis in the next section, the shape of the fundamental mode itself may vary significantly depending on the level of inelasticity and the location(s) of damage.

Furthermore, the deformation estimate obtained from a pushover analysis may be highly inaccurate for structures where higher mode effects are significant. The method, as currently prescribed in codes and seismic guidelines, explicitly ignores the contribution of the higher modes to the total response. In the cases where this contribution is significant, the pushover estimates may be totally misleading [46] [47].

5.4 TIME HISTORY METHOD

Dynamic time history analysis is used to determine the dynamic response of a structure through the direct numerical integration of the dynamic equations [48].

The non-linear calculation method has been performed in order to evaluate the maximum horizontal forces, vertical forces and the deformation on shear walls due to an artificial earthquake that takes into consideration the maximum peak ground acceleration in Dubai.

For the time history calculations, artificial time histories are generated for a type I spectrum for soil class A according to EN 1998-1. Figure 5-31 shows the response spectrum and the synthetic acceleration profile with a length of 10 seconds for a ground acceleration $a_{gR} = 1.66 \text{ m / s}^2$. See figure (5-32).

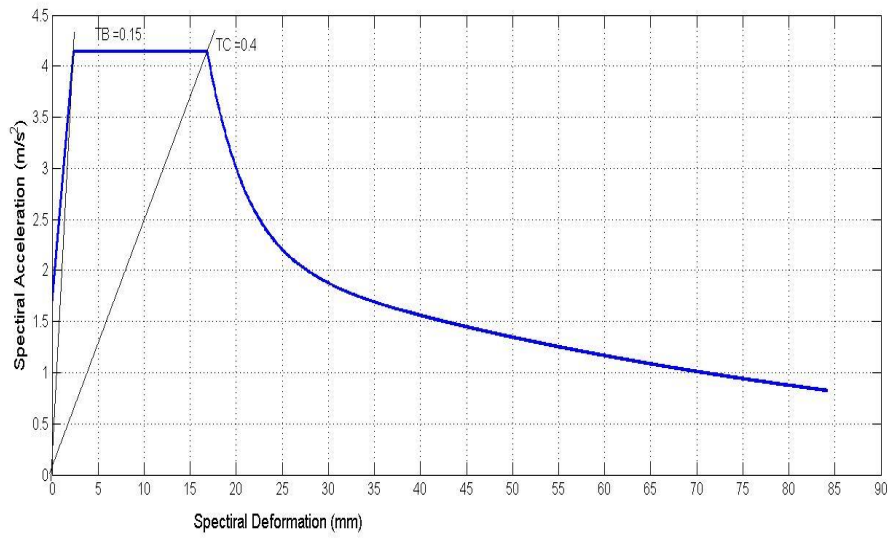


Figure 5-31 Response spectrum based on DIN EN 1998-1 (Type 1 – Class A) soil condition

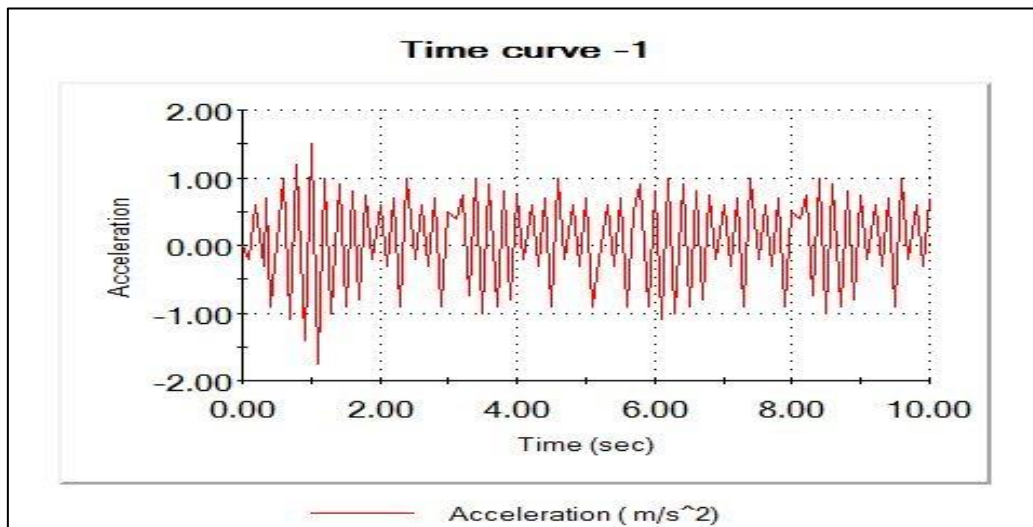


Figure 5-32 Time history of the peak ground horizontal acceleration

5.4.1 Horizontal strength calculation according to the time history method

The non-linear time history calculation of a bearing wall is made with the computer program Solid Works version 2013.

The following figures show the time history for the horizontal shear strength τ in each plane direction for all walls which lie in the x-direction (Figures 5-33, 5-34, 5-35 and 5-36).

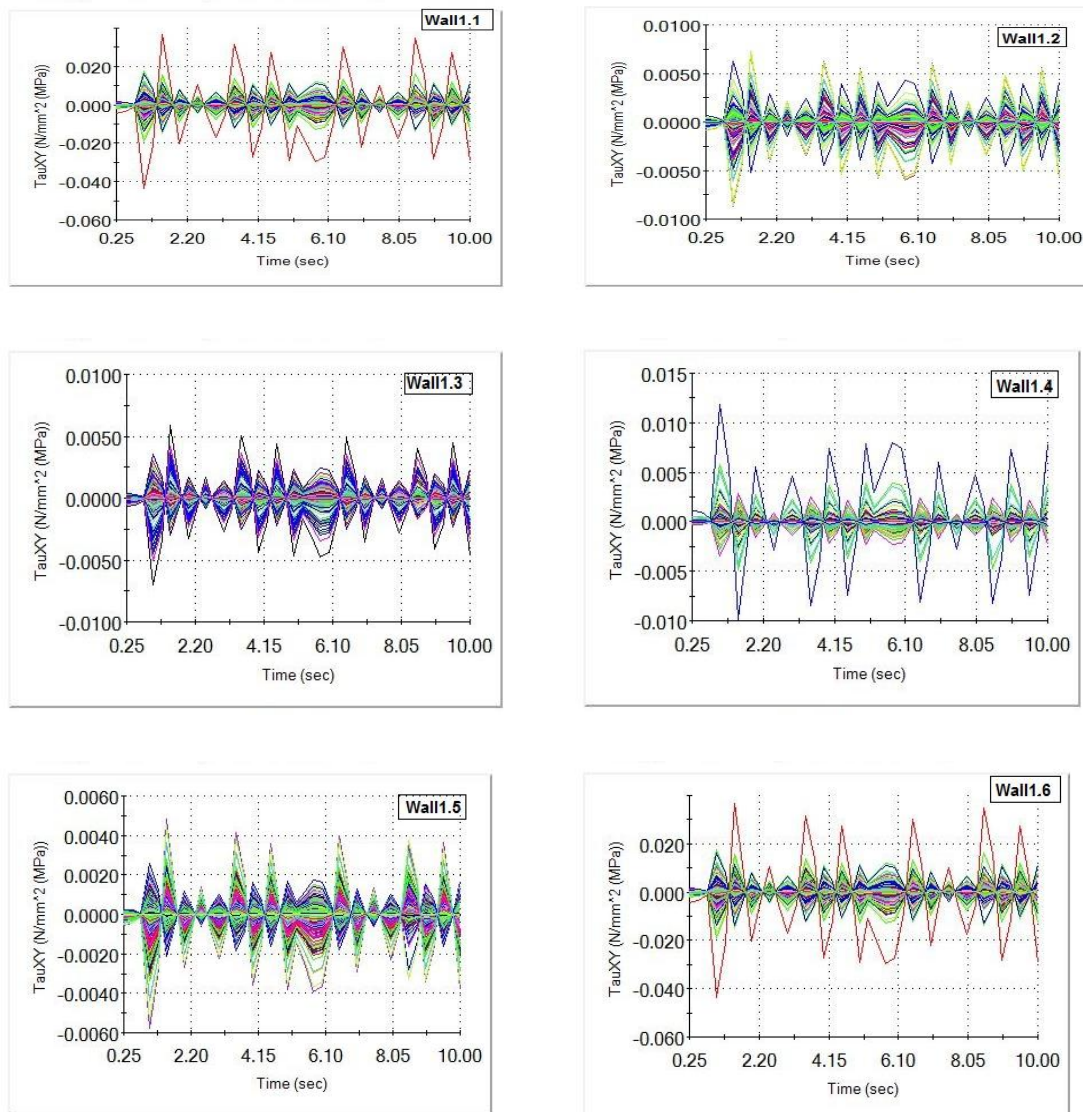


Figure 5-33 Horizontal shear stress due to the earthquake effect for Wall 1 in yz-plane

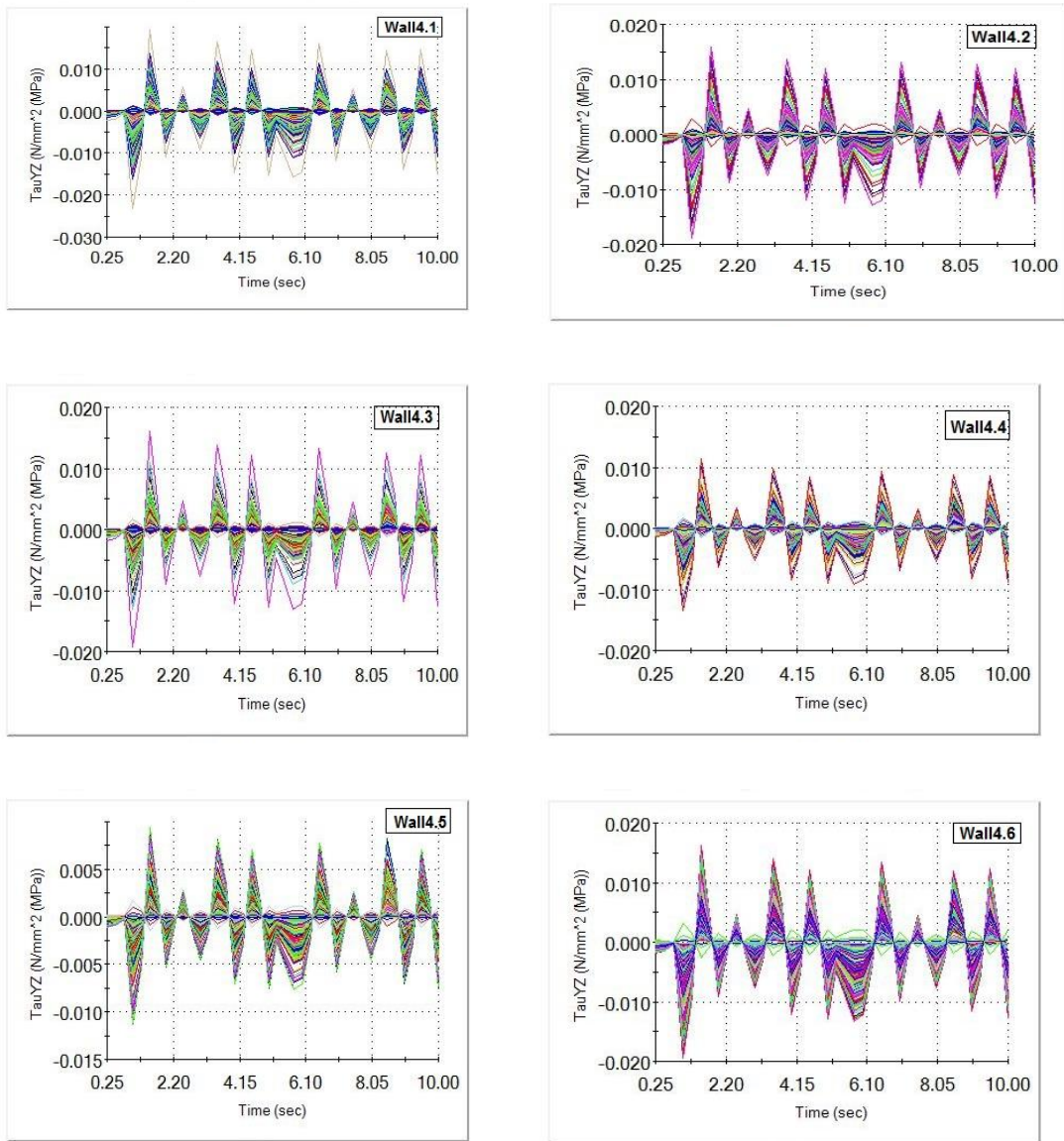


Figure 5-34 Horizontal shear stress due to the earthquake effect for Wall 4 in yz-plane

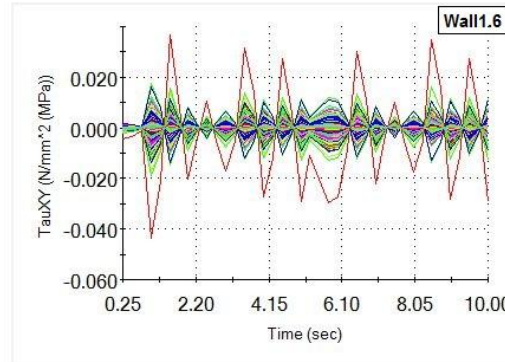
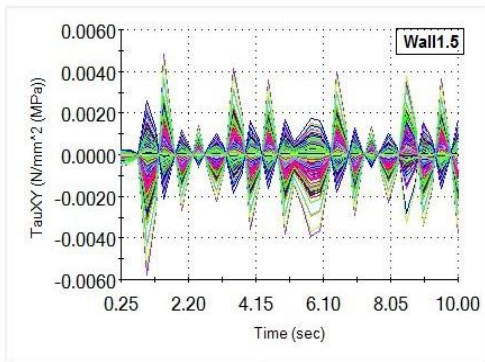
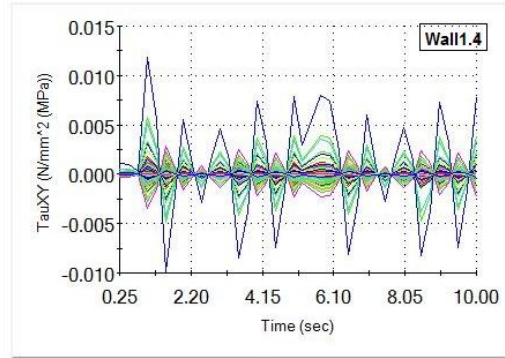
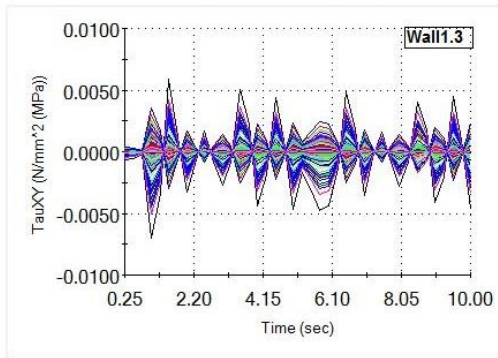
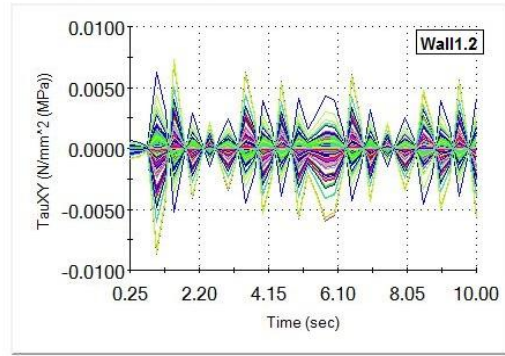
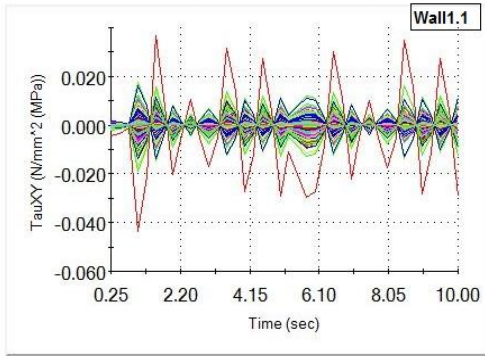


Figure 5-35 Horizontal shear stress due to the earthquake effect for Wall 1 in xy-plane

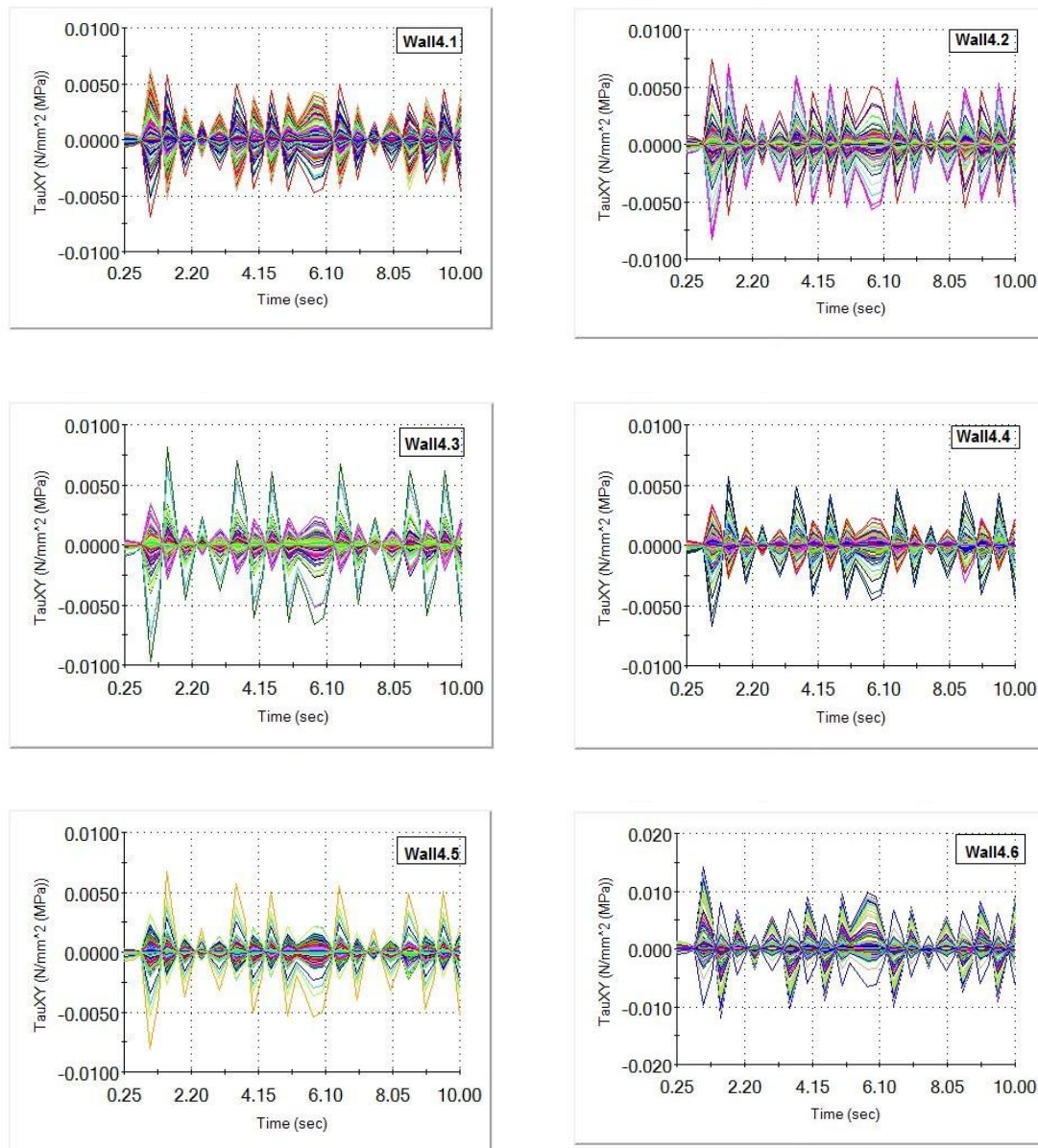


Figure 5-36 Horizontal shear stress due to the earthquake effect for Wall 4 in xy-plane

5.4.1.1 Summary of the horizontal shear strength results

The investigation into wall behaviour through the time history analysis method, using a finite element simulation, shows that the shear wall will be affected with shear stresses shown in Table 5-19. τ represents the shear stress in the yz and yx plane direction due to the earthquake and V_{RS} the shear force acting on the related wall according to the time history method.

Table 5-19 Approximate shear forces on shear walls in x-direction

Wall Number	L	t	Max. τ_{yz}	Max. τ_{yx}	V_{RS}
	m	M	N/mm ²	N/mm ²	KN
1.1	1.3	0.325	-0.041	-0.041	-17.32
1.2	1.7	0.325	-0.015	-0.0058	-8.29
1.3	1.5	0.325	-0.016	0.0052	-7.80
1.4	1.025	0.325	0.018	0.0115	6.00
1.5	1.7	0.325	-0.0164	-0.0059	-9.06
1.6	1.3	0.325	-0.041	-0.041	-17.32
4.1	1.35	0.325	0.03	-0.0052	13.16
4.2	1.7	0.325	-0.019	-0.0056	-10.50
4.3	1.7	0.325	-0.019	-0.0059	-10.50
4.4	1.7	0.325	-0.014	-0.0053	-7.74
4.5	1.7	0.325	0.013	-0.0056	7.18
4.6	1.8	0.325	-0.019	0.0145	-11.12

5.4.2 Deformation capacity calculation according to the time history method

The determined load-deformation capacity in accordance with the time history method has been calculated using the SolidWorks software program. The deformation result for the building was calculated through the total time of the artificial earthquake as accumulated absolute deformation (positive and negative direction) for 10 seconds (see Figure 5-37). The result showed that at the time $t = 0.5$ s, the deformation in the building reaches a value of 20 mm. This is comparable to the pushover method which reaches approximately the same value of deformation at the same time period.

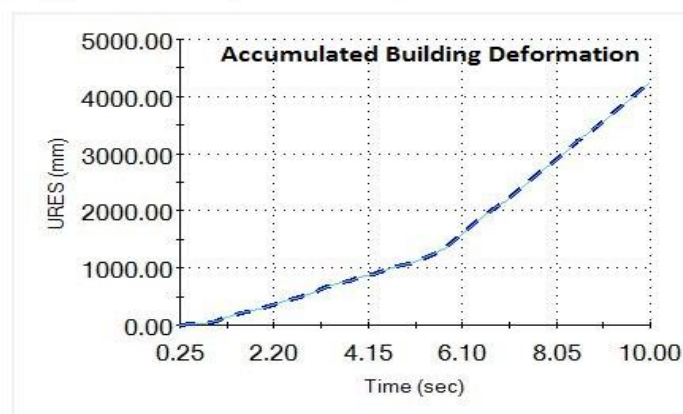


Figure 5-37 Accumulated absolute total deformation for the building through 10 sec.

Theory advantages and disadvantages

The time history method is often used for assessment purposes. The computing effort is higher than the response spectrum method and much higher than for the equivalent lateral force method. The scope of application of this theory is primarily to review existing structures and calculate ductility needs, displacements and stresses due to a specific earthquake.

Unlike modal response spectrum analysis, which provides the best estimates of the peak response by statistical means such as the SRSS and the CQC rules, peak response quantities determined by dynamic time history analysis are exact, falling within the framework of the reliability and representativeness of the non-linear modelling of the structure. The only drawbacks to the approach are its sophistication and the relative sensitivity of its outcome to the choice of input ground motions [49].

6. RETROFITTING METHODS AND NUMERICAL MODELING

The retrofitting of existing structures with insufficient seismic resistance accounts for a major portion of the total cost of hazard mitigation. Thus, it is of critical importance that structures that need seismic retrofitting are identified correctly and optimal retrofitting is conducted in a cost-effective fashion. Once the decision is made, seismic retrofitting can be performed through several methods with various objectives, such as increasing the load, deformation, and/or energy dissipation capacity of the structure. This chapter briefly outlines conventional as well as emerging retrofit methods. A numerical analysis for a retrofit method for the clay mosque in Hatta village, Dubai is also presented.

Conventional upgrading techniques usually include the addition of walls and foundations and strengthening of frames. Most of these techniques lead to costly consequences such as heavy demolition, lengthy construction time, reconstruction, and occupant relocation [50] [51].

Seismic retrofit becomes necessary if it is shown that, through a seismic performance evaluation, the building does not meet minimum requirements according to the current building code and may suffer severe damage or even collapse during a seismic event. Seismic retrofitting of buildings is a relatively new activity for most structural engineers. The retrofitting of a building requires an appreciation for the technical, economic and social aspects of the issue in hand. Changes in construction technologies and innovation in retrofit technologies present added challenge to engineers in selecting a technically, economically and socially acceptable solution [52] [53].

6.1 RETROFITTING METHODS FOR UNREINFORCED WALLS

Unreinforced structures in various categories have numerous retrofitting methods, some of which are under experiment and research. Applying these approaches to structures is projected to amplify the structure's firmness and ductility [54]. Nevertheless, at times the retrofitting cost is not practical and thus advanced technology is required. Therefore, the method is not appropriate for developing nations (which to retrofit buildings), particularly in

rural areas [55]. This work has introduced the most appropriate approaches for retrofitting various unreinforced.

6.1.1 Surface Treatment

The surface treatment is a frequent approach that has been developed largely via experience [56]. Due to the fact that the retrofitting approach covers the masonry walls' surface, it is sometime not appropriate for past buildings which are of architectural value. Current approaches in this type are as follows;

1. Bamboo-Band Retrofitting Technique

The technique of Bamboo-band retrofitting is straightforward enough and it can be understood and used by non-experts even without special skills. This technique enhances the adobe masonry building's seismic capacity considerably. The retrofitting system comprises both horizontal and vertical bamboo which is utilized as external reinforcement, figure (6-1).

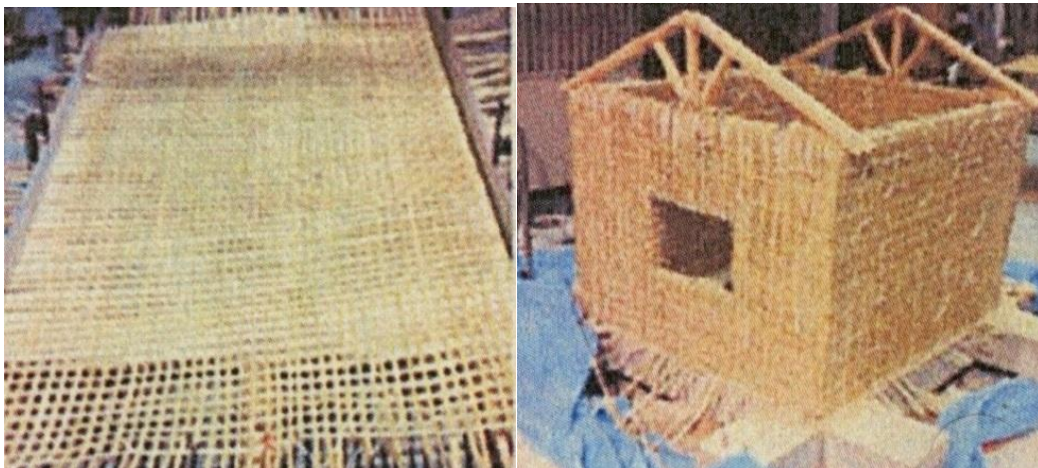


Figure 6-1 Preparing and applying bamboo-band mesh

Initially, bamboo band mesh should be organized on a square grid such that a band is able to cross over another one in diverse layers at succeeding crossing points. The process is comparable to the process of weaving basket. One should place straws at roughly two hundred mm pitch. The holes are often prepared through drilling on the walls. The mesh that has been prepared is actually installed both on the inside and the outside of a wall and it is wrapped around the house's corner. The outside and inside

meshes are often fixed using Polypropylene strings (referred to as PP strings) that are passed throughout the hole. Research indicates that the masonry building that are retrofitted using this approach may withstand input energy that is twice larger compared to what the non-retrofitted sample can do. Nevertheless, bricks that surround the bamboo may not offer suitable bamboo meshes' protection. Among the merits of this approach include its Low cost and it does not require workers with specialized skills.

2. Shotcrete

Researchers argue that Shotcrete is an approach of covering masonry walls that are reinforced using mesh of bars and they have sprayed concrete. The retrofitting approach is more suitable and cost ineffective compared to other approaches of retrofitting. The shotcrete layer's thickness can be tailored to seismic demand. Generally, the superimposed thickness should be about 60 mm. Expert acknowledges that the Shotcrete superimpose is characteristically strengthened using a joined wire fabric which is approximately minimum ratio of steel for controlling crack. In transferring the shear stress over the interface of shotcrete-masonry, cut off dowels (6 to 13 mm width at 25 to 120 mm) are set into holes using cement grout or epoxy by drilled into the wall of the masonry wall. See figure (6-2).



Figure 6-2 Applying Shotcrete

3. FRP (Fiber -Reinforced Polymer)

FRM is a complex material that is made of a polymer matrix strengthened using fibers. The fibers are often made of carbon, others glass and aramid. The substance has light weight and it does not corrode. When one applies this approach to a wall that has not

been strengthened, it elevates the in-plane as well as the out-of-plane wall's strength. Various tests on walls that are unreinforced retrofit with conducted epoxy linked carbon FRP , figure (6-3). Outcomes indicated the in-plane as well as out-of-plane reinforcement are considerably amplified due to retrofit [57].



Figure 6-3 FRP retrofitting method

6.1.2 Post-Tensioning

This is another method used broadly in enhancing the URM walls' flexural capacity and tensile .For URM walls' retrofit, this approach is used by center drilling from the masonry walls' top and post-tensioning those vertically walls to their foundation. The method entails an application of a compressive force to the walls of the masonry. Whereas this approach appears expensive, it has numerous merits since it does not change the structure's appearance. More importantly, the structure occupants are not disturbed as it is applied. See figure (6-4).



Figure 6-4 Applying post-tensioning method

6.1.3 Injection

Injection material is injected continuously into masonry walls via low pressure packers in an offset grid arrangement. In this manner faulty joints capillaries, pores and hollow cavities in the bricks are filled in with the injection material, figure (6-5).

Since this method does not affect the surface of the wall, it is popular for historical buildings with special architectural features. This technique is very useful for improving the compressive and shear strength of URM walls by restoring their initial stiffness. However, if injection is applied to some parts of the building, it must be proved that any partial increase of structure strength is not dangerous for other parts or the whole wall.



Figure 6-5 Applying the injection method to an existing masonry brick wall

6.1.4 Add new structural members to scale up the seismic performance

Various structural members are often added to the current buildings including Braces from diverse material for buildings which are often incorporated in the building to improve the earthquake performance, figure (6-6). New shear wall and other structural member can be built inside the construction [58].



Figure 6-6 Examples of seismic retrofitting methods

6.1.5 Reduce the seismic force inputted to the building

This method requires strong engineering experience to construct the additional members to the existing building, figure (6-7). It can be achieved through many techniques, such as:

- Installation of seismic isolation devices in the foundation.
- Installation of seismic isolation devices in the columns on an intermediate floor.
- Installation of vibration control braces to absorb earthquake energy.

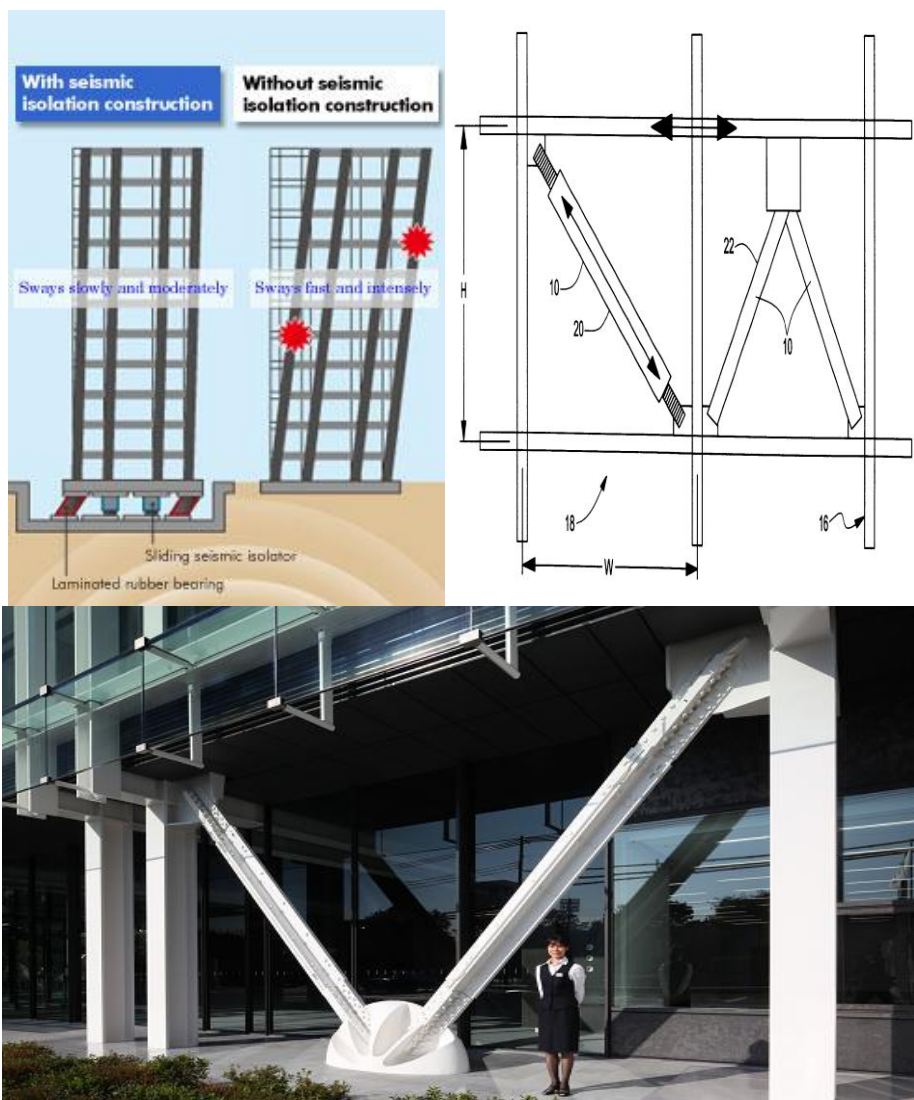


Figure 6-7 Examples of reducing seismic force

6.2 NUMERICAL MODELLING AND RESPONSE SPECTRUM ANALYSIS FOR SEISMIC EXCITATION

The numerical modelling in this section includes finite element analyses. The finite element simulation has been carried out for the clay mosque in Hatta, Dubai.

In the previous chapters, analytical and numerical analysis showed that this mosque has poor characteristics when it comes to seismic events. Therefore, the aim of the following simulation is to investigate the proximity shear stresses and wall deformations after two different retrofitting methods. Wood is used to retrofit the mosque using two different techniques. Different types of wood can be used in this method; however, because of the mosque has important historical value, oak and beech is used. At the end of this chapter, a compression of the simulation results has been introduced for both different techniques.

The building is a historical mosque in Dubai and consists of three separate parts: the prayer hall, office and the minaret. The bearing walls are entirely unreinforced clay, and the roof is made of a thin layer of clay and wooden balconies. As mentioned earlier, the building is located in the Hatta region, which has a reference ground acceleration of $a_{gr} = 1.7 \text{ m/s}^2$ see Figure (6-8). The material properties used for the simulation analysis can be found in table (5-14).

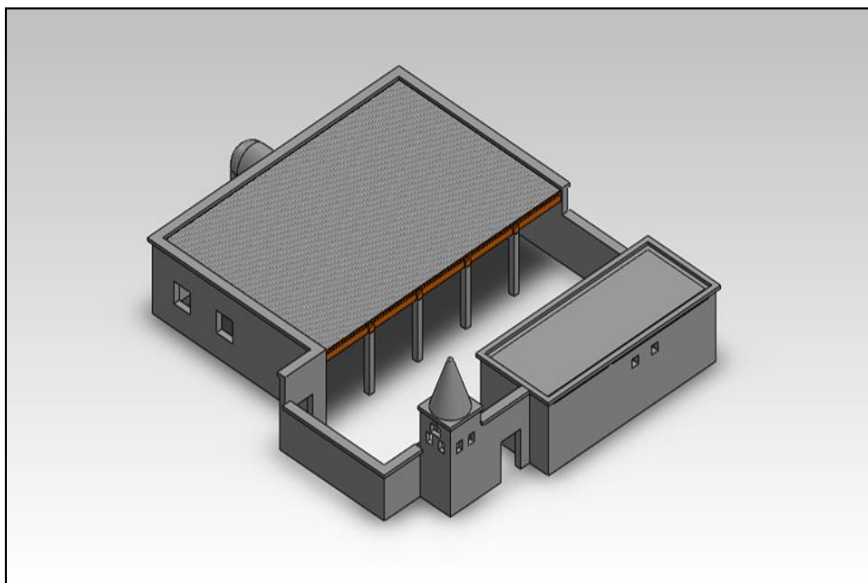


Figure 6-8 Clay mosque

6.2.1 Model simulation without retrofitting

In order to investigate the building's behavior through a seismic event, the building has been modeled without retrofitting using the Soft Works simulation program and analyzed using the response spectrum method. The shear stresses in the three directional planes have been obtained through this analysis and shown in the figures (6-9).

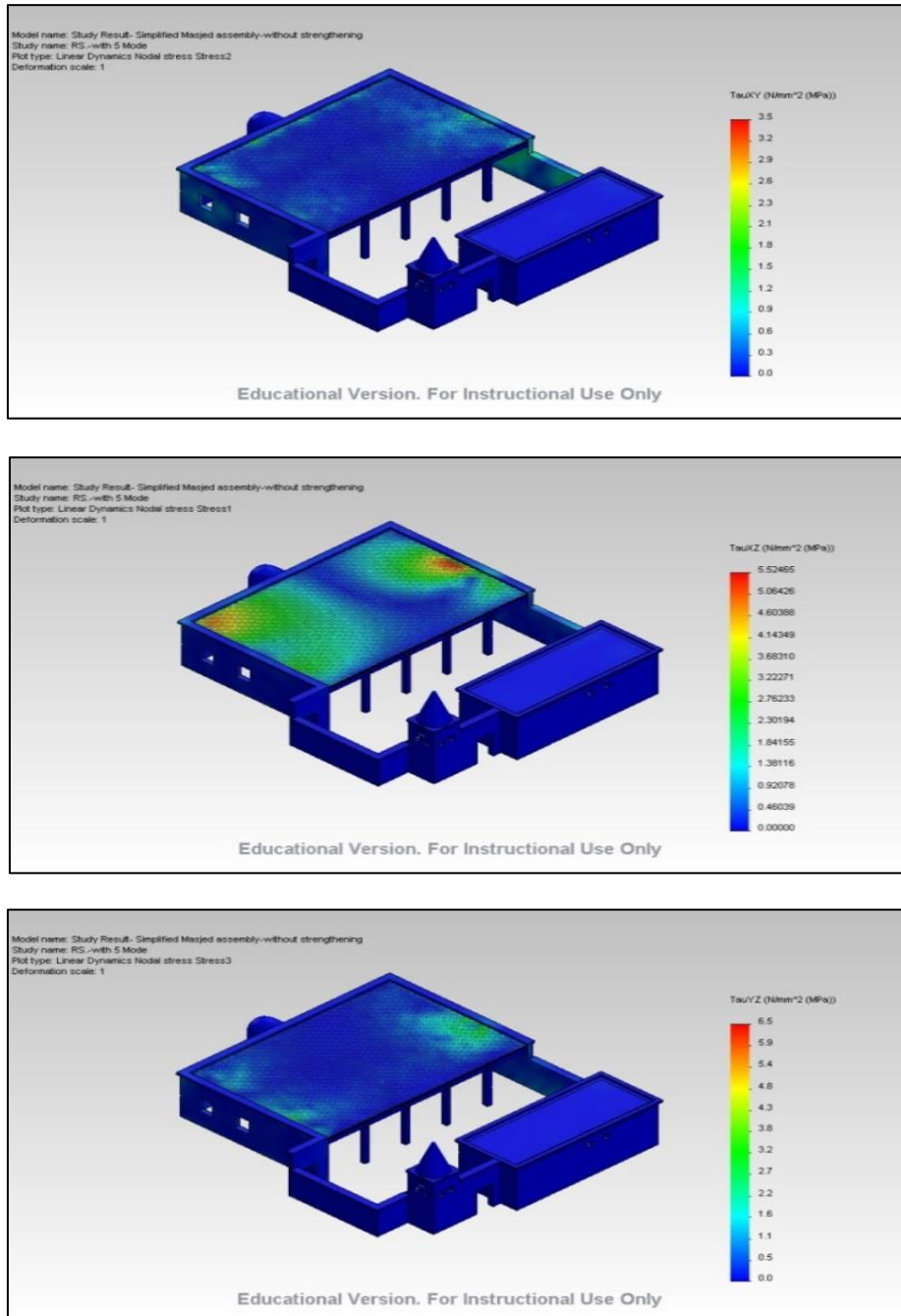


Figure 6-9 Shear stresses in x-y, y-z and x-z directions for the Mosque without retrofitting

As shown in the simulation results, the building is subjected to high shear stresses due to the earthquakes effect. Clay has a 0.5 N/mm^2 shear stress, which needs to be upgraded against seismic influence.

6.2.2 Model simulation with wood cross-bracing retrofitting

The first retrofitting method in this simulation is the use of the wood as cross (x)-bracing fitted to the wall sections between the openings. This method was developed in order to reduce the harmful shear stresses which increase due to seismic effects and to improve the performance of the building. Cross bracing is a form of reinforcement in construction that involves putting braces from the right-hand corner of the floor to the left-hand corner of the ceiling and *vice versa*. See figure (6-10).

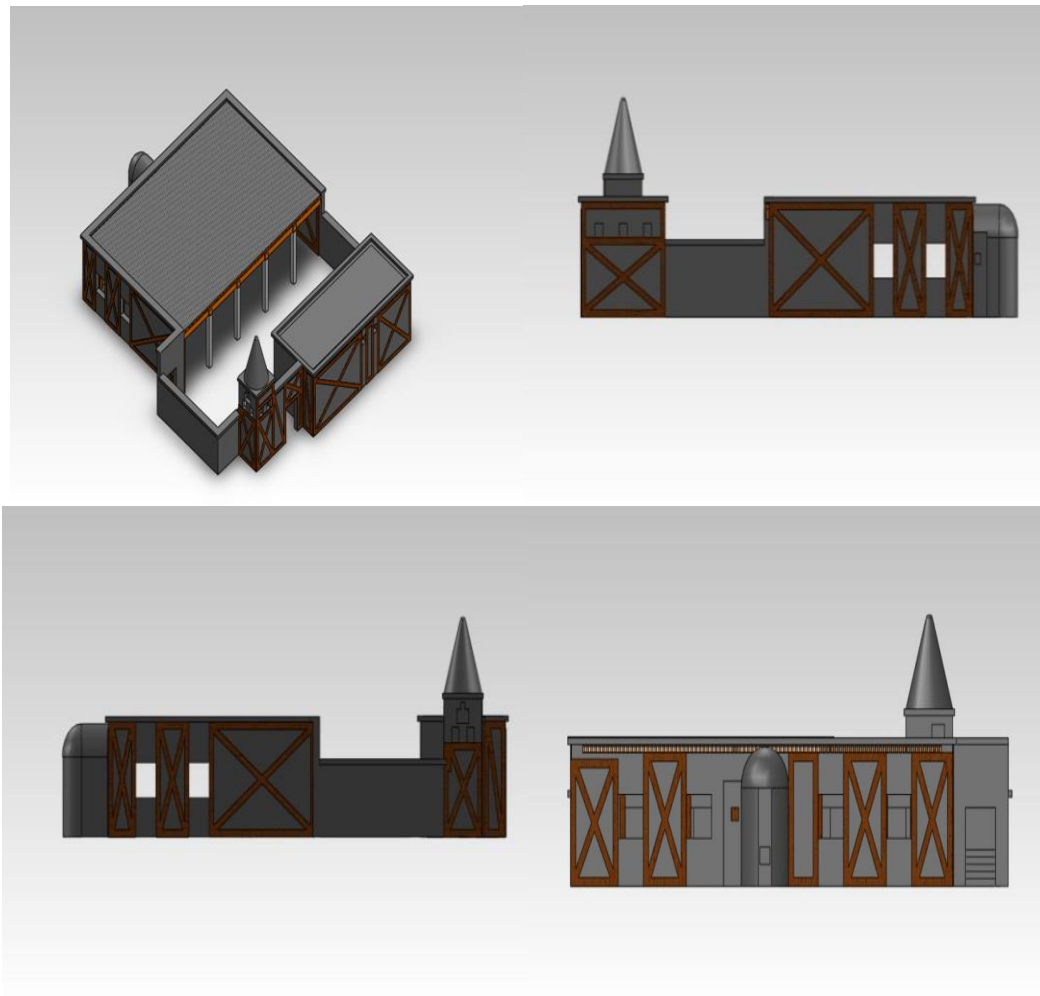


Figure 6-10 Model with wood X-bracing retrofitting

The result is an X-shaped brace that pushes the floor and ceiling against one another, thus increasing the structure's stability. Bracing is efficient because the diagonals work in axial stress and therefore call for minimum member sizes in providing stiffness and strength against horizontal shear.

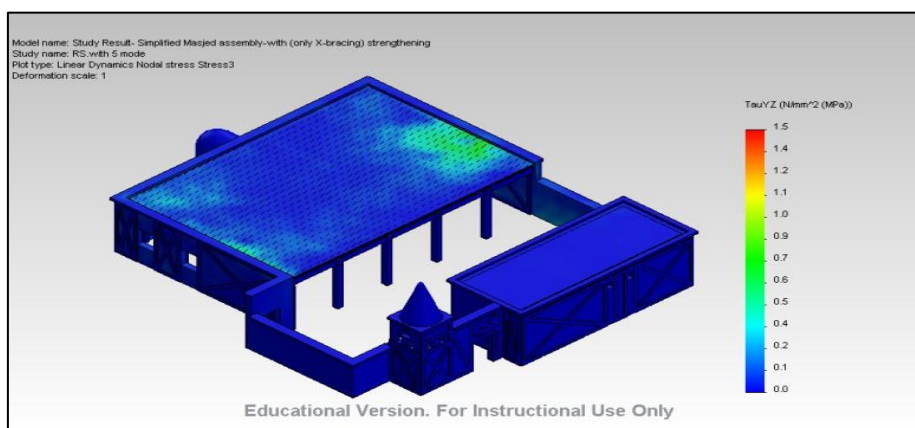
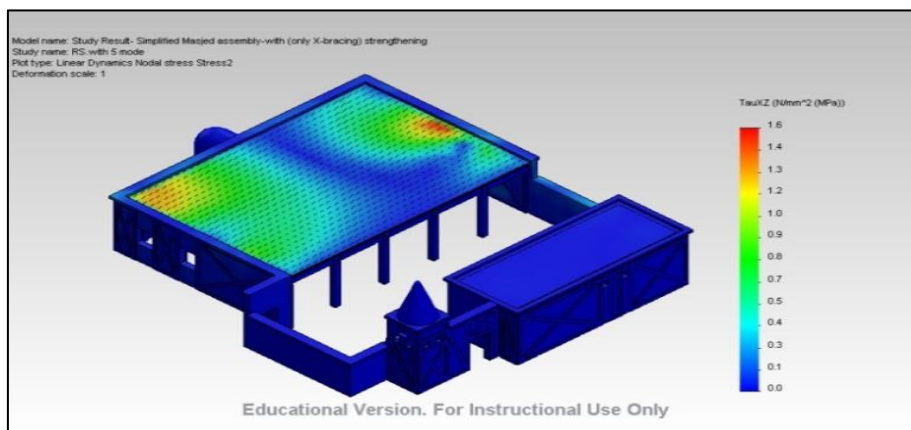
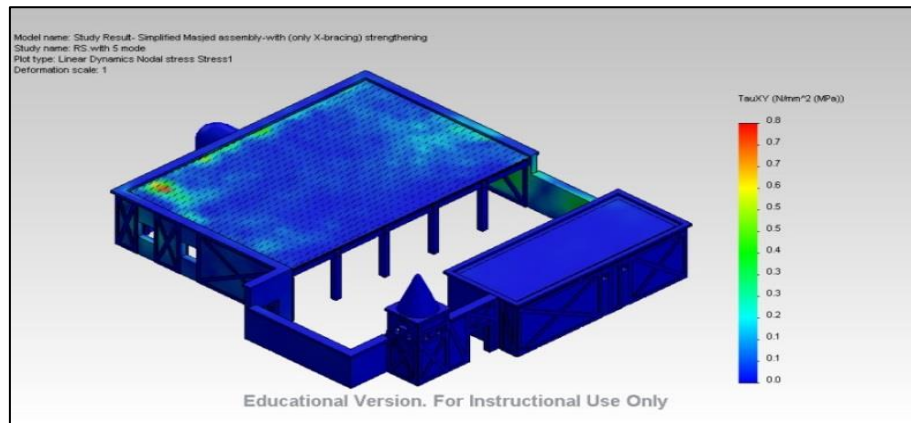


Figure 6-11 Shear stresses in x-y, y-z and x-z directions for the mosque after wood X-Bracing retrofitting

After the first retrofitting method, the numerical simulation shows a reduction in shear stresses in clay walls at a value of 0.1 N/mm^2 in various plane directions. In section 4.2.4, the experiments carried out on a clay wall section with a wood diagonal X-bracing corroborated the effect of constructing diagonals using this method.

6.2.3 Model simulation with wood X-Bracing and fixed wooden plate retrofitting

A better constructional method for obtaining increased robustness in building behaviour during earthquake events is to construct the diagonal X-braces on a 2cm solid wood plate and fixing them to the clay wall sections from both sides of the wall. See figure (6-12).

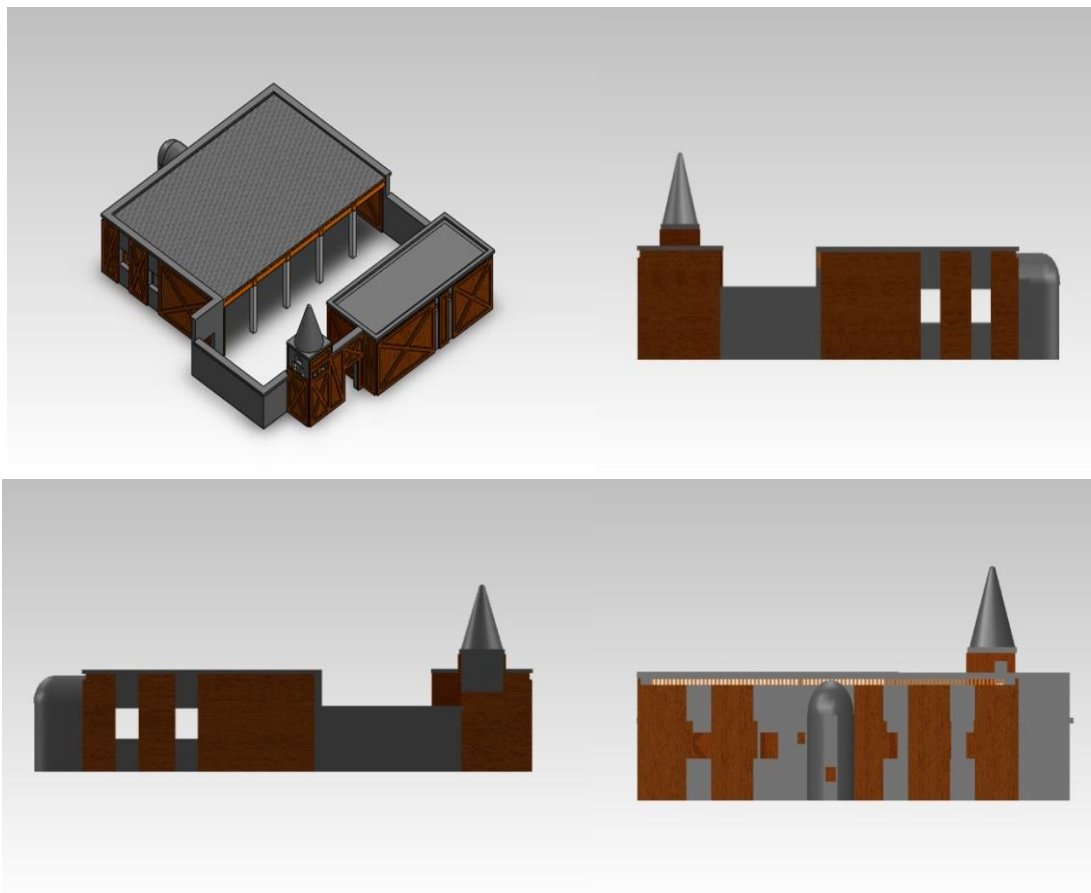


Figure 6-12 Model with wood x-Bracing and fixed wooden plate retrofitting

This method is not only beneficial from a structural standpoint, but also complements the architectural style of this historical building, which was originally constructed using both clay and wood. Disadvantages might be the high cost and requirement for proficient interior design skills. It also increases the building's mass which in turn increases the inputting earthquake force.

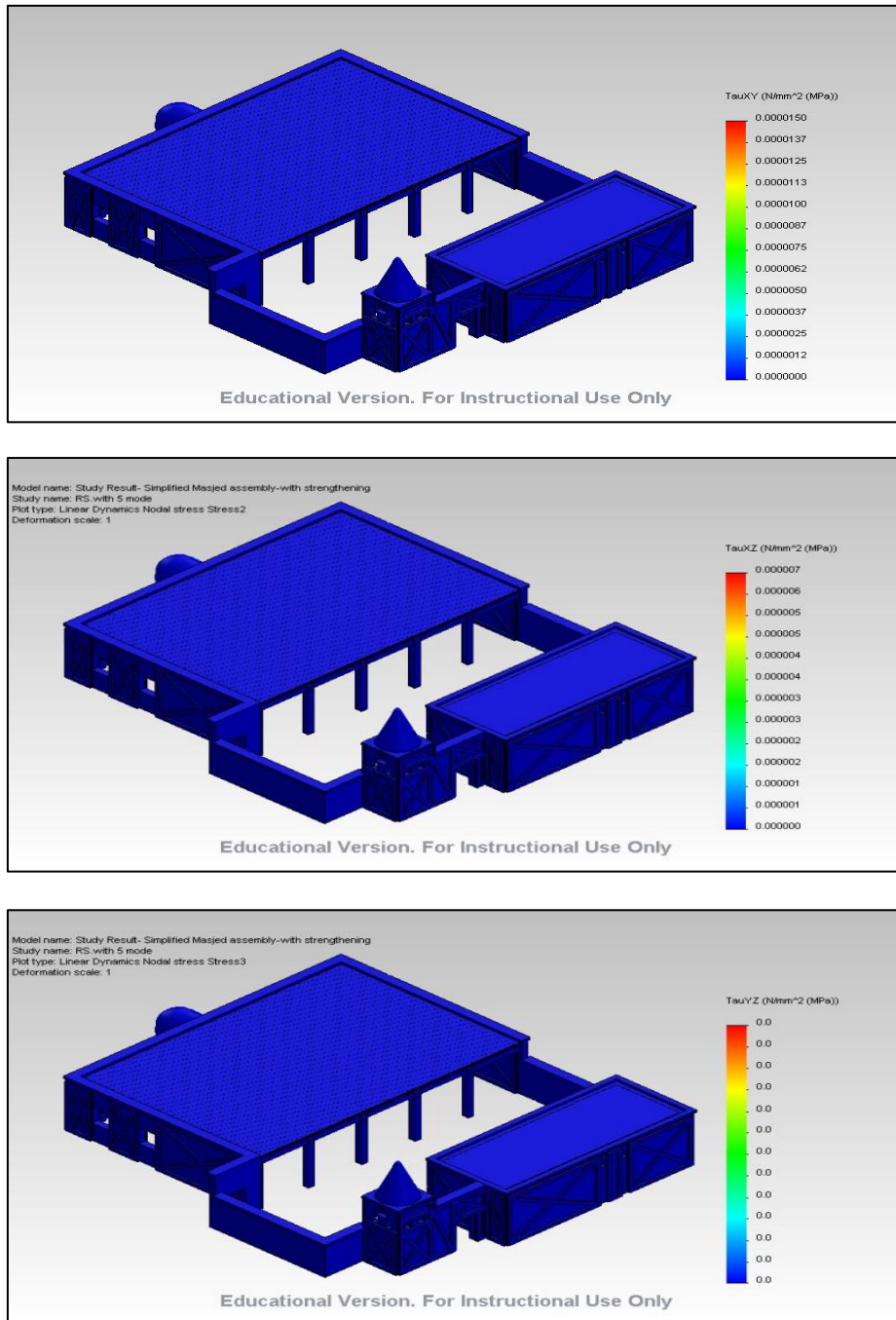


Figure 6-13 Shear stresses in x-y, y-z and x-z directions for the mosque wood X-bracing and fix plate retrofitting

The simulation results under the response spectrum analysis method showed a strong improvement in building shearing capacity by reducing the shear stresses that occurred at the clay walls and enhancing the seismic resistant qualities of the structure see Figure (6-13).

The solid wooden plate and X-bracing have worked as outer reinforcement for the clay walls and supported both sides against shear forces and any out of plane failure.

6.2.4 Numerical analysis for the top displacement

One point that should be considered throughout this analysis is horizontal top shift displacement of the clay walls. These deformations may lead to disaster, especially if the roof can no longer be supported. In chapter 5, the wall's horizontal top displacement was statically and dynamically calculated for the prayer hall, while here in this section figure (6-14), a numerical analysis using the response spectrum analysis method has been implemented on the whole mosque building before and after retrofitting.

The results show that the clay building suffers a maximum horizontal displacement of up to 20 mm.

The results for the two retrofitting methods showed a reduction in shift displacement with cross bracing of up to 50 % and a reduction of up to 90% for top shifting displacement when using X-bracing and a wooden plate.

This can be explained through the fixing of walls against the deformations, especially the wall parts between openings, which are considered to be high risk during an earthquake.

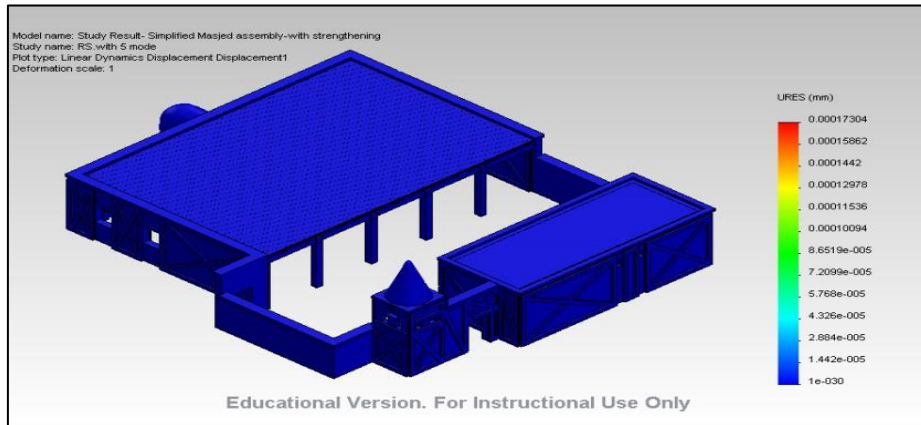
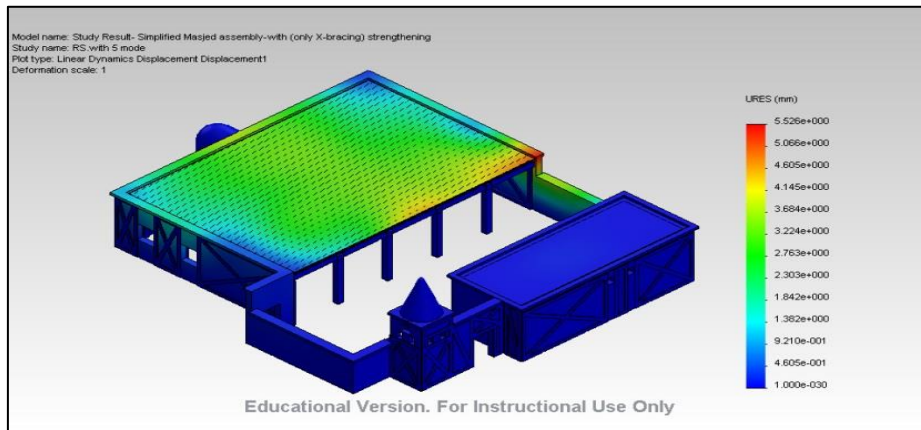
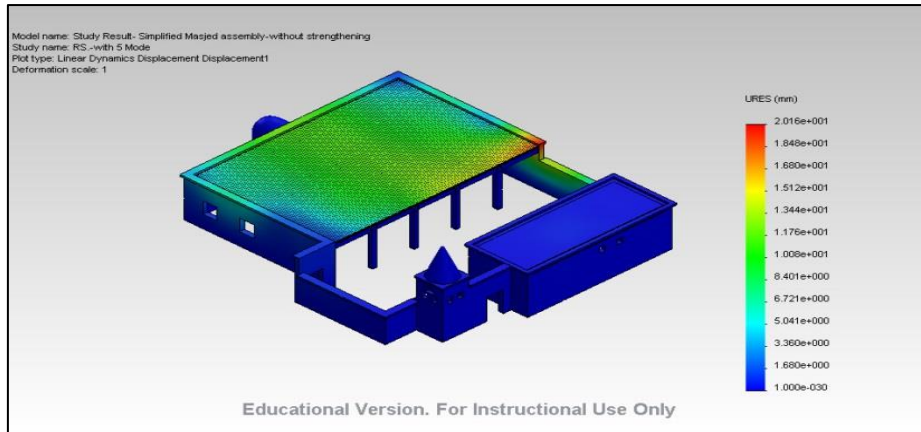


Figure 6-14 Maximum top displacement for the model before and after the two methods of retrofitting

6.3 COMPARISON OF THE NUMERICAL ANALYSIS RESULTS

In order to deduce the influence of the retrofitting methods, a results comparison of the finite element simulation analysis for the response spectrum method is shown in Table (6-1).

The table presents the shear stresses in each directional plane and the top horizontal shift displacement for each wall of the mosque building, Figure (6-15).

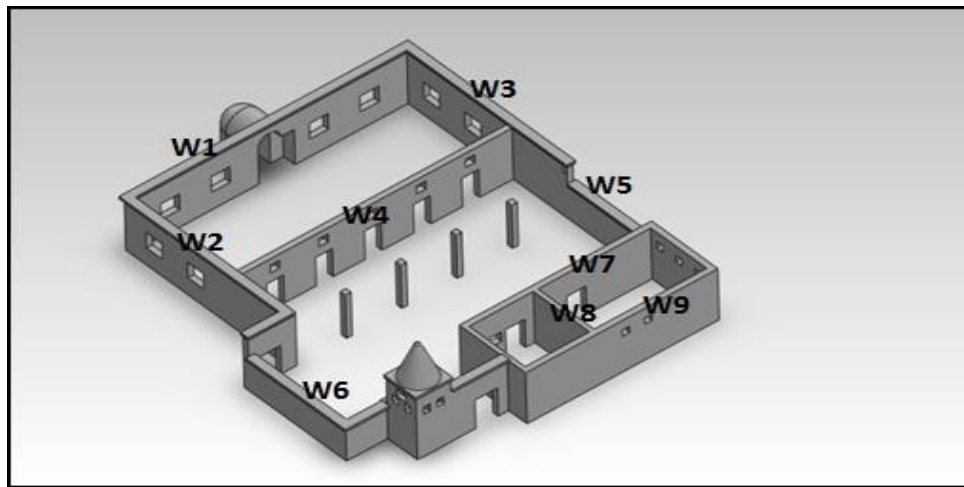


Figure 6-15 Walls numbering as used for the compression

Table 6-1 Comparison of the numerical analysis results

Wall #	Max. T_{xy} [N/mm ²]			Max. T_{xz} [N/mm ²]			Max. T_{yz} [N/mm ²]			Max. Top Displacement [mm]		
	Without Retrofitting	With X-Bracing	With X-Bracing and Fixed plate	Without Retrofitting	With X-Bracing	With X-Bracing and Fixed plate	Without Retrofitting	With X-Bracing	With X-Bracing and fixed plate	Without Retrofitting	With X-Bracing	With X-Bracing and fixed plate
W1	3.52	0.8	0	2.74	0.75	0	6.4	1.48	0	11.8	3.55	0
W2	1.6	0.3	0	2.2	0.71	0	3.55	1.09	0	6.4	1.77	0
W3	1.9	0.41	0	3.3	1.76	0	5.9	1.18	0	20.35	5.49	0
W4	1.6	0.45	0	2.05	0.58	0	4.17	1.4	0	4.99	1.35	0
W5	0.47	0.14	0	0.19	0.27	0	0.44	0.09	0	1.7	0.43	0
W6	0.09	0.015	0	0.4	0.019	0	0.11	0.025	0	0.269	0.047	0
W7	0.23	0.048	0	0.2	0.07	0	1.17	0.046	0	0.3	0.054	0
W8	0.123	0.03	0	0.13	0.023	0	0.19	0.47	0	0.55	0.13	0
W9	0.085	0.01	0	0.04	0.011	0	0.05	0.011	0	0.5	0.011	0

7. SUMMARY AND CONCLUSION

We cannot prevent natural disasters from striking, but we can prevent or limit their impact by making buildings strong enough to resist their destructive forces. In the case of earthquakes, it is possible, as this study demonstrates, to neutralize their harm by applying basic engineering and planning principles that are inexpensive and not beyond the skills of most building industries.

This work presents some of the most important aspects of earthquake influence on historical clay buildings. The model which has been chosen is a mosque of great historical importance in Hatta Village in Dubai.

The experimental results on clay specimens provide important clay mechanical specifications which are used as input for the analytical and numerical methods.

The methods used for determining the clay walls' performance under seismic effects consider the linear and non-linear behaviour of clay during earthquake events. The theory implemented for this purpose helped to predicate the shear stresses and deformation values that arise in clay walls under static and dynamic conditions. The analysis showed that a high level of shear stress will negatively affect the clay walls and might lead to a full building collapse.

After investigating the linear and non-linear behaviour of the clay building, a solution and retrofitting methods were introduced by which it is possible to sufficiently reduce the shear stresses and wall shift deformation and give more stability for the building against earthquake effects.

The two retrofitting methods were proven through a finite element program implemented in accordance with the response spectrum method. The first method used wooden cross-bracing for the clay walls and showed a strong improvement in shear capacity. The second method used a solid wooden plate and wooden cross bracing and showed an excellent strength improvement for the building's clay walls.

As recommendations for further research, further investigation could be conducted into the behaviour of clay used in combination with other building materials such as concrete or different types of brick.

Another possibility is to develop and test more retrofitting methods by using new and different materials that can be combined easily with clay buildings and show strong performance against earthquakes.

8. REFERENCES

- [1] Marcial Blondet and Gladys Villa Garcia M., ADOBE CONSTRUCTION, Catholic University of Peru, Peru.
- [2] EN1998-1:2004 Eurocode 8: Design of structures for earthquake resistance
- [3] <http://www.solidworks.com>
- [4] Clay constructions in Arabic countries/Dr.Mansor Aljded / Prince Saud University
- [5] Eyad Aldoghaim/Verbesserung der seismischen Kapazität von Mauerwerkswänden durch Verwendung von Elastomerlagern/ Kassel im Januar, 2011
- [6] Müller, F. P.; Keintzel, E.: Erdbebensicherung von Hochbauten. Berlin.Ernst & Sohn,1984.
- [7] Trifunac, M. D., and Brady, A. G., 1975. A study on duration of strong earthquake ground motion, *Bull. Seismol. Soc. Am.* **65**, 581–626.
- [8] Bachmann H.: Erdbebensicherung von Bauwerken. Birkhäuser Verlag Basel, 1995.
- [9] Der Kiureghian A.: A response spectrum method for random vibrations. Earthquake Engineering Research Center, Report UCB/EERC-80/15, University of California, Berkeley 1980.
- [10] Thomas Wenk:Dissertation: Nichtlineare dynamische Berechnung von Stahlbetonrahmen unter Erdbebeneinwirkung/ Zürich August 2000
- [11] Paret T.F., Sasaki K.K., Eilbeck D.H., Freeman S.A.: Approximate Inelastic Procedures to Identify Failure Mechanisms from Higher Mode Effects. Proceedings of the Eleventh World Conference on Earthquake Engineering, Paper No. 966, Elsevier,New York 1996
- [12] Freeman S.A., Nicoletti J.P., Tyrell J.V.: Evaluations of Existing Buildings for Seismic Risk- A Case Study of Puget Sound Naval Shipyard, Bremerton, Washington. Proceedings of the U.S. National Conference on Earthquake Engineering, Earthquake Engineering Research Institute, Oakland, California, 1975.
- [13] Freeman S.A.: The Capacity Spectrum Method as a Tool for Seismic Design. Proceedings of the 10th European Conference on Earthquake Engineering (XIthECEE),Sept. 6-11, 1998, Paris, France. A.A. Balkema, Rotterdam, Brookfield 1998.
- [14] Chopra A.K.: Dynamics of Structures. Prentice-Hall Inc., Englewood Cliffs, New Jersey 1995.
- [15] Anderheggen E.: Nichtlineare Finite Element Methoden: Eine Einführung fürIngenieure. Institut für Informatik, ETH Zürich 1986.
- [16] Jeanette Gasparini,Erdbebensicherheit von Lehmsteinbauten untersucht für den Standort Oaxaca, Mexiko, Berlin 2006
- [17] MANN, MÜLLER (Schubtragfähigkeit 1978) Mann, W.; Müller H.; Schubtragfähigkeit von Mauerwerk; Mauerwerks-Kalender 1978; S.35 ff.

- [18] BERNADINI, MODENA, TURNŠEK, VESCOVI (Shear Resistance 1980) Bernardini, A.; Modena, C.; Turnšek, V.; Vescovi, U.; A Comparison of three Laboratory Test Methods used to Determine the Shear Resistance of Masonry Walls; Proceedings of the 7th World Conference on Engineering (IAEE, Istanbul/Turkey 1980); P. 181-184
- [19] GHANEM, ABU-EL-MAGD, HOSNY (Diagonal Tension Test Calculation 1994) Ghanem, G; Abu-El-Magd, S.; Hosny, H.; Suggested Modifications to the Diagonal Tension Test Calculation for Masonry Assemblages; Proceedings of the 10th International Brick and Block Masonry Conference, Vol.3, Calgary Canada, 1994; S.1325-1334
- [20] Marcial Blondet and Rafael Aguilar, SEISMIC PROTECTION OF EARTHEN BUILDINGS, Peru 2007.
- [21] Blondet M, Torrealva D, Vargas J, Velasquez J and Tarque N. 2006. "Seismic Reinforcement of Adobe Houses Using External Polymer Mesh". First European Conference on Earthquake, Engineering and Seismology. Geneva, Switzerland.
- [22] Bruckner A. ,Bauen mit Lehm an Hand von Beispielen aus Österreich, Deutschland, Südtirol; Diplomarbeit am Institut für Baustofflehre, Bauphysik und Brandschutz der TU-Wien, 1996
- [23] www.rael-sanfratello.com
- [24] Volhard, Franz / Röhlen, Ulrich: Lehm-Bau-Regeln : Begriffe, Baustoffe, Bauteile, 3. Auflage, Braunschweig: Vieweg & Sohn, 2007
- [25] DIN 18952: Prüfung von Baulehm, Berlin: Fachnormenausschuss Bauwesen im Deutschen Normenausschuss, 1956.
- [26] DIN 18953: Baulehm, Lehm-Bauteile, Berlin: Fachnormenausschuss Bauwesen im Deutschen Normenausschuss, 1951
- [27] EN 1015-11: Prüfverfahren für Mauermörtel, Teil 11: Bestimmung der Biege- und Druckfestigkeit von erhärtetem Mörtel, Wien: Österreichisches Normungsinstitut, 2003
- [28] Neville, A.M., 1996. Properties of Concrete (Fourth and Final Edition), John Wiley & Sons, Inc, New York
- [29] EN1996-Eurocode 6: ÖNORM B1996-1-1: Eurocode 6: Bemessung und Konstruktion von Mauerwerksbauten, Wien: Österreichisches Normungsinstitut, Ausgabe: 2009-03-01.
- [30] Dierks, Klaus / u.a.: Lehm-Bau in Theorie und Praxis, Berlin: Unterlagen zum Seminar, 1998
- [31] Mandadjieva, Joana: Baustoffeigenschaften von Lehm, Wien: Institut für Baustofflehre, Bauphysik und Brandschutz, 1997
- [32] Minke, Gernot: Das neue Lehm-Bau-Handbuch, 5. Auflage, Staufen bei Freiburg: Ökobuch Verlag, 2001
- [33] Volhard, Franz: Leichtlehm-Bau. Alter Baustoff - neue Technik, 4.Auflage, Karlsruhe: C.F.Müller, 1990

- [34] <http://www.seismo.geodesy.ae>, Dubai seismic network , Seismic Hazard Assessment.
- [35] Khader Abu-Dagga, A Framework for Seismic Fragility Assessment of Model Buildings in Sharjah, United Arab Emirates, University of Sharjah 2009
- [36] ASCE (2006). Automated People Mover Standards, ASCE Journal Vol 51; 54-76
- [37] American Public Transport Association (1999). Manual for the development of rail transit system safety program plans. Sterling, V.A.
- [38] Agarwal, P. and Shrikhande, M., (2006), Earthquake Resistant Design of Structures, 2nd Edition, Prentice-Hall of India Private Limited, New Delhi
- [39] Cardone, D. and Dolce, M., (2003), Seismic Protection of Light Secondary Systems through Different Base Isolation Systems, Journal of Earthquake Engineering, 7 (2), 223-250.
- [40] Both, D., Dubinsky,R., and Hil P. (1998). Summary of findings and bibliography for the Department of Energy's innovative residential retrofit delivery system demonstrations. New York: RAND Corporation
- [41] Sonja P., (2011), Property Assessed Payments for Energy Retrofits: Strategic Recommendations for an optimal "PAPER" Program. Sustainable Alternatives Consulting, 2011. 54 pages.
- [42] Meskouris K./ Hinzen K.-G./ Butenweg Ch./Mistler M., Bauwerk und Erdbeben 3. Auflage
- [43] Christoph Gellert, Diss. Nichtlinearer Nachweis von unbewehrten Mauerwerksbauten unter Erdbebeneinwirkung,2010
- [44] EN1998-3:2004 Eurocode 8: Design of structures for earthquake resistance
- [45] Kolbitsch, Andreas:Erhaltung und Erneuerung von Hochbauten, Wien: Skriptum zur Vorlesung U., Institut für Hochbau und Technologie, 2011
- [46] Bachmann H.: Kapazitätsbemessung und plastisches dynamisches Verhalten von Stahlbetontragwerken. Beton- und Stahlbetonbau, Heft 4, 1999. IBK Sonderdruck Nr. 0023, Institut für Baustatik und Konstruktion, ETH Zürich 1999.
- [47] Bachmann IL. Linde P.. Wenk T.: Capacity Design and Nonlinear Dynamic Analysis of Earthquake-Resistant Structures. IBK Sonderdruck Nr. 0002, Institut für Baustatik und Konstruktion. ETH Zürich 1994.
- [48] Hugo Bachmann: Erdbebensicherung von Bauwerken 2. Auflage, BirkhÄuser Verlag, Basel-Bosten,Berlin 2002.
- [49] Chopra A.K.: Dynamics of Structures. Prentice-Hall Inc., Englewood Cliffs, NewJersey 1995.
- [50] Hugo Bachmann: Seismic Conceptual Design of Buildings – Basic principles for engineers, architects, building owners and authorities , Biel 2002.
- [51] Vargas J, Blondet M, Ginocchio F, Villa-Garcia G. 2005. "35 years of research on SismoAdobe". In Spanish. Internacional Seminar on Architecture, Construction and

Conservation of Earthen Buildings in Seismic Areas, SismoAdobe2005. PUCP. Lima. Peru.

- [52] Blondet M, Villa-Garcia G, and Brzev S. 2003. "Earthquake-Resistant Construction of Adobe Buildings: A Tutorial". Published as a contribution to the EERI/IAEE World Housing Encyclopedia. <http://www.world-housing.net>,2003
- [53] Tolles L, Kimbro E, Webster F, and Ginell F. 2000. Seismic Stabilization of Historic Adobe Structures: Final Report of the Getty Seismic Adobe Project, GSAP. Los Angeles: The Getty Conservation Institute.
- [54] Blondet M, Ginocchio F, Marsh C, Ottazzi G, Villa Garcia G, Yep J. 1988. "Shaking Table Test of Improved Adobe Masonry Houses". 9th World Conference on Earthquake Engineering. Tokyo-Kyoto, Japan.
- [55] Zegarra L, Quiun D, San Bartolome A, and Giesecke A. 1997. Reinforcement of Existing Adobe Dwellings 2nd part: Seismic Test of Modules. In Spanish. XI National Congress on Civil Engineering. Trujillo, Peru.
- [56] CYTED (Programa Iberoamericano de Ciencia y tecnología para el Desarrollo). 1995. "Recommendations for the development of technical regulatins for adobe, rammed earth, blocks and soil-cement buildings". In Spanish. Red Temática XIV.A: HABITERRA. La Paz, Bolivia.
- [57] Blondet M, Torrealva D, Vargas J, Velasquez J and Tarque N. 2006. "Seismic Reinforcement of Adobe Houses Using External Polymer Mesh". First European Conference on Earthquake Engineering and Seismology. Geneva, Switzerland.
- [58] Schemata –workshop ,X- Marks the Brace: Resisting Earthquakes on Capitol Hill's Heritage Buildings, September 19, 2011.